Republic of Iraq
Ministry of Higher Education
and Scientific Research
Al-Nahrain University
College of Science
Department of Physics

Radiation Dose Assessment for Ionizing and Ultraviolet Radiations Using CR-39 , Lexan and LR-115 Nuclear Track Detectors

A Thesis
Submitted to the College of Science/ Al-Nahrain University as a
Partial Fulfillment of the Requirements for the Degree of Master of
Science in Physics

By
Fala Hatem Taha
(B.Sc.in Physics-2011)

Supervised by

Dr.Hussain Ali Al-Jobouri
(Assist. Professor)

June   Shaaban
2014 A.D.   1435A.H

بِسْمِ اللَّهِ الرَّحْمَنِ الرَّحِيمِ

قَالُواْ سُبْحَانَكَ لاَ عِلْمَ لَنَا إِلاَّ مَا عَلَّمْتَنَا إِنَّكَ أَنتَ الْعَلِيمُ الْحَكِيمُ

صَدَقَ اللهُ العَظِيم

"سورة البقرة ٣٢"

Supervisors Certification

We certify that this thesis entitled **" Radiation Dose Assessment for Ionizing and Ultraviolet Radiations Using   CR-39 , Lexan and LR-115 Nuclear Track Detectors "** under our supervision at ' Al-Nahrian University ' as a partial fulfillment of requirements for the Degree of Master of Science in Physics.

Signature:
Name: **Dr.Hussain Ali Al-Jobouri**
Title**: Assist. Prof**.
Address: Department of Physics,
College of Science,
 Al-Nahrian University.

Date: / /2014

In view of the available recommendations, I forward this thesis for debate by the Examination Committee.

_____

Signature:
Name: **Dr. Thamir Abdul-Jabbar Jumah**
Title**: Assist. Prof.**
Address: Head of the department of Physics, College of Science,
 Al-Nahrian University.
Date: / /2014

Examination Committee Certification

We certify that we have read this thesis entitled "**Radiation Dose Assessment for Ionizing and Ultraviolet Radiations Using CR-39, Lexan and LR-115 Nuclear Track Detectors** " and, as an examining committee, examined the student (**Fala Hatem Taha**) in its contents, it is adequate as a thesis for the degree of Master of Science in Physics.

Signature:
Name: **Dr.Laith A. Al-Ani**
Title: Professor
Address: Dept. of physics ,college of science
       Al-Nahrain university
Date: /   /2014
       (Chairman)

Signature:
Name: **Dr. Kareem K. Mohammad**
Title: Assist. Professor
Address:Dept. of physics,college of science
       Al-Nahrain university

Date: / /2014
     (Member)

Signature:
Name: **Dr.Mahmoud A.Elawi**
Title: Assist. Professor
Address: College of Education for
       Pure Science , university of Tikrit

Date: / /2014
     (Member)

Signature:
Name: **Dr. Hussain Ali Al-Jobouri**
Title: Assist. Professor
Address: College of Science/ Al-Nahrain
      University
Date: / /2014
    (Member & supervisor)

I, hereby certify upon the decision of the examining committee

Signature:
Name: **Dr. Hadi M. A. Abood**
Title: Assistant Professor
Address: Dean of the College of Science
      Al-Nahrain University
Date: /   /2014

Dedication

To

my parents

For instilling in me the drive and ambition for making it to where I am, and for always loving me through the tough time.

Fala

Acknowledgments

Abstract

The aim of this study is the radiation dose assessment of gamma rays-γ and ultraviolet-UV radiation on nuclear track detector-NTDs types CR-39 , Lexan and LR-115 through measuring the absorbance-A by using uv-visible spectroscopy technique and measuring the spectral deviation of Fourier transform infrared- FTIR technique .

The radiation response for gamma rays was measured at low dose range 1Gy to 10 Gy and high dose range 10 Gy to 195 kGy .There is gamma ray response for all NTDs used in this study . Results revealed gamma radiation response at low and high radiation doses for Lexan and LR-115 detector   using   optical   absorbance-A ,while the radiation response for CR-39 detector appears only at high dose range .

The results show that absorbance -A   increases with increasing of gamma radiation dose, where it was observed that Lexan detector has a radiation response much better than CR-39 and LR-115   detectors through measuring increasing in the absorbance-A value at the wavelength 800 nm . There is deviation in some of wavenumbers-W of FTIR spectrum measured for CR-39 detector. This deviation appears at low dose range from 1Gy to 10 Gy with increasing of gamma radiation dose at wavenumbers-W 1405 and 1456 cm^{-1} , while the deviation does not appear in Lexan and LR-115 detectors .

Also, for uv-irradiation there is an increase in absorbance-A with uv-irradiation in dose at the range from 1 J/cm² to 360J/cm² . LR-115 detector has   uv-radiation response better than CR-39 and   Lexan detectors through measuring the increasing in absorbance-A at the wavelength 650 nm.

The deviation in FTIR spectrum caused by uv-irradiation appears at the wavenumbers-W 1338 , 940 and 2907 cm^{-1} for CR-39 , Lexan and LR-115 detector respectively. The deviation in CR-39 and Lexan detectors is more clear than in LR-115 detector.

From the results of this study , a possibility appears for the case of NTDs type CR-39 , Lexan and LR-115 as gamma and uv radiation dosimeters in medical and environmental fields.

List of Contents

List of Figures

List of Tables

List of Symbols

Symbol	Definition
f	Frequency.
λ	Wavelength.
E	Energy.
c	Speed of light in vacuum.
h	Planck's constant.
eV	Electron volts.
α	Alpha particles.
β	Beta particles.
γ	Gamma rays.
i.e.	That is.
etc.	And other things.
T_B	Etching time
D_T	Nuclear track diameter.
T_B	Etching time.
V_D	Etching velocity.
N_T	Number of tracks.
V_B	Etching velocity.
$\mathcal{E}_p$	Permittivity.
et. al.,	And all, or and others.
μm	Micrometer.
a.m.u	atomic mass unit

List of Abbreviations

Abbreviation	Definition
AERE	Association of Environmental and Resource Economists.
AFM	Atomic Force Microscopy.
ARS	Acute radiation syndrome.
CN	Cellulose nitrate.
DSC	Differential scanning calorimetry.
DNA	Deoxyribonucleic acid.
EDXR	Energy-dispersive X-ray fluorescence.
EM	Electromagnetic.
EMR	Electromagnetic radiation.
FTIR	Fourier Transform Infrared spectroscopy.
ICRP	International Commission on Radiological Protection.
SEM	Scanning electron microscopy.
SSNTDs	Solid State Nuclear Track Detectors.
TEM	Transmission electron microscopy.
UV	Ultraviolet radiation.
UV-VIS	UV–Visible spectroscopy.
PADC	Poly allyl diglycol carbonate.
PMMA	poly(methyl methacrylate).
XRD	X-ray diffraction.

Chapter One

Introduction and General Review

Chapter One
Introduction and General Review

1.1. History of the electromagnetic spectrum

For most of history, light was the only known part of the electromagnetic spectrum. The ancient Greeks recognized that light traveled in straight lines and studied some of its properties, including reflection and refraction. Over the years the study of light continued and during the 16th and 17th centuries there were conflicting theories which regarded light as either a wave or a particle. The first discovery of electromagnetic waves other than light came in 1800, when William Herschel discovered infrared radiation [1]. He was studying the temperature of different colors by moving a thermometer through light split by a prism. He noticed that the highest temperature was beyond red. He theorized that this temperature change was due to "calorific rays" which would be in effect a type of light ray that could not be seen. The next year, Johann Ritter worked at the other end of the spectrum and noticed what he called "chemical rays" (invisible light rays that induced certain chemical reactions) that behaved similar to visible violet light rays, but were beyond them in the spectrum [2].

They were later renamed ultraviolet radiation. In 1895 Wilhelm Röntgen noticed a new type of radiation emitted during an experiment with an evacuated tube subjected to a high voltage. He called these radiations x-rays and found that they were able to travel through parts of the human body but were reflected or stopped by denser matter such as bones. Before long, many uses were found for them in the field of medicine. The last portion of

the electromagnetic spectrum was filled in with the discovery of gamma rays.

In 1900 Paul Villard was studying the radioactive emissions of radium when he identified a new type of radiation that he first thought consisted of particles similar to known alpha and beta particles, but with the power of being far more penetrating than either. However, in 1910, British physicist William Henry Bragg demonstrated that gamma rays are electromagnetic radiation, not particles, and in 1914, Ernest Rutherford (who had named them gamma rays in 1903 when he realized that they were fundamentally different from charged alpha and beta rays) and Edward Andrade measured their wavelengths, and found that gamma rays were similar to x-rays, but with shorter wavelengths and higher frequencies.

1.1.1. Range of the electromagnetic spectrum

Electromagnetic waves are typically described by any of the following three physical properties: the frequency f , wavelength λ , or photon energy E. Frequencies observed in astronomy range from 2.4×10^{23} Hz (1 GeV gamma rays) down to the local plasma frequency of the ionized interstellar medium (~1 kHz) as shown in figure (1.1). Wavelength is inversely proportional to the wave frequency [3].
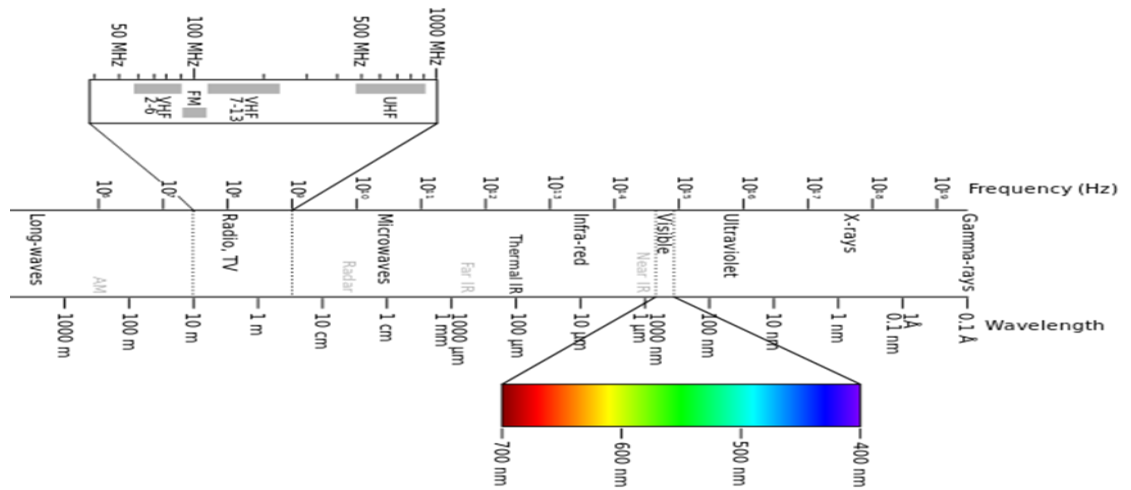
Figure 1.1 The electromagnetic spectrum [3]

so gamma rays have very short wavelengths that are fractions of the size of atoms, whereas wavelengths on the opposite end of the spectrum can be as long as the universe. Photon energy is directly proportional to the wave frequency, so gamma ray photons have the highest energy (around a billion electron volts), while radio wave photons have very low energy (around a femtoelectronvolt). These relations are illustrated by the following equations:

$$f = \frac{c}{\lambda}, \quad or \ f = \frac{E}{h}, \quad or \ f = \frac{hc}{\lambda}, \tag{1.1}$$

where: c = 2.99792458×10^8 m/s is the speed of light in vacuum and

h = 6.62606896 ×10^{-34} J s = 4.13566733×10^{-15} eV s is

Planck's constant [4].

Whenever electromagnetic-EM waves exist in a medium with matter, their wavelength is decreased. Wavelengths of electromagnetic radiation, no matter what medium they are traveling through, are usually quoted in terms of the vacuum wavelength, although this is not always explicitly stated. Generally, electromagnetic radiation is classified by wavelength into radio

wave, microwave, terahertz (or sub-millimeter) radiation, infrared, the visible region we perceive as light, ultraviolet, x-rays and gamma rays. The behavior of EM radiation depends on its wavelength. When EM radiation interacts with single atoms and molecules, its behavior also depends on the amount of energy per quantum (photon) it carries. Spectroscopy can detect a much wider region of the EM spectrum than the visible range of 400 nm to 700 nm.

1.2. Radiation

In physics, radiation is a process in which energetic particles or energetic waves travel through a vacuum, or through matter-containing media that are not required for their propagation. Waves of a mass filled medium itself, such as water waves or sound waves, are usually not considered to be forms of "radiation" in this sense. Radiation can be classified as either ionizing or non-ionizing according to whether it ionizes or does not ionize ordinary chemical matter. The word radiation is often colloquially used in reference to ionizing radiation (e.g. x-rays, gamma rays), but the term radiation may correctly also refer to non-ionizing radiation (e.g., radio waves, microwaves, heat or visible light) as well. The particles or waves radiate (i.e., travel outward in all directions) from a source. This aspect leads to a system of measurements and physical units that are applicable to all types of radiation. Because radiation expands as it passes through space, and as its energy is conserved (in vacuum), the power of all types of radiation follows an inverse-square law in relation to the distance from its source.

Both ionizing and non-ionizing radiation can be harmful to organisms and can result in changes to the natural environment. In general, however, ionizing radiation is far more harmful to living organisms per unit of energy deposited than non-ionizing radiation, since the ions that are produced, even at low radiation powers, have the potential to cause DNA damage. By contrast, most non-ionizing radiation is harmful to organisms only in proportion to the thermal energy deposited, and is conventionally considered harmless at low powers that do not produce a significant temperature rise. Ultraviolet radiation in some aspects occupies a middle ground, as it has some features of both ionizing and non-ionizing radiation.

Although nearly all of the ultraviolet spectrum that penetrates the Earth's atmosphere is non-ionizing, this radiation does far more damage to many molecules in biological systems than can be accounted for by heating effects (an example is sunburn). These properties derive from ultra-violet's power to alter chemical bonds, even without having quite enough energy to ionize atoms.

The question of harm to biological systems due to low-power ionizing and non-ionizing radiation is not settled. Controversy continues about possible non-heating effects of low-power non-ionizing radiation, such as non-heating microwave and radio wave exposure. Non-ionizing radiation is usually considered to have a safe lower limit, especially as thermal radiation is unavoidable and ubiquitous. By contrast, ionizing radiation is conventionally considered to have no completely safe lower limit, although at some energy levels, new exposures do not add appreciably to background radiation. The evidence that small

amounts of some types of ionizing radiation might confer a net health benefit in some situations, is called radiation hormesis [5].

1.2.1. Ionizing radiation

Radiation with sufficiently high energy can ionize atoms; that is to say it can knock out electrons from atoms and create ions. This occurs when an electron is stripped (or "knocked out") from an electron shell of the atom, which leaves the atom with a net positive charge. Because living cells and, more importantly, the DNA in those cells can be damaged by this ionization, it can result in an increased chance of cancer. Thus "ionizing radiation" is somewhat artificially separated from particle radiation and electromagnetic radiation, simply due to its great potential for biological damage. While an individual cell is made of trillions of atoms, only a small fraction of those will be ionized at low radiation powers. The probability of ionizing radiation causing cancer is dependent upon the absorbed dose of the radiation, and is a function of the damaging tendency of the type of radiation (equivalent dose) and the sensitivity of the irradiated organism or tissues (effective dose). Roughly speaking, photons and particles with energies above about 10 electron volts (eV) are ionizing.

Alpha particles, beta particles, cosmic rays, gamma rays, and x-ray radiation, all carry enough energy to ionize atoms.

In addition, free neutrons are also ionizing since their interactions with matter are inevitably more energetic than this threshold. Ionizing radiation originates from radioactive materials, x-ray tubes, particle accelerators, and is naturally present in the environment. It is invisible and not directly detectable by human senses; as a result, instruments such as Geiger counters are usually

required to detect its presence. In some cases, it may lead to secondary emission of visible light upon its interaction with matter, as in the case of Cherenkov radiation and radio-luminescence.

Ionizing radiation has many practical uses in medicine, research and construction, but presents a health hazard if used improperly.

Exposure to radiation causes damage to living tissue, high doses result in skin burns, radiation sickness and death, while low but persistent doses result in cancer tumors and genetic damage [5]. However, calculating exact risk and chance of cancer forming in cells caused by ionizing radiation is still wildly unknown and currently estimates are loosely made off of population based data from the atomic bombing in Japan (which shouldn't be generalized to populations in other countries).

The International Commission on Radiological Protection-ICRP states that "The Commission is aware of uncertainties and lack of precision of the models and parameter values.", "Collective effective dose is not intended as a tool for epidemiological risk assessment, and it is inappropriate to use it in risk projections." and "in particular, the calculation of the number of cancer deaths based on collective effective doses from trivial individual doses should be avoided" [6].

Electromagnetic radiation -EMR is represented as self-propagating waves. EMR has electric and magnetic field components that oscillate in phase perpendicular to each other and also to the direction of energy propagation. EMR is classified into types according to the frequency range of the waves, these types include (in order of increasing frequency): radio waves, microwaves, terahertz radiation, infrared radiation, visible light,

ultraviolet radiation, x-rays and gamma rays. These, radio waves have the longest wavelengths (lowest energy) and gamma rays have the shortest and hence the highest energy. A small window of frequencies, called the visible spectrum or light, is sensed by the eyes of various organisms.

Ionizing electromagnetic radiation is that for which the photons making up the radiation have energies larger than about 10 electron volts. The ability of an electromagnetic wave (photons) to ionize an atom or molecule thus depends on its frequency, which determines the energy of a photon of the radiation. An energy of 10 eV is about 1.6×10^{-18} joules, which is a typical binding energy of an outer electron to an atom or organic molecule [7]. This corresponds with a frequency of 2.4×10^{15} Hz, and a wavelength of 125 nm (this is in far ultraviolet) or less [8].

1.2.1.1. Ultraviolet radiation

Ultraviolet of ionizing wavelengths from 10 nm to 125 nm ionizes air molecules, and this interaction causes it to be strongly absorbed by air. Ionizing uv therefore does not penetrate Earth's atmosphere to a significant degree, and is therefore sometimes referred to as vacuum ultraviolet. Although present in space, this part of the uv spectrum is not of biological importance, because it does not reach living organisms on Earth. Some of the ultraviolet spectrum that does reach the ground (the part that begins above energies of 3.1 eV, or wavelength less than 400 nm) is non-ionizing, but is still biologically hazardous due to the ability of single photons of this energy to cause electronic excitation in biological molecules, and thus damage them by means of unwanted

reactions. An example is the formation of pyrimidine dimers in DNA, which begins at wavelengths below   365 nm (3.4 eV), which is well below ionization energy. This property gives the ultraviolet spectrum some of the dangers of ionizing radiation in biological systems without actual ionization occurring. In contrast, visible light and longer-wavelength electromagnetic radiation, such as infrared, microwaves, and radio waves, consists of photons with too little energy to cause damaging molecular excitation, and thus this radiation is far less hazardous per unit of energy [8].

1.2.1.2. X-ray

X-rays are electromagnetic waves with a wavelength less than about 10^{-9} m (greater than 3×10^{17} Hz and 1,240 eV). A smaller wavelength corresponds to a higher energy according to the equation $E = hc/\lambda$. A "packet" of electromagnetic waves is called a photon. When an x-ray photon collides with an atom, the atom may absorb the energy of the photon and boost an electron to a higher orbital level or if the photon is very energetic, it may knock an electron from the atom altogether, causing the atom to ionize. Generally, larger atoms are more likely to absorb an x-ray photon since they have greater energy differences between orbital electrons. Soft tissue in the human body is composed of smaller atoms than the calcium atoms that make up bone, hence there is a contrast in the absorption of x-rays. X-ray machines are specifically designed to take advantage of the absorption difference between bone and soft tissue, allowing physicians to examine structure in the human body [7].

1.2.1.3. Gamma radiation

Gamma $-\gamma$ radiation consists of photons with a wavelength less than 3×10^{-11} meters (greater than 10^{19} Hz and 41.4 keV) [5]. Gamma radiation emission is a nuclear process that occurs to rid the decaying nucleus of excess energy after it has emitted either alpha or beta radiation. Both alpha and beta particles have an electric charge and mass, and thus are quite likely to interact with other atoms in their path. Gamma radiation, however, is composed of photons, which have neither mass nor electric charge and, as a result, penetrates much further through matter than either alpha or beta radiation.

Gamma rays can be stopped by a sufficiently thick layer of material as shown in figure (1.2) , where the stopping power of the material per given area depends mostly (but not entirely) on the total mass along the path of the radiation, regardless of whether the material is of high or low density. However, as is the case with x-rays, materials with high atomic number such as lead or depleted uranium add a modest (typically 20% to 30%) amount of stopping power over an equal mass of less dense and lower atomic weight materials (such as water or concrete) [7].
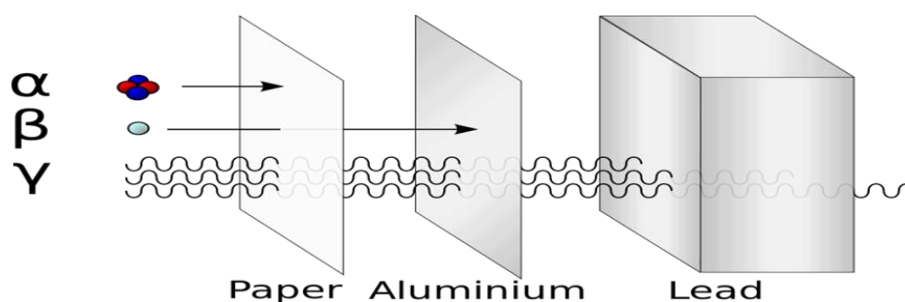
Figure 1.2 Illustration of the relative abilities of three different types of ionizing radiation to penetrate solid matter. Typical alpha particles (α) are stopped by a sheet of paper, while beta particles (β) are stopped by an aluminum plate. Gamma radiation (γ) is dampened when it penetrates lead [7]

1.2.1.4. Alpha radiation

Alpha particles are helium-4 nuclei (two protons and two neutrons). They interact with matter strongly due to their charges, and at their usual velocities only penetrate a few centimeters of air, or a few millimeters of low density material (such as the thin mica material which is specially placed in some Geiger counter tubes to allow alpha particles in). This means that alpha particles from ordinary alpha decay do not penetrate skin and cause no damage to tissues below.

Some very high energy alpha particles compose about 10% of cosmic rays, and these are capable of penetrating the body and even thin metal plates. However, they are of danger only to astronauts, since they are deflected by the Earth's magnetic field and then stopped by its atmosphere.

Alpha radiation is dangerous when alpha-emitting radioisotopes are ingested (breathed or swallowed). This brings the radioisotope close enough to sensitive tissue for the alpha radiation to damage cells. Per unit of energy, alpha particles are at least 20 times more effective at cell-damage as gamma rays and x-rays. Examples of highly poisonous alpha-emitters are radium, radon, and polonium.

1.2.1.5. Beta radiation

Beta-minus (β^-) radiation consists of an energetic electron. It is more ionizing than alpha radiation, but less than gamma. Beta radiation from radioactive decay can be stopped with a few centimeters of plastic or a few millimeters of metal. It occurs when a neutron decays into a proton in a nucleus, releasing the beta particle and an antineutrino. Beta radiation from linear particle

accelerators is far more energetic and penetrating than natural beta radiation. It is sometimes used therapeutically in radiotherapy to treat superficial tumors.

Beta-plus (β^+) radiation is the emission of positrons, which are the antimatter form of electrons . When a positron slows down to speeds similar to those of electrons in the material, the positron will annihilate an electron, releasing two gamma photons of 511 keV in the process. Those two gamma photons will be traveling in (approximately) opposite direction . The gamma radiation from positron annihilation consists of high energy photons, and is ionizing .

1.2.2.   Non-ionizing radiation

The kinetic energy of particles of non-ionizing radiation is too small to produce charged ions when passing through matter. For non-ionizing electromagnetic radiation , the associated particles (photons) have only sufficient energy to change the rotational, vibrational or electronic valence configurations of molecules and atoms. The effect of non-ionizing forms of radiation on living tissue has only recently been studied Nevertheless, different biological effects are observed for different types of non-ionizing radiation [5 , 9].

Even "non-ionizing" radiation is capable of causing thermal-ionization if it deposits enough heat to raise temperatures to ionization energies. These reactions occur at far higher energies than with ionization radiation, which requires only single particles to cause ionization . A familiar example of thermal ionization is the flame-ionization of a common fire, and the browning reactions in

common food items induced by infrared radiation, during broiling-type cooking .

1.2.2.1. Non-ionizing electromagnetic radiation

The electromagnetic spectrum is the range of all possible electromagnetic radiation frequencies [5]. The electromagnetic spectrum (usually just spectrum) of an object is the characteristic distribution of electromagnetic radiation emitted by, or absorbed by, that particular object. The non-ionizing portion of electromagnetic radiation consists of electromagnetic waves that (as individual quanta or particles) are not energetic enough to detach electrons from atoms or molecules and hence cause their ionization. These include radio waves, microwaves, infrared, and (sometimes) visible light. The lower frequencies of ultraviolet light may cause chemical changes and molecular damage similar to ionization, but is technically not ionizing. The highest frequencies of ultraviolet light, as well as all x-rays and gamma-rays are ionizing .

The occurrence of ionization depends on the energy of the individual particles or waves, and not on their number. An intense flood of particles or waves will not cause ionization if these particles or waves do not carry enough energy to be ionizing, unless they raise the temperature of a body to a point high enough to ionize small fractions of atoms or molecules by the process of thermal-ionization (this, however, requires relatively extreme radiation intensities).

1.2.2.1.1. Ultraviolet light

As noted above, the lower part of the spectrum of ultraviolet, from 3 eV to about 10 eV, is non-ionizing. However, the effects of non-ionizing ultraviolet on chemistry and the damage to biological systems exposed to it (including oxidation, mutation, and cancer) are such that even this part of ultraviolet is often compared with ionizing radiation.

1.2.2.2. Other types of non-ionizing electromagnetic radiation

a- Visible light

Light, or visible light, is a very narrow range of electromagnetic radiation of a wavelength that is visible to the human eye, or 380–750 nm which equates to a frequency range of 790 to 400×10^{12} Hz respectively.

b- Infrared

Infrared (IR) light is electromagnetic radiation with a wavelength between 0.7 and 300 micrometers, which corresponds to a frequency range between 430 to 1×10^{12} Hz respectively.

c- Microwave

Microwaves are electromagnetic waves with wavelengths ranging from as short as one millimeter to as long as one meter, which equates to a frequency range of 300 GHz to 300 MHz .

d- Radiowaves

Radiowaves are a type of electromagnetic radiation with wavelengths in the electromagnetic spectrum longer than infrared light . Like all other electromagnetic waves, they travel at the speed of light . Naturally occurring radio waves are made by lightning, or by certain astronomical objects. Artificially generated radio waves are used for fixed and mobile radio communication, broadcasting, radar and other navigation systems, satellite communication, computer networks and innumerable other applications.

1.3. History of solid state nuclear track detectors

The usability of solid state nuclear track detector-SSNTDs technique has been enhanced by various methods of track visualization and evaluation introduced over the past one –decade or more [10] . Starting with the observation of few feel trails of damage in sheet of mica exposed to fission fragments some forty years ago, the discipline based on their correct interpretation has emblazoned resounding success story in the second half of the 20th century [11]. The first documentation of etchable tracks in dielectrics was reported in 1958 by Young [12] , working at Atomic Energy Research Establishment -AERE at Harwell in England. He discovered that LiF crystal held contact with Uranium foil irradiated with thermal neutrons, revealed a number of etch pits after treatment with a chemical reagent . He seasoned that with respect to the chemical properties , the damage trial of a fission fragment is similar to that of dislocation .

In 1959, Silk and Barnes [13] , also working at Association of Environmental and Resource Economists-AERE reported direct observation of this damaged region in mica. They published for the first time the electron photomicrograph of the tracks of fission fragments in natural mica. [14 , 15] introduced fission fragment and other heavy charged partial in many solids (mica, plastic,…etc.) and observed their tracks directly by an electron microscope as well as after selective chemical etching by an optical microscope . Subsequently, they showed that this was a general phenomenon, were observed in many other dielectrics including other minerals, glasses and polymers [16, 17].

More directly useful researches have included medical and biological used as well as industrial applications [18].

One can add that, due to realization of the great potentialities of nuclear tracks, a completely research journal named "Nuclear Tracks Detection " renamed as "Nuclear Tracks" and currently entitled as "Nuclear Tracks and Radiation Measurements" is being published by pergammon press since 1976 [19]. Another jornal "Nuclear Instrument and Method", have devoted full volumes to the papers read at international conferences and spring school held on development and application of SSNDs [20].

1.4. Solid state nuclear track detectors SSNTD's

Solid-state nuclear track detectors-SSNTDs are insulating materials have the capabilities for measuring concentration and spatial distribution of isotopes if they emit heavy charge particles , either directly or as a result of specific nuclear reaction [21]. The damage of these particles along their path is called track (latent track), may become visible under an ordinary optical microscope

after etching with suitable chemical [22]. The damage track detectors can be the quantity of importance is the energy left near the particle trajectory, which determines the chemical track reactivity [21].

The solid state nuclear track detectors are formed in a variety of materials that fall into two main categories: inorganic solids such as crystals and glasses, and organic solids such as polymers . These types differ in their sensitivity which increases with increasing of incident particle atomic number.

1.4.1. The types of solid state nuclear track detectors

a- Inorganic detectors

Inorganic detectors are compounds where carbon and hydrogen do not enter in structure, and create (Ionic Bond) between their atoms. Table (1.1) show some kinds of the inorganic detectors and their chemical composition [23].

b- Organic detectors

Organic detectors are compounds where carbon and hydrogen enter in its structure, and create a (covalent bond) between its atoms, this type of SSNTDs has a sensitivity larger than inorganic detectors because the bounds of C-C, C-H are easily broken after exposing to the radiation, also the organic detectors have a high analytic power larger than inorganic detectors, while the threshold energy for organic detectors is less than inorganic detectors [24]. Table (1.1) show some kinds of the organic detectors and their chemical composition [23].

Some of commonly used SSNTD's are given in table (1.1).

Table 1.1 Commonly used SSNTD's materials **[23]**

	Detector	Atomic composition	General etching conditions	Least ionizing ion seen
Inorganic materials	Quartz	SiO_2	KOH Soln., 210 °C, 10 min	100 MeV ^{40}Ar
	Muscovite Mica	$Kal_3Si_3O_{10}(OH)_2$	48%HF,23° C, 3 sec - 40 min	2MeV ^{20}Ne
	Silica Glass	SiO_2	48%HF, 23°C, 3 sec	16MeV ^{40}A
	Flint Glass	$18SiO_2:4PbO:1.5Na_2O:K_2O$	48%HF, 23°C, 3 sec	MeV ^{20}Ne 4-2
Organic materials	Polyallyl Digolycol Carbonate (**CR-39**)	$C_{12}H_{18}O_7$ (CR-39)	6 N NaOH, 60°C, 1-6 hrs	1 MeV H
	Bisphenol A-polycarbonate(**Lexan**, Makrofol)	$C_{16}H_{14}O_3$	6 N NaOH, 60°C, 60 min	0.3 MeV ^4He
	Cellulose Nitrate (Daicell, **LR-115**)	$C_6H_9O_9N_2$ (CN)	6-3 N NaOH, 50°C, 40 min	0.5 MeV H

1.5. Applications of solid state nuclear track detectors

As already mentioned, the SSNTDs can perform background free detection of fission fragments in the presence of high doses of light charged particles, gamma rays and neutrons . They are ideal for the study of rare type of heavy charged reaction products emitted in nuclear reactions . They have been advantageously employed in the measurement of spontaneous fission decay constant of a number of heavy nuclides , and other parameters of great importance in nuclear sciences [25, 26] .

The advantage of SSNTD over nuclear track emulsion in detecting charged particles have resulted in an almost complete replacement of the latter in many fields of application [27]. They have already found numerous applications in physics, medicine, geophysics and technology [28].

The physical applications includes:

1. Nuclear fission and spallation reactions [28].

2. Lifetime of heavy unstable nuclear particles.

3. Ternary fission [29 , 30].

 4. Neutron dosimtry [31].

   In medicine, selectively etched tracks in the track detectors have

been used to determine:

 1. The deposition of inhaled UO_2 particles in rat's lung [32].

 2. The micro-distribution of inhaled alpha emitters

[33].

  3. The concentration of radioactive nuclides in tissues   [34]

and in blood [35] .

    In geophysics these detectors have been used in geochronology [36] , also in fission track dating of lunar samples and meteorites [31].

    In technology, these detectors have been used as a fine sieve for the filtration of cancer blood cells [37, 38] , in aerosol filtration [39], and in studies of personal dosimeter to measure neutron fluxes at nuclear reactors.

1.6. Health effects of ionizing radiation

    All ionizing radiation causes similar damage at a cellular level, but because rays of alpha particles and beta particles are relatively non-penetrating, external exposure to them causes only localized damage, e.g. radiation burns to the skin. Gamma rays and neutrons

are more penetrating, causing diffuse damage throughout the body (e.g. radiation sickness, cell's DNA damage, cell death due to damaged DNA, increasing incidence of cancer) rather than burns. External radiation exposure should also be distinguished from internal exposure, due to ingested or inhaled radioactive substances, which depending on the substance's chemical nature, can produce both diffusion and localized internal damage.

Even low doses of gamma radiation, such as those experienced by professionals who use x-ray machines in the medical field, can damage DNA and cause genetic mutations, according to a study on the government's PubMed database. The study showed that amounts as low as 5 rad or 5 c Gy (a standard measurement for the amount of energy one kilogram of matter absorbs) can damage a person's genetic material. Damaged DNA often leads to cancer and chromosome mutations.

Gamma rays are usually the main culprit when people suffer from radiation sickness, reports the Merck Online Medical Manual. Technically known as "acute radiation syndrome," radiation sickness symptoms develop in two to 31 days of exposure to gamma radiation. Typical effects from ARS include nausea, vomiting and general fatigue due to the body's weakened immune system.

1.6.1. Positive health effects of ionizing radiation

Although gamma absorbed through the skin can cause several health risks, the medical field often uses gamma radiation to kill bacteria and sterilize equipment , according to medical supplier Steritech . The DNA-damaging effect of gamma radiation destroys germs , which have much less DNA than animals and humans.

Gamma irradiation is a "cold process" that does not increase the temperature of an object.

1.6.2. Solution to prevent the effect of gamma rays

The Environmental Protection Agency claims that one can reduce exposure to gamma radiation through a few preventative steps.

Always wear protective clothing around radiation. Anything emitting gamma radiation should bear a symbol that can review. Gamma radiation occurs naturally in some isotopes of potassium, but the most controllable way to avoid gamma rays is to limit medical   x-rays.

1.6.3. Health effects of uv_ radiation exposure

Some uv exposure is essential for good health. It stimulates vitamin D production in the body. In medical practice, uv lamps are used for treating psoriasis (a condition causing itchy, scaly red patches on the skin) and for treating jaundice in new born babies .

Excessive exposure to ultraviolet radiation is associated with different types of skin cancer, sunburn, accelerated skin aging, as well as cataracts and other eye diseases. The severity of the effect depends on the wavelength (Figure 1.3) , intensity, and duration of exposure. Understanding these risks and taking sensible precautions will help you enjoy the sun while reducing your chances of sun-related health problems:

- Skin cancer (melanoma and nonmelanoma)
- Premature aging and other skin damage
- Cataracts and other eye damage

- Immune system suppression

EFFECTS OF UV ON THE SKIN
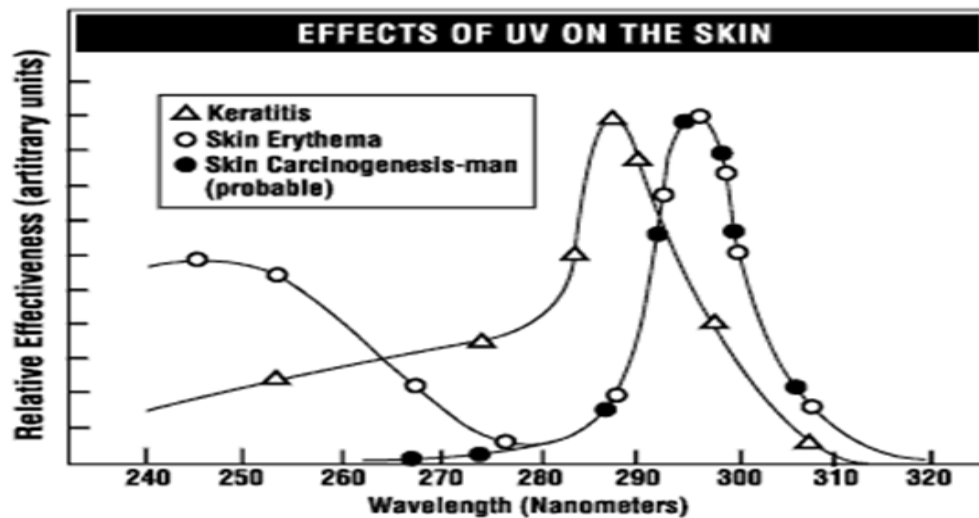
Figure 1.3   Relative sensitivity of the eye and the skin to uv radiation of different wavelengths

1.6.4. Effects on the skin

The shortwave UV radiation UV-C poses the maximum risk. The sun emits UV-C but it is absorbed in the ozone layer of the atmosphere before reaching the earth. Therefore, UV-C from the sun does not affect people. Some man-made UV sources also emit UV-C. However, the regulations concerning such sources restrict the UV-C intensity to a minimal level and may have requirements to install special guards or shields and interlocks to prevent exposure to the UV.

The medium wave UV (UV-B) causes skin burns, erythema (reddening of the skin) and darkening of the skin. Prolonged exposures increase the risk of skin cancer. The uv-irradiation source used in this study has wave length 254 nm and the amount of power 15W.

Long wave UV radiation (UV-A) accounts for up to 95% of the   uv radiation that reaches the earth's surface . Although

UV-A is less intense than UV-B , it is more prevalent and can penetrate deeper into the skin layers, affecting the connective tissue and blood vessels, which results in premature aging .

Certain chemicals and medications act as photosensitizing agents and enhance the effect of uv radiation from sunlight or other sources. Such agents include thiazide diuretics (drugs which cause excessive urine production), drugs used in the treatment of high blood pressure, certain antibiotics (tetracyclines, sulfonamides) , cosmetics , and thiazine tranquilizers .

These are just a few examples; this is not intended to be a comprehensive list. However, it is important to know that these photosensitizing effects can occur in case people are exposed to uv radiation at work. For example, an inexperienced welder, who was taking a phenothiazine anti-depressant drug, suffered damage in both eyes in the part of the retina that absorbs short wavelength light (bilateral maculopathy) . He began complaining of eye problems a day after he was arc welding for two minutes without wearing any eye protection .This damage, that fortunately was reversible after several months , occurred because the drug he was taking sensitized him to the uv radiation to which he was exposed . Various plants such as carrot , celery, dill , fig , lemon and some types of weeds are known to cause photosensitivity.

Exposure to fluids from these plants , especially if crushed, followed by exposure to sunlight can cause dermatitis. Citrus fruit handlers and vegetable harvesters , gardeners , florists and bartenders are at risk for experiencing dermatitis following exposure to certain plants and then to sunlight (phytophotodermatitis) . Coal tar and creosote are examples of photosensitizing agents in the workplace.

Effects of repeated exposures (chronic effects) include skin aging and skin cancer. There is a strong causal link between skin cancer and prolonged exposure to solar uv and from artificial sources.

1.7. NTDs used in this study

1.7.1. CR-39 track detector

Poly allyl diglycol carbonate -PADC which is generally referred as CR-39 is the most sensitive of the nuclear track recording plastics [31] . The chemical form of CR-39 is $C_{12} H_{18} O_7$ as shown in figure (1.3) . This plastic detector is made by polymerization of the oxydi-2 , 1-ethanediyl, di-2-propenyl ester of carbonic acid. It contains two of monomer ally functional groups $[CH_2 = CH - CH_2 -]$ and has the following structure:
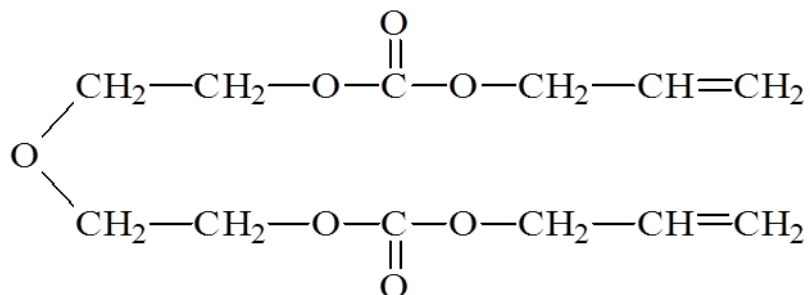
Figure 1.4 Chemical structure of CR-39 $C_{12} H_{18} O_7$ [31] .

It has the unique properties of being inert to light, x-ray, and gamma and beta radiation, but reactive with alpha particles . CR-39 detectors are widely used in different branches of sciences such as nuclear and fission physics , charged-particle radiography, radon dosimetry and radiobiological experiments .

The general characteristics of CR-39 can be summarized as [40]:

1. Amorphous polymer.

2. Optically clear.

3. Environmentally very stable.

4. Having a closed packed and uniforms molecular structure.

5. Having non – solvent chemical etchant.

6. Highly cross – linked thermoset.

7. Sensitive to heavy ion damage $Z/\beta > 10$ where β is the ratio of particle velocity to the velocity of light.

In the radiation detection application, CR-39 is used as a solid-state nuclear track detector to detect the presence of ionising radiation. Energetic particles colliding with the polymer structure leave a trail of broken chemical bonds within the CR-39. When immersed in a concentrated alkali solution (typically Sodium Hydroxide) hydroxide ions attack and break the polymer structure , etching away the bulk of the plastic at a nominally fixed rate .

However, along the paths of damage left by charged particle interaction the concentration of radiation damage allows the chemical agent to attack the polymer more rapidly than it does in the bulk , revealing the paths of the charged particle ion tracks. The resulting etched plastic therefore contains a permanent record of not only the location of the radiation on the plastic but also gives spectroscopic information about the source . Principally used for the detection of alpha radiation emitting radionuclides (especially radon gas) , the radiation-sensitivity properties of CR-39 are also used for proton and neutron dosimetry and historically cosmic ray investigations .

Irradiation of polymer rich substances by high energy ionizing radiation such as x-rays or gamma rays causes many changes in

the polymer. It may degrade polymeric materials by random fracture of the main chain with the number of fractures being proportional to the radiation dose [41,42] . The bond breaking may give rise to free radicals [41,43] ionic species, It has been reported that irradiating plastic detectors with gamma rays or uv (which do not induce any tracks themselves) can affect the properties of track registrations on these detectors [25] .

Therefore, many studies were performed to use plastic detectors for gamma dosimetry . It is well established that polymers can be degraded by energetic agencies (e.g., ultraviolet radiation) and chemical agencies (e.g., NaOH). There have been many previous studies indicating that ultraviolet-UV irradiation will affect the bulk etch and track etch responses [44,46].

In 2008 [47] found the effect of gamma radiation on optical properties of CR-39 polymer with various doses (20-800 kGy) and determined the values of indirect and direct for band energy gap. Used gamma radiation to irradiate CR-39 and he found the optical band gap (direct and indirect) decreased with photon energy. The number of carbon atom and Urbach energy was determined [48].

One of these fields was the measurement of radiation effects for non-particle radiation as ionizing radiation [49] , and particle radiation as ion beam , neutron and α- particle[50] , and so named nuclear track detector- NTD[48,51]. The main strength of these detectors is that the damage produced by the ionizing particle can be enlarged through chemical etching [52] . These enlarged tracks, and physical properties can be viewed under the optical microscope and fourier transform infrared spectroscopy – FTIR [53] . Nuclear track detector – NTD type CR-39 is one of the trade names of the family of Poly Allyl Diglycol Carbonate– PADC etch track

detectors. When it is etched in sodium hydroxide – NaOH solution , a variety of inorganic and organic compounds are formed as the reaction products , which also have effect on the thickness of CR-39 [54, 55].

1.7.2. Lexan track detector

Lexan polycarbonate $C_{16}H_{14}O_3$ as shown in figure (1.5) is a promising polymer having high transparency in the visible spectrum range, which is used in all fields of life viz. optical [56] , medical , electronic , space applications and for recording ion tracks [57] . Where its low weight, chemical inertness, high impact resistance and relatively low cost are of major importance. During last few decades , some materials like metals and ceramics have been replaced by the polymers because of their superior advantages. However , some features of polymers should be modified by using treatments like ionizing beam , laser or uv radiation [58] .
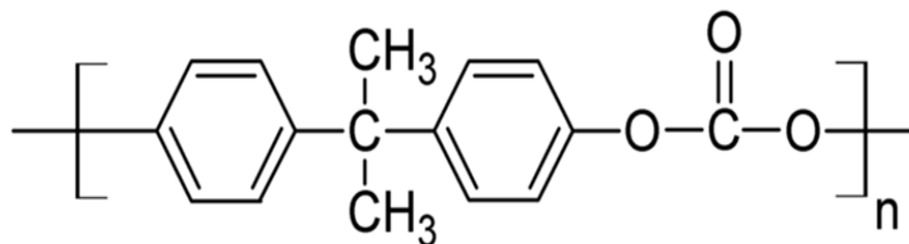
Figure1.5 Chemical structure of Lexan $C_{16}H_{14}O_3$ [56] .

The changes induced in the polymer by uv radiation depend on the time of exposure and also on the wavelength of uv radiation. In case of short wavelength uv irradiation, the energy is sufficient enough to break polymer bonds leading to scission of the polymer chains. In addition, depending upon the polymer structure, the free

radicals generated may combine with other radicals resulting in cross-linking. uv irradiation effects on polyallyl diglycol carbonate-PADC detector have been studied by Tse et.al.[59].

The radiation induced changes in the properties of polymer are very specific with respect to type of polymer , radiation and its environment [6o] . The polymers which are difficult to process by chemical methods can be easily modified using irradiation [61]. This leads to changes in structural [62] , thermal , optical [63] and surface morphological properties [63] due to the radiochemical alterations such as unsaturation, evolution of gases , formation of carbon clusters, change in free volume , creation of defects , amorphization etc . As a result, irradiation of polymers has shown great potential for the fields such as microelectronics, biomedical, device technology nano-materials and materials science [64] . Literature survey indicates that the effects of radiation on Lexan polycarbonate are being extensively studied including exposure of Lexan polycarbonate to gamma [47] . and RF plasma showed modification in optical, chemical and surface morphological properties. It was further observed that there was a substantial chemical and thermal modification in the Lexan polycarbonate sample such as breaking of C–O single bond and formation of phenolic bond and gradual decrease in the glass transition temperature with the increase in ion fluence of 100 MeV silicon ions [65] .

As per literature survey , until now , no study has been carried out on the characterisation of structural , optical and mechanical modifications of uv-irradiated Lexan polycarbonate . Therefore , in the present investigation, an attempt has been made to study the effect of uv radiation ($\lambda = 250$ nm) on the above-

mentioned properties of Lexan polycarbonate using x-ray diffraction , Fourier Transform Infrared-FTIR spectroscopy , scanning electron microscope , differential scanning calorimetry , uv–visible spectroscopy, impedance analysis , tensile testing and rheometry analyses [66] .

1.7.3. LR-115 track detector

Cellulose nitrate films $C_6H_9O_9N_2$ as shown in figure (1.6) (commercially available as LR-115 films from DOSIRAD , France) have been commonly used as SSNTDs in which visible tracks can be formed after ion irradiation and suitable chemical etching [67,68]. depending critically on the thickness of etched-away cellulose nitrate-CN layer during chemical etching . However , Yip et. al. [69] showed that its bulk etch rate was affected by the amount of stirring so actual monitoring of the thickness of the CN layer is necessary whenever using this SSNTD [70] . In particular , so-called a priori non-destructive methods are needed before completion of chemical etching [71] .
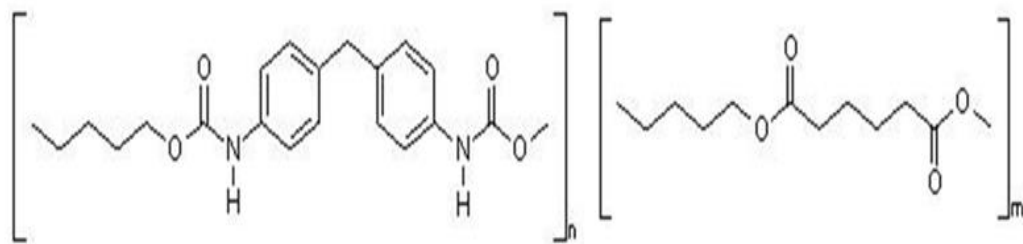
Figure1.6 Chemical structure of LR-115 $C_6H_9O_9N_2$ [69] .

It is the so called "gravimetric" method [72] . However, this method is limited by the accuracy of mass measurements . Proposed a method to measure the thickness of the active layer of LR-115 SSNTDs based on the absorption of fluorescence x-ray

photons by the active layer [73] . Nevertheless , there is a risk that x-ray radiation affects the track and bulk etching velocities . For example , [74,75] have shown x-ray degradation of cellulose nitrates. Proposed another spectroscopic method by using Fourier transform infrared-FTIR spectroscopy [76] . Proposed a method based on a color commercial document scanner to determine the active layer thickness of the LR-115 [77] .

1.8. Analyses of FTIR spectra of CR-39

CR-39 detector is a highly crosslinked thermoset fabricated by polymerization of the allyl diglycol carbonate monomer [78] . IR spectroscopy allows the identification of different absorption bands [79,80], decreased when the thickness of the CR-39 detector decreases , so these are characteristic of the CR-39 detector . The wave numbers corresponding to these absorptions (transmission troughs) , and the corresponding assignment of the functional groups and the modes of vibration are summarized in table (1.2) .

Table 1.2 The wave numbers of the more significant absorption peaks (transmission troughs) in the FTIR spectrum of CR-39 detector, and the corresponding assignment of the function groups and the modes of vibration [81].

Position of the peak (cm^{-1})	Functional Groups/modes of vibration
3636	OH asymmetric stretching vibrations
3549	OH symmetric stretching vibrations
3470	First overtone of C=O stretching vibration of ester
2958, 2911	CH_2 asymmetric stretching vibrations
2875	CH_2 symmetric stretching vibrations
1744	C=O stretching vibrations of carbonate group
1650	C=C stretching vibrations of vinyl group
1456, 1405, 1360, 1338	CH_2 deformation vibrations
1260	C-O-C asymmetric stretching vibrations of carbonate
1137	C-O-C asymmetric stretching vibrations of ether
1096	C-O-C symmetric stretching vibrations of carbonate
1026	C-O-C symmetric stretching vibrations of ether
910	C=C deformation vibrations
877	CH_2 deformation vibration of $-CH=CH_2$ group

1.9. Analyses of FTIR spectra of Lexan

The FTIR spectrum of the Lexan   a type of polycarbonate features a higher carbonyl C=O stretching frequency than simple esters   (1774 cm^{-1} IR and 1775 cm^{-1} Raman) and an aryl ester band at   1230 cm^{-1} (IR) and 1236 cm^{-1} (Raman).The other bands in the spectra of this material are assigned to the aromatic ring and the dimethyl branched substituent . These are as follows: the aromatic ring bands,   a doublet at 1602 and 1594 cm^{-1} , and a band at 1506 cm^{-1} for the IR ,   a doubles at 1605 and 1594 cm^{-1}

and a band at 1510 cm^{-1} for the Raman , 1,4-disubstituted aromatic ring bands at 1081 , 1015 , and 831 cm^{-1} for the IR and the at 1181 , 1114 , 709 , and 638 cm^{-1} for the Raman; and a weak doublet at 1386 and 1366 cm^{-1} for IR and at 1388 and 1366 cm^{-1} for the Raman . In the latter case , the intensity of the lower-frequency methyl band is slightly greater than of the high-frequency one , due to R — C $(CH_3)_2$R structure [similar to — $CH(CH_3)_2$ structure , as stated in the section on polyethylene] . High-frequency carbonyl absorptions are also observed in acid anhydrides, such as maleic anhydride-ethylene copolymers and poly-amide-imides. The polycarbonate can be differentiated from these polymers by comparison of the IR spectra , table (1.3) shows the assignment for the Raman spectra of Lexan[82] .

Table 1.3 Peak assignment for the Raman spectra of Lexan [82].

Raman frequency (cm⁻¹)	Vibration
1774	C=O Stretch
1604	Ring Stretch
1560	Ring Stretch
1468	CH def
1232	C-O Stretch
1170	CH wag (in-plane)
1118	CH wag (in-plane)
1038	C-O Stretch
1004	Ring Stretch
940	CH wag (out of plane)
918	C-CH$_3$ Stretch
880	CH wag (out of plane)
813	CH wag (out of plane)
712	Ring def (out of plane)
643	Ring def (out of plane)

1.10. Analyses of FTIR spectra of LR-115

The FTIR spectrum of the unetched LR-115   is characterized by transition   at the following wavenumbers (cm⁻¹): 2907   [C–H stretch], 1614 [–ONO$_2$–] , 1524 [N–O asymmetric stretch] , 899 [CCO– stretch], 680 [NO$_2$ deformation vibration] , 632 [–OH out of plane deformation vibration] and 520 [NO$_2$ rocking vibration] , with the corresponding functional groups/modes of vibration shown in square brackets after the wave numbers . The wave numbers corresponding to these absorptions (transmission troughs)

, and the corresponding assignment of the function groups and the modes of vibration are shown in table (1.4). The infrared transmittance at these wave numbers will be studied for different residual active-layer thickness .

Table 1.4 The wave numbers of the more significant absorption peaks (transmission troughs) in the FTIR spectrum of the unetched colorless LR-115. and the corresponding assignment of the function groups and the modes of vibration [83].

Position of the peak (cm^{-1})	Functional group/modes of vibration
2907	C–H stretch
1614	$-ONO_2-$
1524	N–O asymmetric stretch
899	CCO– stretch
680	NO_2 deformation vibration
632	–OH out of plane deformation vibration
520	NO_2 rocking vibration

1.11. Review of previous studies

Several studies have been conducted to measure the use and impact of nuclear track detectors and their use as dosimeters of ionizing radiation and non-ionizing radiation using several techniques.   Below we give a summary of some of these studies, according to the irradiation dose used and other types of radiation.

a- Gamma-ray

- N. E. IPE, et. al., (1985) [84] had determine the effect of pre-gamma irradiation on track density , bulk etch rate and light absorbance in   CR-39 were investigated. CR-39 detectors were

irradiated with gamma doses over a range of 0 to 280 kGy (0 to 28 Mrad) . The detectors were overlaid with 0.77 mm of polyethylene and exposed to a known fluence of Cf -252 spontaneous fission neutrons .

UV spectrophotometric measurements showed significant changes in light absorbance for gamma irradiated CR-39 .

- D. Sinha et. al., (1997) [85] had studied the effect of gamma radiation in Polyafiyldiglycol carbonate-PADC detectors and studied in the dose range of 10^0 - 10^6 Gy. Some of the properties like bulk-etch rate , track- etch rate, activation energy for bulk and track-etching have been found out for different gamma doses from ^{60}Co Source in PADC.

- D. Sinha et. al., (1998) [86] showed that the photon induced modifications in Triafol-TN and Triafol-BN polymers that have been studied in the dose range of 10^1-10^6 Gy at room temperature using a ^{60}Co source. To monitor the chemical and structural changes induced by gamma rays , UV , IR , and ESR studies were carried out . Thermal studies were also conducted for understanding the effects of gamma irradiations on these polymers .

- D. Sinha et. al., (2001) [87] used the polyallyl diglycol carbonate-PADC detectors that were exposed to different doses of gamma radiation ranging from 10^1 to 10^6 Gy from a ^{60}Co source . The effect of gamma doses on etch-rates were studied . Etch-rate values were found to increase at the dose of 106 Gy for all types of PADC detectors . The influence of gamma exposure on sensitivity and etching efficiency of these detectors was also determined.

- T. Yamauchi et. al., (2001) [88] measured the depth-dependent bulk etch rate that has been examined for the gamma-irradiated

CR-39 at doses ranging from 20 to 100 kGy. The thickness of the damaged region in gamma-irradiated CR-39 plastics, in which the bulk etch rate was significantly enhanced , was found to be limited in the thin layer near the surface and decreases with increasing the dose-rate , while it barely depends on the total dose. This indicates that it is possible to apply CR-39 plastics as high dose gamma-dosimeter by assessing both the bulk etch rate in the damaged region and its thickness in principle .

- M. A. Maleka et. al., (2002) [89] produced the CO_2 gas inside CR-39 plastic track detectors irradiated by both x-rays and γ -rays and found to diffuse out with time . The diffusion half-time of the gas was measured for both the irradiation cases . For x-rays , the irradiation doses ranged from 220 to 500 kGy and the half-time was found to decrease with increase in irradiation dose from 7.7 to 6.0 days. For γ –rays , the irradiation doses ranged from 130 to 950 kGy and the half-time of the gas diffusion was also found to decrease with increase in irradiation dose from 9.0 to 4.0 days .

- Ahmed K. Abdullah , (2006) [90] measured the energy gap of some glassy polymers –PC , PS and PMMA , he had studied the effect of gamma–ray and uv light radiation on the energy gap of these polymers and then the effect of dyes (anthracene) on the energy gap for these materials for exposure times (0 to 34 hr) . It's found that the energy gap of pure polymers and doped polymers measurement was changed depending on the gamma and uv dose and the mechanism of interaction between molecules of polymers and dye .It was found that the addition of anthracene to polymers leads to a reduction in the energy gap generally.

- P.C. Kalsi et. al., (2008) [91] determined the bulk-etch rates of a newly developed track detector called poly-[N-allyloxycarbonyl

diethanolamine-bis allylcarbonate] (PNADAC) homopolymer at different temperatures to deduce its activation energy. The effects of gamma irradiation on this new detector in the dose range of 4.7–14.5 Mrad have also been studied using uv–visible spectroscopic technique. The optical band gaps of the unirradiated and the gamma-irradiated detectors determined from the uv–visible spectra were found to decrease with the increase in gamma dose.

- Jyotsna A. Sapkal et. al., (2009) [92] obtained the effects of gamma irradiation in the dose range of $1.0 - 20.0$ Mrad on the etching and optical characteristics of Tuffak polycarbonate $(C_{16}H_{14}O_3)_n$ nuclear track detector that have been studied by using etching and uv–visible spectroscopic techniques. The result showed that bulk etch rates increase and the activation energies for bulk etching decrease with the increase in gamma dose. The optical band gaps determined from the uv–visible spectra were found to decrease with the increase in gamma dose. These results have been explained on the basis of scission of the detector due to gamma irradiation.

- Kh. M. Abdel Raouf , (2013) [93] studied the CR-39 irradiated with γ-rays , x-rays and alpha particles by FTIR spectroscopy . He made a comparison between the effect of many types of radiation on the sensitivity of CR-39 detector by using the FTIR spectrometer. It was found that, investigated CR-39 is so sensitive for all types of radiation used that was used as a dosimeter for these types of radiation. In this work the optical density of the detector was calculated and then it is used to determine α-range.

b- UV-radiation

- R. Shweikani et. al., (2002) [94] showed the effects of solar ultraviolet (SUV) and ultraviolet type A (UVA) produced by a solar uv simulator on CR-39 detectors that were studied . This was done using three techniques: 1—Alpha tracks diameters and tracks densities , 2—UV–Vis spectrometry and 3—FTIR spectrometry. The results showed that the e1ect of UVA on CR-39 was not clear using the three techniques. While, the e1ect of SUV was clear when using uv–visible and FTIR spectrometric, and not clear when using track parameters.

- K.C.C. Tse et. al., (2006) [95] studied the effects of ultraviolet –UV photons at different wavelengths (namely UVA , UVA + B and UVC) on PADC (polyallyl diglycol carbonate) were investigated in this study . The chemical modifications were studied by Fourier Transform Infrared (FTIR) spectrometry and the corresponding nano-mechanical properties were also determined. The scission process could be revealed by the decreasing net absorbance at particular wavelengths in the infrared (IR) spectra. It was also observed that a UVC exposure caused a comparatively higher bulk etch rate at the beginning of etching. However, the bulk etch rate decreased with the depth of the PADC sample due to the lower rate of oxygen diffusion into deeper regions .

- Tse Chun Chun , (2007) [81] discussed the effects of uv exposure on solid-state nuclear track detectors-SSNTDs . The study confirms that uv exposures can drastically change

the bulk etch rate (V_b) and track etch rate (V_t) of CR-39 detectors at short uv wavelength . In this study, the changes in the chemical, physical and mechanical properties of CR-39 detectors under UV irradiation were studied together with the corresponding photo-degradation mechanisms in order to explain the variation of the etching behavior of CR-39 detectors in NaOH/H_2O .

- Chhavi Agarwal et. al., (2010) [96] determined the effects of uv irradiation (λ =254 nm) on polyester nuclear track detector that have been investigated employing bulk-etch technique, uv– visible spectrophotometry and infra-red spectrometry (FTIR) . The activation energy values for bulk etching were found to decrease with the uv-irradiation time indicating thesciss ion of the polymer. Not much shift in the absorption edge due to uv irradiation was seen in the uv–visible spectra. FTIR studies also indicate the scission of the chemical bonds, thereby further validating the bulk-etch rate results.

- Rana H. Mahmmod , (2012) [97] performed a study of the effect of ultraviolet radiation (244 nm) on the physical properties of the solid state nuclear track detector CN-85 has (100μm) thickness . Samples were radiated by ultraviolet radiation for (1, 3 ,7, 9 ,11) hr. The results show the effects of the radiation on the samples. The real dielectric constant €1 change from 7.9 at 1hr. radiated to 10.1 at 11hr radiated . The extinction coefficient K_0 changed from 2.25×10^{-4} at 1hr. radiated to 9.0×10^{-5} at 11hr radiated. It has been found that the values of energy gaps decreasing from 2.0eV at 1hr radiated to 1.22eV at 11hr radiation. The amount of

energy gap decreased with increasing UV dose. The results show the amount of maximum absorption between 308 nm to 312 nm.

- Firas M. Al-Jomaily et. al., (2012) [98] studied the ultraviolet radiation dosimetry that was determined by using CN-85 , CR-39 ,LR-115 nuclear track detectors – NTD with measuring of ; number of track-N_T , etching time-T_B , nuclear track diameter - D_T and etching velocity -V_D . By this study appear the increasing in etching time-T_B of NTD samples which irradiated by uv-radiation do not show pure effect on the number of track - N_T , comparing with un-irradiated samples . The increasing in uv-irradiation make decreasing in etching time- T_{opt} for CR-39 , CN-85 , LR-115 nuclear track detectors with percent of 20% , 25% , 50% respectively , comparing with un– irradiated sample at the radiation dose 3.77×10^3 erg /mm^2 . The increasing of irradiation dose makes increasing in nuclear track diameter-D_T with increase in etching time-T_B at the radiation dose 300×10^3 erg / mm^2 for LR-115 detector . This study showed that there was increasing in the percent value of etching velocity -V_B with increasing in radiation dose for CR-39 , CN-85 . The increasing in nuclear track diameter- D_T with increasing in radiation dose was appearing as a result of energy of radiation and produced free radicals which interact with chemical etching solution .This study was optioned by using nuclear track detectors CN-85 , CR-39 for determination the radiation dosimetry through measuring of etching velocity -V_B butter than LR-115 detector .

- K. Hareesh, et. al., (2013) [99] study used Lexan polycarbonate films that were irradiated by uv radiation at wavelength $\lambda = 250$ nm under different time exposures of 1, 2, 4, 6 and 7 hr Structural, optical and mechanical modifications were studied by X-ray diffraction-XRD , Fourier transform infrared spectroscopy –FTIR , scanning electron microscopy-SEM , differential scanning calorimetry-DSC , uv–visible spectroscopy , impedance analysis , tensile testing and rheometry methods . The glass transition temperature was observed to decrease after irradiation as revealed by DSC measurement . uv–visible spectra showed decrease in optical band gap after irradiation due to chain scission in the Lexan polycarbonate.

- K. Hareesh et. al., (2012) [66] studied the changes in the microstructural parameters of Lexan polycarbonate films irradiated with uv radiation at a wavelength of $\lambda = 250$ nm were investigated using wide-angle x-ray scattering measurements. uv–visible spectroscopy study revealed the formation of photo-stabilizers after irradiation. In the photoluminescence spectrum, the intensities of the peaks at 426 nm in the emission spectra and at 375 nm in the excitation spectra were observed to decrease with an increase in the exposure time. Raman spectra exhibit only minor shifts in some of the bands after the films were irradiated . Infrared spectroscopic study revealed that the carbonate linkage was the radiation-sensitive linkage and that the benzene ring does not undergo any changes after being irradiated.

c- Other types of irradiation

- C.S. CHONG et al., 1997 [100] made a study on the uv-visible and FTIR spectra of CR-39 plastics irradiated with 50 kVp tube x-rays in the dose range 0 to 45 MR. The optical transmittance over the wavelength region of 200-1000rim decreases with the   x-ray exposure , much greater decrease being observed in the   uv region . The IR absorption spectra of the irradiated samples show the presence of two new strong absorption bands at the frequencies 655 and 2340 cm $^{-1}$, indicative of the gas CO_2: produced inside the plastic. The absorbance of these bands increases linearly with the x-ray dose .

- D. Nikezic et. al., (2002) [101] obtained the three-dimensional and analytical theory for track growth in solid state nuclear track detector that was incorporated in a computer program for calculating track parameters and for plotting track-wall profiles and contours of the track opening in the LR115 detector irradiated by alpha particles.

- F.M.F. Ng, K.N. Yu , (2006) [76] studied the energy-dispersive x-ray fluorescence –EDXRF spectrometry previously proposed to measure the thickness of the cellulose nitrate layer of the commonly used LR-115 solid-state nuclear track detector -SSNTD. Their work is devoted to the investigation whether the x-ray radiation involved in EDXRF spectrometry will induce degradation of the cellulose nitrate . For this purpose , Fourier transform   infrared –FTIR spectroscopy was employed to examine the nitrate functions (at the wavenumber 1598 cm^{-1}) and the glycosidic bonds (at 1146 cm^{-1}) for various

irradiation time involved in the EDXRF spectrometry. No significant changes were observed even for x-ray irradiation up to 3000 live seconds, which was equivalent for 10 separate scans and should be far more than enough for a determination of the cellulose nitrate layer thickness. Therefore , EDXRF remains a fast and non-destructive method to measure the active layer thickness of the cellulose nitrate SSNTD.

- Amer H. Ali , (2009) [102] showed has work , the effect of 514nm argon laser radiation on the alpha particles tracks diameters, tracks growth velocity and the tracks appearing time in LR-115 nuclear track detector has been studied. Increasing the exposure time of laser radiation were found to improve the above mentioned parameters up to7min of exposure time, then it was decrease gradually with exposure time and become near data of standard sample of detector at 15 min.

- Sallama .S. Hummadi, (2010) [103]   measured the uranium concentration in male and female children's teeth samples collected from different countries. The obtained results show that the concentration is ranging from (0.3204±0.06 ppm) in Oman for female to (0.1965±0.04 ppm) in UAE for male, the uranium concentration was the highest in Oman for female.

- Hussain Ali Al-Jobouri et. al., (2012) [104] showed the effect of   x-ray radiation that has been studied by measurement of the permittivity $-\mathcal{E}p$ and transmission ratio _T% on CR-39 sheets a nuclear solid state track detector by microwave and Fourier Transformer Infrared FTIR spectroscopy techniques respectively. The permittivity $-\mathcal{E}p$ increases with dose increase of x-ray radiation from 2 - 6.032 mGy. In addition , obtained there was dropping in the permittivity-$\mathcal{E}p$ from the value 600

CV^{-1} m^{-1} at the radiation dose 6.032 mGy to the value 47 $CV^{-1}m^{-1}$. And there was reciprocal point at 10.5 mGy, then still εp value constant at this value with increasing of radiation dose until to 18 mGy. The absolute difference -DT of the transmission ratio -T% , which is measured by FTIR spectroscopy between irradiated-TR and unirradiated-T_0 [DR = |T_R - T_0|] of CR-39 sheets, has been decreased at the wave number 2250 cm^{-1} and 2450 cm^{-1} to a reciprocal point of 14. 0 mGy and then increased to 18.0 mGy. This study suggests the use of CR-39 sheets as dosimeter for x-ray radiation by measuring the permittivity –εp and the transmission ratio -T% .

1.12. The aim of study

The main purpose of the present work is to find the radiological response to gamma rays and uv-radiation by using different types of NTDs CR-39 , Lexan and LR-115 by analytical optically by uv-visible and FTIR-spectroscopy . Also, we make an attempt to show the reliability of the detectors use as radiation dosimeters according to mathematical relationships derived.

Chapter Two

Materials and Methods

Chapter Two
Materials and Methods

2.1. Materials

This chapter describes the use of three types for solid state nuclear track detectors-SSNTDs CR-39 , Lexan and LR-115, used in this study   The specifications of these detectors is described in the following items

2.1.1. CR-39 Track Detector

CR-39 is type of organic solid state nuclear track detector in the form of sheets with thickness 1200 μm , obtained from TASTRAK (Pershore Moulding ,Track Analysis System Ltd., UK) .Its composition is $C_{12}H_{18}O_7$, molecular weight 274 a.m.u., density 1.32 g/cm^3 . These sheets were cut into small pieces each with (2 cm $\times$2 cm).

2.1.2. Lexan Track Detector

Lexan is a type of organic solid state nuclear track detectors. Its composition is $C_{16}H_{14}O_3$, in the form of sheets of thickness 175 μm , obtained from company Co. Chan Zhou Weldin. These sheets were cut into small pieces each with (2 cm $\times$2 cm).

2.1.3. LR-115 Track Detector

Cellulose nitrate-CN is a type organic solid state nuclear track detectors-SSNTDs (commercially known as LR-115 , with composition $C_6H_9O_9N_2$), The CN SSNTDs which are used in the present study were purchased from DOSIRAD, France (LR-115 film, Type 2, strippable). The SSNTDs consist of a red layer of CN on a 100 μm clear polyester base substrate. For the purpose of our

experiments, only the CN layer is required, so this SSNTD will hereafter referred to my CN layer stripped from the polyester base. These sheets were cut into small pieces each with (2 cm ×2 cm).

2.2. Sources of irradiation

In this study we have used two types of sources of radiation ionizing radiation (Gamma-ray) and ultraviolet radiation for the irradiation of samples as follows:

2.2.1. Gamma Irradiation
a- Low doses of gamma irradiation

The irradiation of low doses in this study was carried out by the source of gamma rays in the hospital radiation nuclear medicine in Iraq from obtained CIS BIO INTERNATIONAL (French) as shown in fig.(2.1), at the beginning of 1998 and reached a number of long-lived radioactive sources for use in the treatment has reached the source of Cobalt-60 the value of dose rate of Cobalt-60 was 0.45 Gy/min.
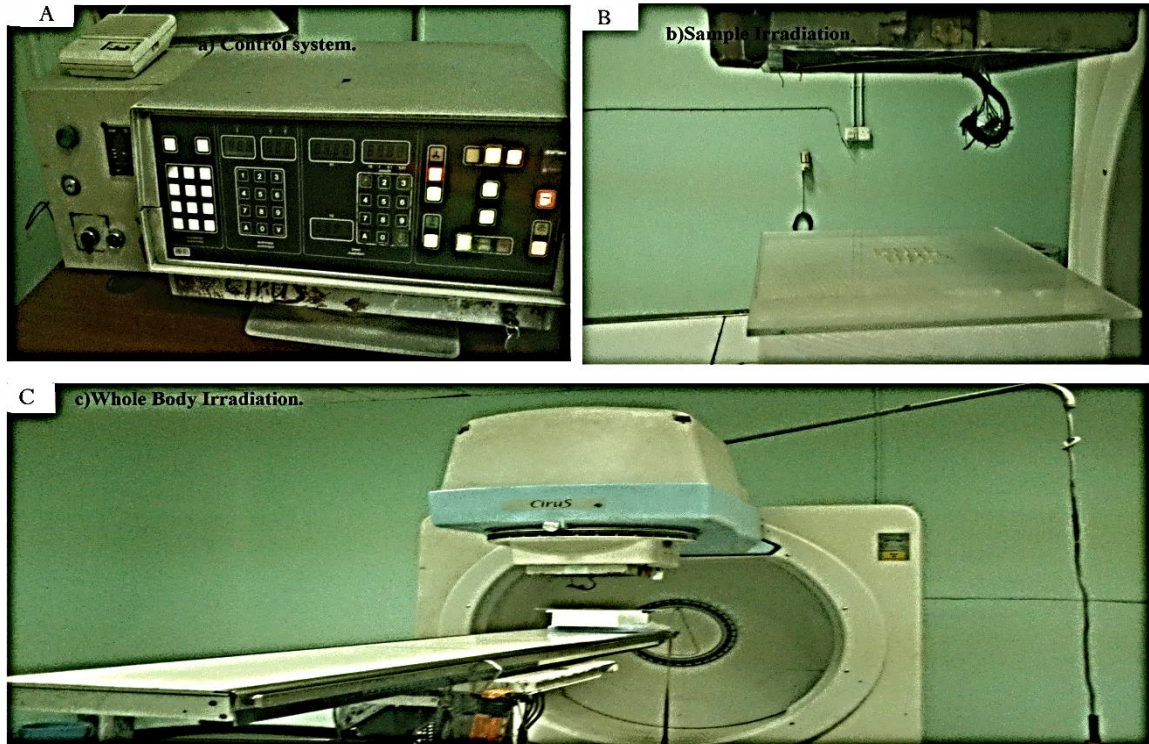
Figure 2.1 CIS BIO INTERNATIONAL system of gamma-ray source Co-60 . There in the hospital radiation nuclear medicine in ministry of health of Iraq
A- Control system **B-** Irradiation sample   **C-** Whole body irradiation

b- High doses of gamma irradiation

The irradiation with high doses in this study was irradiated in air with energetic gamma- rays, using Co-60 source (Gamma cell 900) of strength rate 4.5Ci, which emits mono-energic 1.17 and 1.33MeV gamma-rays, and has a half-life of 5.3years , manufactured by the Bhabha Atomic Research Center-BHA /Trombay / Bombay /India and shown in figure (2.2) . The dose rate of this source was   254.48 Gy / h (or 4.23 Gy/min) in (1-1-2014). This gamma cell 900 is located in the department of physics, college of science, university of Baghdad.

1	Stirrer motor
2	Central drawer
3	Sample chamber
4	External cabinet
5	Removable Cover
6	Lead Flask (Biological Shield)
7	Source cage
8	Mechanical driving system
9	Wire Rope
10	Platform
11	Concrete Pit
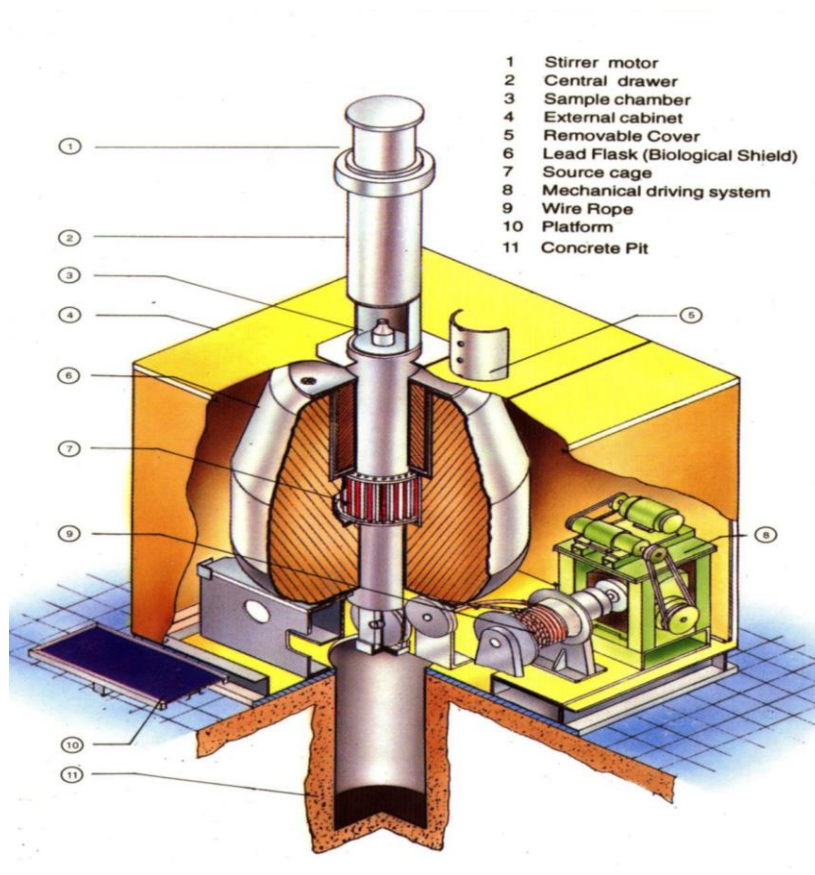
Figure 2.2 Gamma cell 900 system model by Bhabha Atomic Research Center-BHA
/ Trombay / Bombay /India , this system is located in the department of physics, college of science, university of Baghdad

2.2.2. Ultraviolet irradiation

Fig.(2.3) shows the uv-irradiation system used in this study. This system is located in the department of bio-technology in the college of science _ Al-Nahrain university, its model is FLUO-LINK FLX ,which irradiates with different doses of uv- radiation . The distance between the source and the samples was 4 cm with a wavelength 254 nm and   amount of energy 15W .

Figure 2.3 Vilber Lourmat FLX-20M Transilluminator 312/254 nm UV-irradiation
system   model and the amount of power 15W, the uv-radiation range
was 1 J/cm^2 to 360 J/cm^2, this system is located in the department of
bio-technology in the college of science / Al-Nahrain university

2.3. Materials Analysis

2.3.1. UV-visible (UV-VIS) spectroscopy

Ultraviolet–visible spectroscopy (UV-Vis or UV/Vis) refers to
absorption spectroscopy or reflectance spectroscopy in the
ultraviolet-visible spectral region. This means it uses light in the
visible and adjacent (near-UV and near-infrared -NIR) ranges. The
absorption or reflectance in the visible range directly affects the
perceived color of the chemicals involved.

In this region of the electromagnetic spectrum, molecules
undergo electronic transitions. This technique is complementary to
fluorescence spectroscopy, in that fluorescence deals with
transitions from the excited state to the ground state, while
absorption measures transitions from the ground state to the excited
state [105].

The system is located in the department of physics the college of science - Al-Nahrain university and shown in fig. (2.4) . The wavelength range used in this study was 200-800nm .All the samples of NTDs CR-39 , Lexan and LR-115 measured in uv-visible spectroscopy were adjusted directly in sample unit in the space of Cavite cell.

Figure 2.4 UV-visible Spectroscopy system , model UV-1601PC from SHIMADZU Company
the system is located in the department of physics the college of science / Al-Nahrain university

2.3.2. FTIR-Spectroscopy

Fourier transform infrared spectroscopy-FTIR [106] is a technique which is used to obtain an infrared spectrum of transmission , emission, photoconductivity or Raman scattering of

a solid, liquid or gas. An FTIR spectrometer simultaneously collects spectral data in a wide spectral range.

This confers a significant advantage over a dispersive spectrometer which measures intensity over a narrow range of wavelengths at a time. FTIR spectroscopy used in this study was FTIR-8300 model from SHIMADZU company. The system was located in the department of chemistry in the college of science / Al-Nahrain University as shown in fig. (2.5). The wavenumber range used in this study was 400-4000 cm^{-1} .

All the samples of NTDs CR-39 , Lexan and LR-115 measured in FTIR-Spectroscopy were adjusted directly in sample unit in the space of cavite cell.
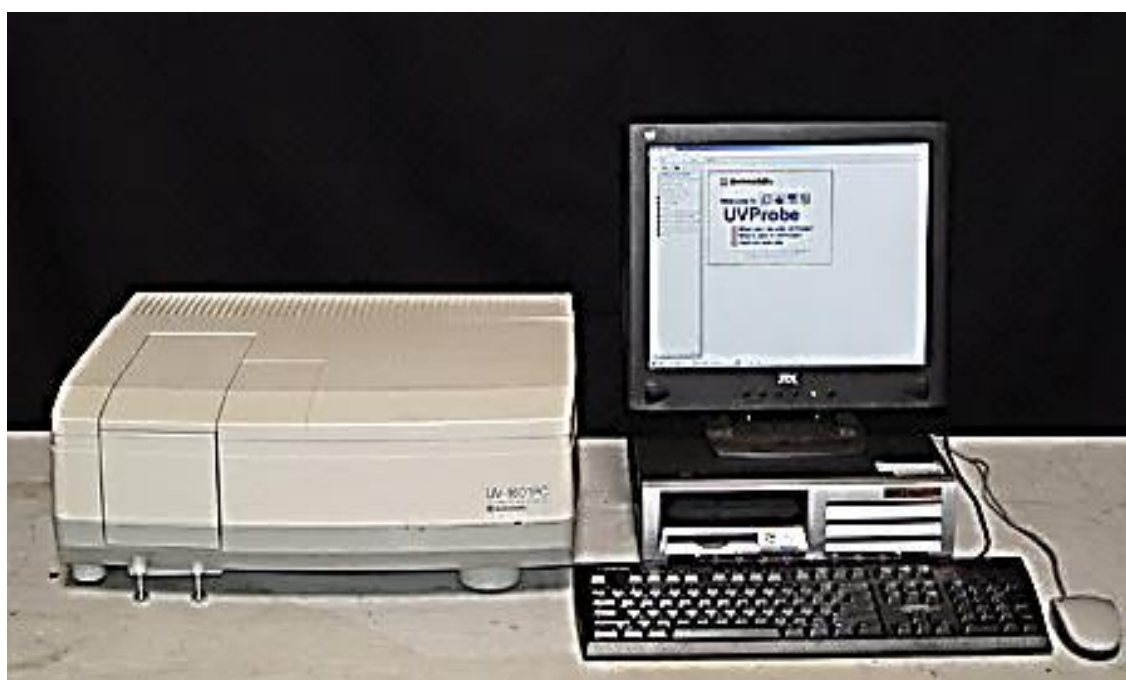

Figure 2.5 Fourier transform infrared spectroscopy-FTIR system, model FTIR-8300 from SHIMADZU Company the system located in department of chemistry in the college of science - Al-Nahrain University

2.4. Methods

2.4.1. Samples irradiation

2.4.1.1. Gamma-ray irradiation

a- The conditions of low doses of gamma irradiation were :

- The distance between source of Co-60 and samples was 6cm.

- The dose rate of the source of Co-60 was 0.45 Gy/min.
- The range of gamma irradiation was (1-10Gy).
- All the irradiation of low doses were in air at room temperature.

b- The conditions of high doses of gamma irradiation were :

- Co-60 source and samples were irradiated by gamma cell 900.
- The dose rate of the source of Co- 60 was 254.48 Gy / h in (1-1-2014). The range of gamma irradiation was 10 Gy to 195 kGy .
- All the irradiation of high doses were in air at room temperature.

2.4.1.2. Ultraviolet-UV irradiation

- The distance between source of uv-irradiation and samples was 4cm.
- The uv-irradiation source has wave length 254 nm and power 15W.
- The range of uv- irradiation with different doses (1, 5 ,30 , 60, 120 , 240 , 360 J/cm²).
- All the irradiation of doses were in air at room temperature.

Chapter Three

Results and Discussion

Chapter Three

Results and Discussion

3.1. Effect of Gamma-ray and UV-irradiation on NTDs Using UV-visible Spectroscopy Technique

In this study we used uv-visible spectroscopy technique to measure the effect of gamma-ray and uv irradiation.

3.1.1. Effect of gamma irradiation on NTDs using uv-visible spectroscopy technique

3.1.1.1. NTD type CR-39

When using gamma irradiation of CR-39 detector at low doses range (1-10 Gy) by source of low doses, no radiation response appeared at this range through the measurements of absorbance-A from wavelengths 200 nm to 800 nm.

Figure (3.1) show the change that appears in absorbance-A measured by uv-visible technique at the range 300 - 400 nm to the samples of nuclear track detector type CR-39 irradiated by gamma-ray with the dose range from 10 Gy to 195 kGy compared with unirradiated sample . This figure shows that there is an increase in absorbance-A with the increase of radiation dose-D (Gy). The change in absorbance-A with irradiation doses appears at the wavelengths 300 and 304 nm as shown in figures (3.2) and figure (3.3) .

Figure 3.1 Absorbance-A measured by uv-visible spectroscopy
technique with wavelength range 300 – 400 nm for
unirradiated and gamma-irradiated samples at dose range
from 10 to 195 kGy for CR-39 detector

Figure (3.2) and figure (3.3) shows the polynomial relationship between the absorbance-A and gamma irradiation dose-D at wavelengths 300 and 304 nm , and this is given by equation (3.1) and equation (3.2) respectively . These equations reflect that the radiation response appears by gamma irradiation dose-D (Gy) with absorbance-A measured by uv-visible spectroscopy technique , and given by following equations

$$D\ (Gy)\ =\ 2 \times 10^4 A^2\ -\ 3 \times 10^3 A\ -\ 9 \times 10^3 \tag{3.1}$$

If A $\geq$ 75×10

$$D\ (Gy)\ =\ 3 \times 10^4 A^2\ -\ 9 \times 10^3 A\ -\ 5 \times 10^3 \tag{3.2}$$

If A $\geq$ 0.58

where D (Gy): gamma irradiation dose , A: absorbance

The maximum response of gamma radiation 195 kGy at wavelength 304 nm corresponds to absorbance-A value 2.6 as shown in figure (3.3) .
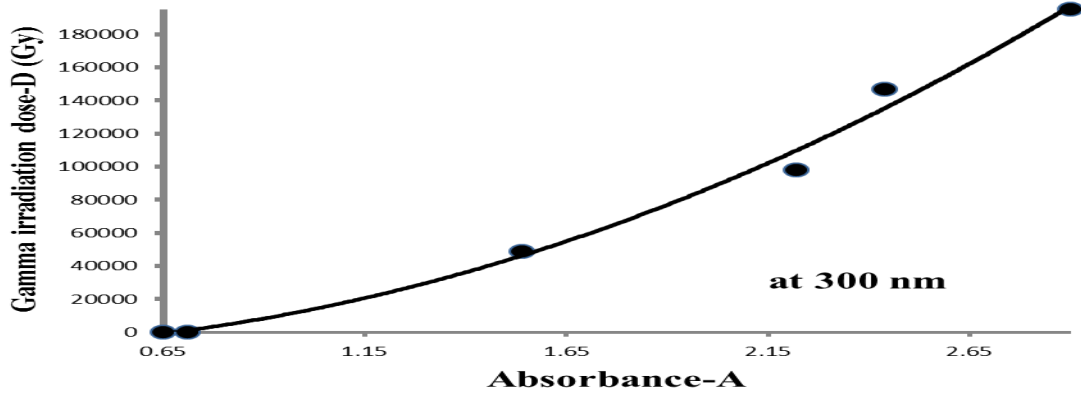
Figure 3.2 Absorbance-A vs. gamma irradiation dose-D (Gy) for CR-39 detector at wavelength 300 nm
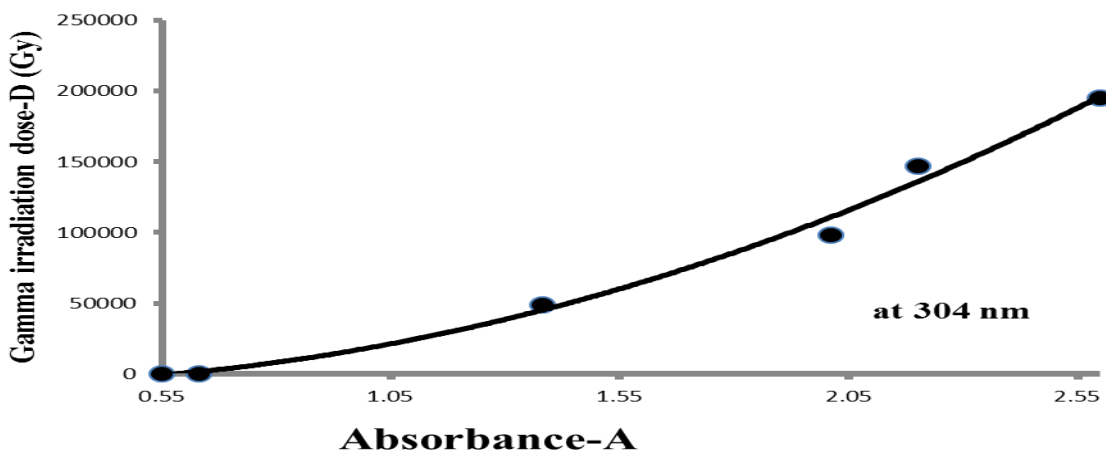
Figure 3.3 Absorbance-A vs. gamma irradiation dose-D (Gy) for CR-39 detector at wavelength 304 nm

3.1.1. 2. NTD type Lexan

Figure (3.4) show the change that appears in absorbance-A measured by uv-visible technique at range 400 - 800 nm to the samples of nuclear track detector type Lexan irradiated by gamma-ray at the range from 2 Gy to 10 Gy compared with unirradiated sample . This figure shows that there is uv-radiation response by

increase of   absorbance-A with   increase of radiation dose- D (Gy). And this response appears at the wavelengths 400 , 500 , 600 ,700 and 800 nm as shown in the following figures (3.5) , (3.6) , (3.7) , (3.8) and (3.9) respectively .
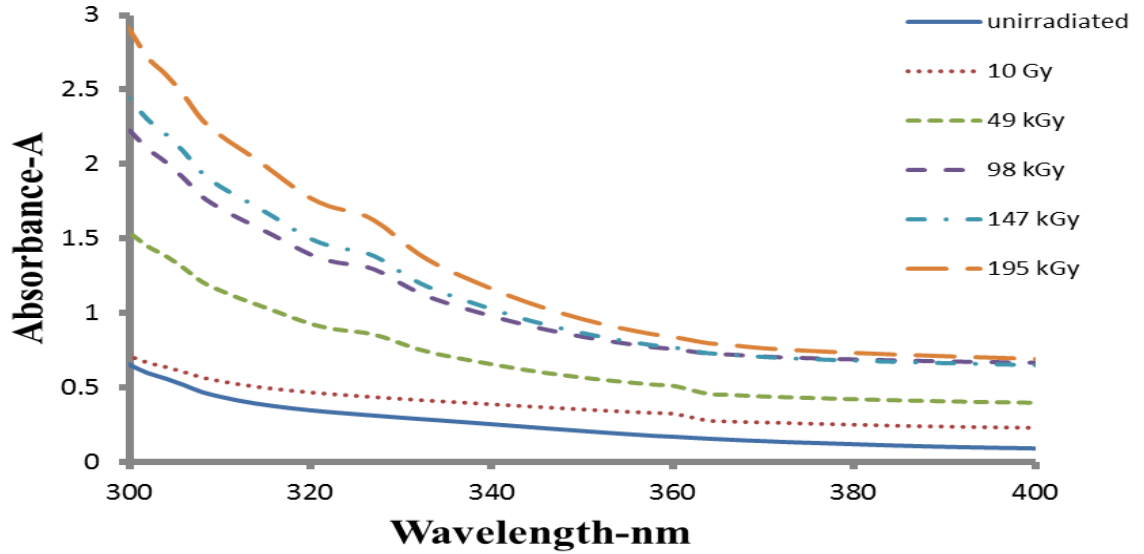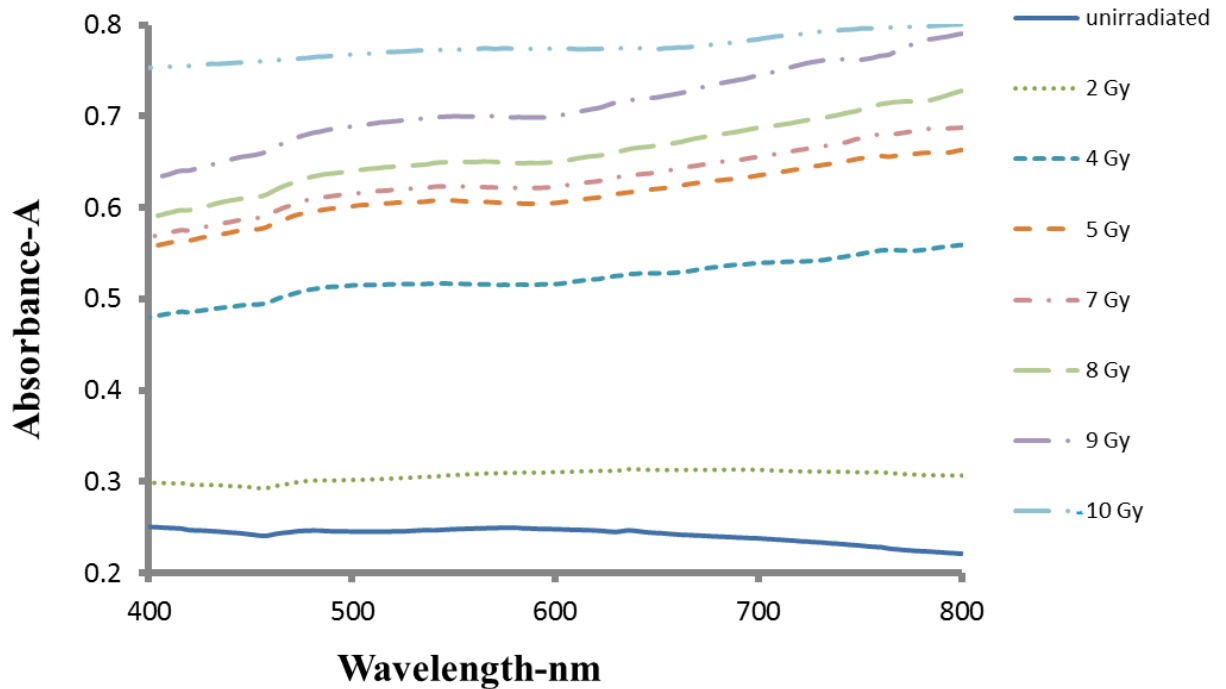

Figure 3.4 Absorbance-A measured by uv-visible spectroscopy technique with wavelength range   400 – 800 nm   for   unirradiated   and gamma - irradiated samples at dose range from 2 to 10 Gy for Lexan detector

Figures (3.5) , (3.6) , (3.7) , (3.8) and (3.9) shows the polynomial relationship between the absorbance-A and gamma irradiation dose-D at wavelengths 400 500 ,600 ,700 and 800 nm respectively. Equations (3.3) , (3.4) , (3.5) , (3.6) and (3.7) are obtained from the polynomial relationship of figures (3.5) , (3.6) , (3.7) , (3.8) and (3.9) respectively . The radiation response of gamma irradiation dose-(Gy) with absorbance-A measured by uv-visible spectroscopy technique , is given by the following equations

$$D(Gy) = A^2 + 19A - 4 \qquad\qquad (3.3)$$

$$\text{If } A \geq 0.2$$

$$D(Gy) = 18A^2 + A - 1 \qquad\qquad (3.4)$$

$$\text{If } A \geq 0.2$$

$$D(Gy) = 16A^2 + 2A - 1 \qquad\qquad (3.5)$$

$$\text{If } A \geq 0.36$$

$$D(Gy) = 21A^2 - 4A + 0.4 \qquad\qquad (3.6)$$

$$D(Gy) = 21A^2 - 6A + 1 \qquad\qquad (3.7)$$

where D (Gy): gamma irradiation dose , A: absorbance

The maximum response of gamma radiation 10 Gy at wavelength   800 nm corresponds absorbance-A value at 0.8 as shown in figure (3.7).

Figure 3.5 Absorbance-A vs. gamma irradiation dose-D (Gy) for Lexan

detector at wavelength 400 nm

Figure 3.6 Absorbance-A vs. gamma irradiation dose-D (Gy) for Lexan detector at wavelength 500 nm

Figure 3.7 Absorbance-A vs. gamma irradiation dose-D (Gy) for Lexan detector at wavelength 600 nm

Figure 3.8 Absorbance-A vs. gamma irradiation dose-D (Gy) for Lexan detector   at wavelength 700 nm

Figure 3.9 Absorbance-A vs. gamma irradiation dose-D (Gy) for Lexan detector at wavelength 800 nm

3.1.1.3. NTD type LR-115

Figure (3.10) shows the change that appears in absorbance-A measured by uv-visible technique at the range 700-720 nm to the samples of nuclear track detector type LR-115 irradiated by gamma-ray at the range from 1Gy to 10 Gy compared with un-irradiated sample .

The figure shows the increase in absorbance-A with the increase of radiation dose. And the increase in absorbance-A with irradiation dose-D (Gy) appears at the wavelengths 700 and 710 nm as shown in figure (3.11) and figure (3.12) respectively.
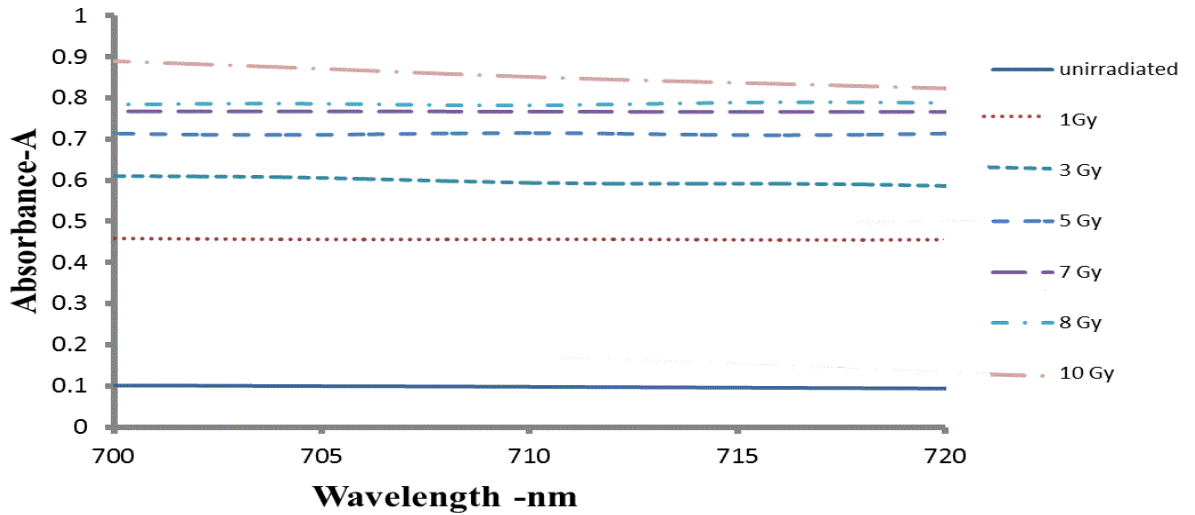
Figure 3.10 Absorbance-A measured by uv-visible spectroscopy technique with wavelength range 700 – 720 nm for un-irradiated and gamma-irradiated samples at dose range from 1 to 10Gy for LR-115 detector

Figure (3.11) and figure (3.12) shown the polynomial relationship between the absorbance-A and gamma irradiation dose-D (Gy) at wavelengths 700 and 710 nm respectively. Equations (3.8) and (3.9) are obtained from the polynomial relationship of figures (3.11) and (3.12) respectively . The radiation response of gamma irradiation dose-D (Gy) with absorbance-A measured by uv-visible spectroscopy technique appears as given by the following equations

$$D(Gy) = 25A^2 - 11.4A + 0.9 \tag{3.8}$$

$$D(Gy) = 27.6A^2 - 13A + 1 \tag{3.9}$$

where D (Gy): gamma irradiation dose , A: absorbance

The maximum response of gamma radiation 10 Gy at wavelength 710 nm corresponds to absorbance-A value at 0.85 as shown in figure (3.9).
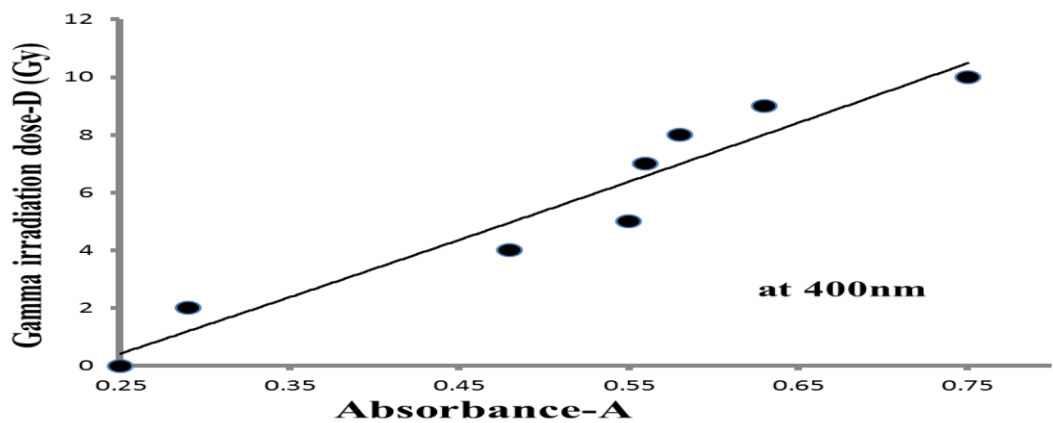
Figure 3.11   Absorbance-A vs. gamma irradiation dose-D (Gy) for LR-115
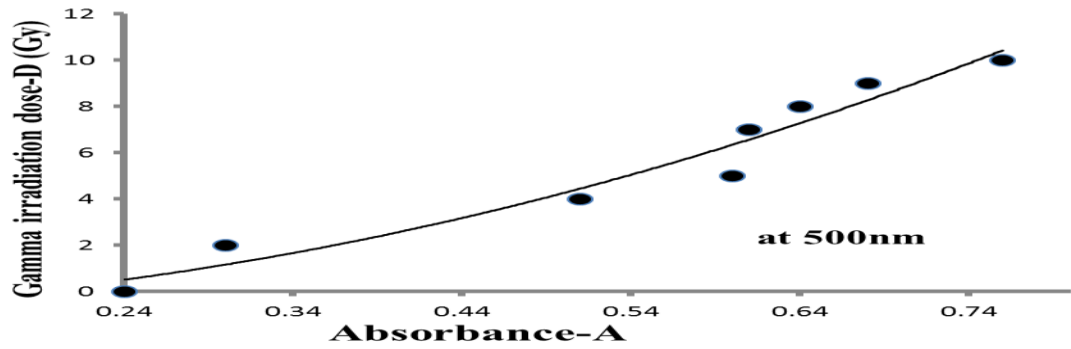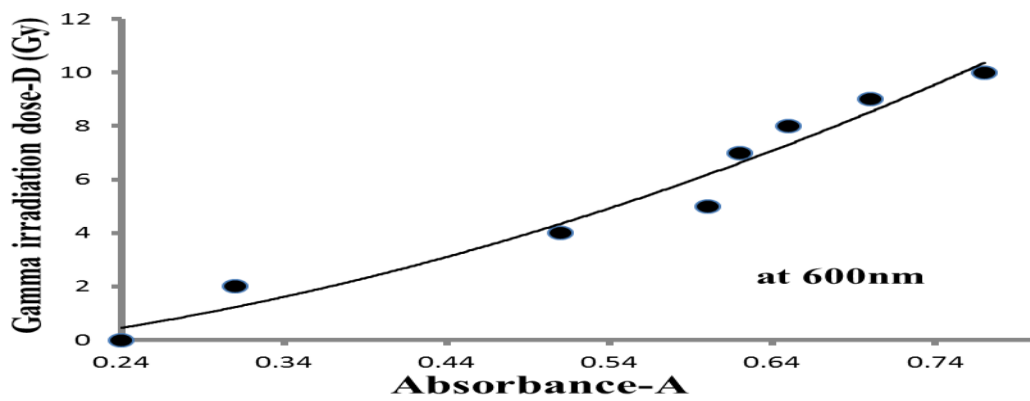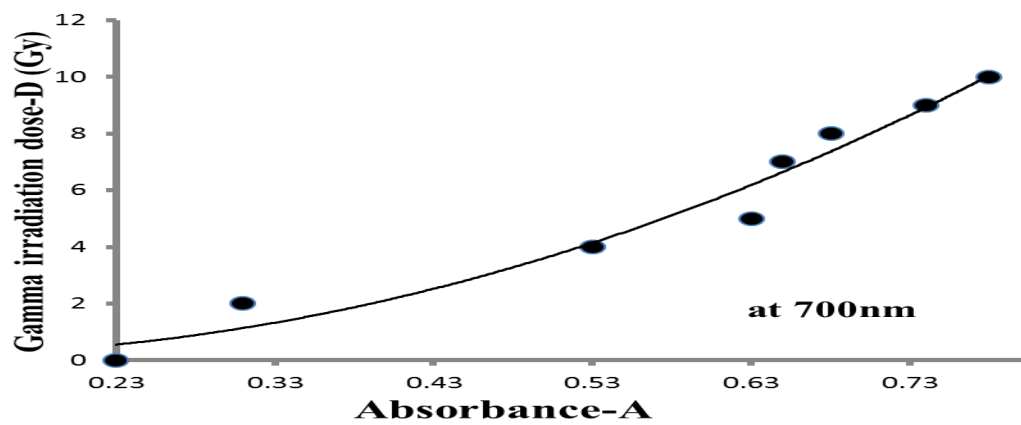detector   at wavelength 700 nm
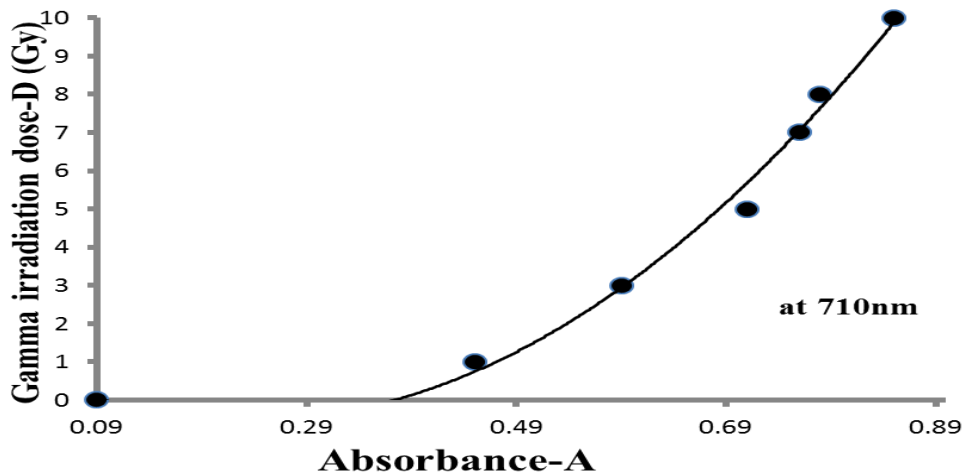
Figure 3.12   Absorbance-A vs. gamma irradiation dose-D (Gy) for LR-115
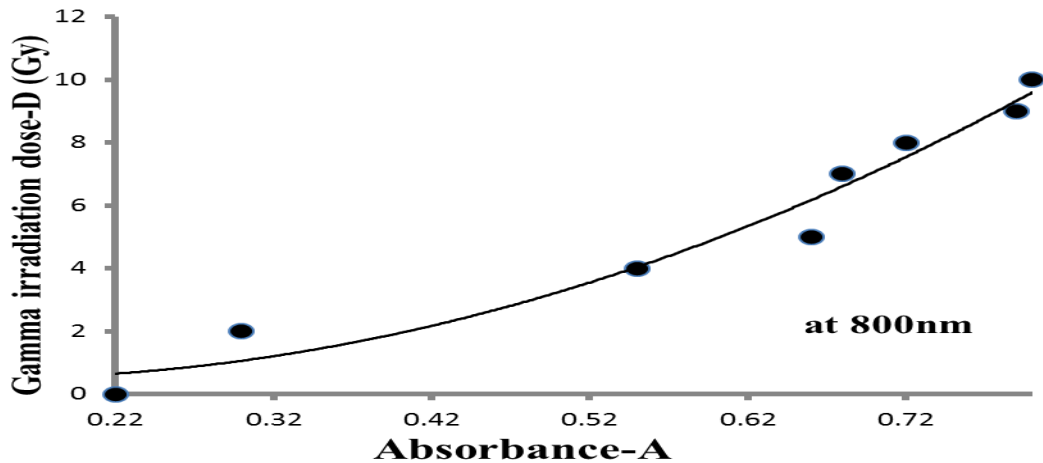detector at wavelength 710 nm

Table (3.1) show the equations which obtained   from the
relationships between gamma irradiation dose with absorbance-A
measured by uv-visible spectroscopy technique for the NTDs types
CR-39 , Lexan and LR-115 .

Table 3.1 Gamma irradiation dose-Gy vs. absorbance-A obtained equations for NTDs types CR-39 , Lexan and LR-115 at different wavelengths using uv-visible spectroscopy technique

Type of NTDs	Equations	Equation no.	Wavelength (nm)
CR-39	$D\ (Gy)\ =\ 2 \times 10^4 A^2\ -\ 3 \times 10^3 A\ -\ 9 \times 10^3$	3.1	300
	$D\ (Gy)\ =\ 3 \times 10^4 A^2\ -\ 9 \times 10^3 A\ -\ 5 \times 10^3$ At high dose gamma irradiation	3.2	304
Lexan	$D(Gy) =\ A^2\ +\ 19\ A\ -\ 4$	3.3	400
	$D(Gy) =\ 18\ A^2\ +\ A\ -\ 1$	3.4	500
	$D(Gy) =\ 16\ A^2\ +\ 2\ A\ -\ 1$	3.5	600
	$D(Gy) =\ 21\ A^2\ -\ 4\ A\ +\ 0.4$	3.6	700
	$D(Gy) =\ 21\ A^2\ -\ 6\ A\ +\ 1$	3.7	800
LR-115	$D(Gy) =\ 25\ A^2\ -\ 11.4\ A\ +\ 1$	3.8	700
	$D(Gy) =\ 27.6\ A^2\ -\ 13\ A\ +\ 1$	3.9	710

That means may use the change in absorbance-A value with uv-visible spectroscopy technique to determine the gamma radiation dose (Gy) absorbed by NTDs   CR-39 , Lexan and LR-115 . The polynomial relationships between gamma radiation dose-Gy and absorbance-A in table (3.1) for NTDs types Lexan was better than the radiation response which appear in CR-39 and LR-115 as shown in figure (3.8) and   figure (3.9) respectively . And these figure reflect this response for gamma-ray at wave length 700 , 800 nm respectively.

3.1.2. Effect of UV-irradiation on NTDs using uv-Visible spectroscopy technique

3.1.2.1. NTD type CR-39

Figure (3.13) shows the increase in absorbance-A measured by uv-visible technique at the range 300 - 330 nm to the samples of nuclear track detector type CR-39 with increase in irradiation dose of uv-radiation at range (10 , 60 , 120 , 240 , 360 J/cm²) compared with un-irradiated sample . The increase in absorbance-A with irradiation dose appear at the wavelength 300 and 304 nm as shown in figures (3.14) and figure (3.15) respectively.

Figure 3.13 Absorbance-A by uv-visible spectroscopy technique with
wavelength range (300 – 330 nm) for un-irradiated and uv-
irradiated samples at dose range (10 , 60 ,120 , 240 , 360 J/cm²)
for CR-39 detector

Figure (3.14) and figure (3.15) shown the polynomial relationship between the absorbance-A and uv-irradiation dose at 300 and 304nm respectively. Equation (3.10) and equation (3.11) are obtained from the polynomial relationship of figure (3.14) and figure (3.15) respectively . The radiation response of uv-irradiation

dose (J/cm²) with absorbance-A measured by uv-visible spectroscopy technique is given by the following equations

$$D\ (J/cm^2) = 2 \times 10^4 A^2 - 4 \times 10^4 A + 1 \times 10^4 \qquad (3.10)$$

$$D(J/cm^2) = 2 \times 10^4 A^2 - 3 \times 10^4 A + 1 \times 10^4 \qquad (3.11)$$

where D(J/cm²): uv- irradiation dose , A: absorbance

The maximum response of uv-radiation dose 360 J/cm² at wavelengths 304 nm corresponds at absorbance-A value 0.83 as shown in figure (3.14).
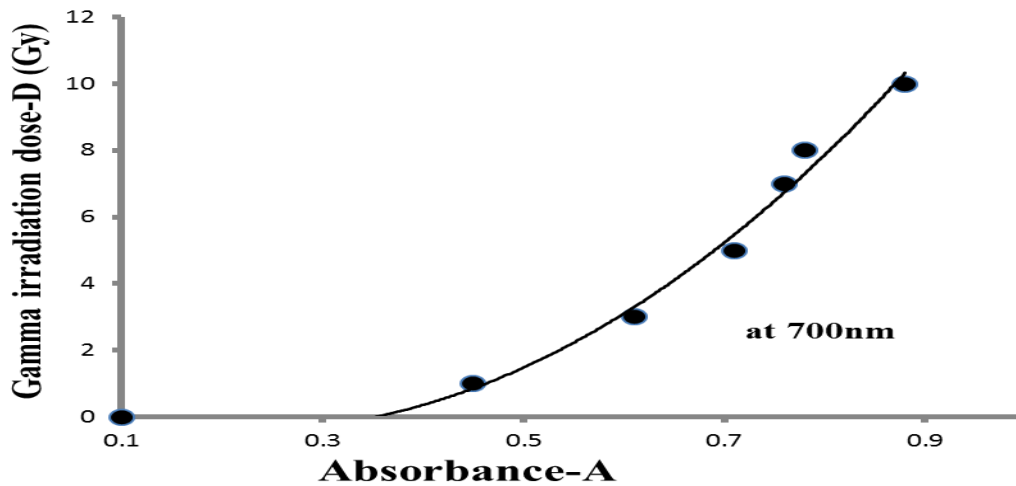

Figure 3.14 Absorbance-A vs. uv-irradiation dose-D (J/cm²) for CR-39 detector at wavelength 300 nm

Figure 3.15 Absorbance-A vs. uv-irradiation dose-D (J/cm²) for CR-39 detector at wavelength 304 nm

3.1.2.2. NTD type Lexan

Figure (3.16) show the increase in absorbance-A measured by uv-visible technique at the range 290 - 330 nm to the samples of nuclear track detector type Lexan with increase of irradiation dose of uv-radiation at the range (10 ,60 ,120 ,240 ,360J/cm²) compared with un-irradiated sample . This figure shows the increase in absorbance-A with increase of radiation dose.
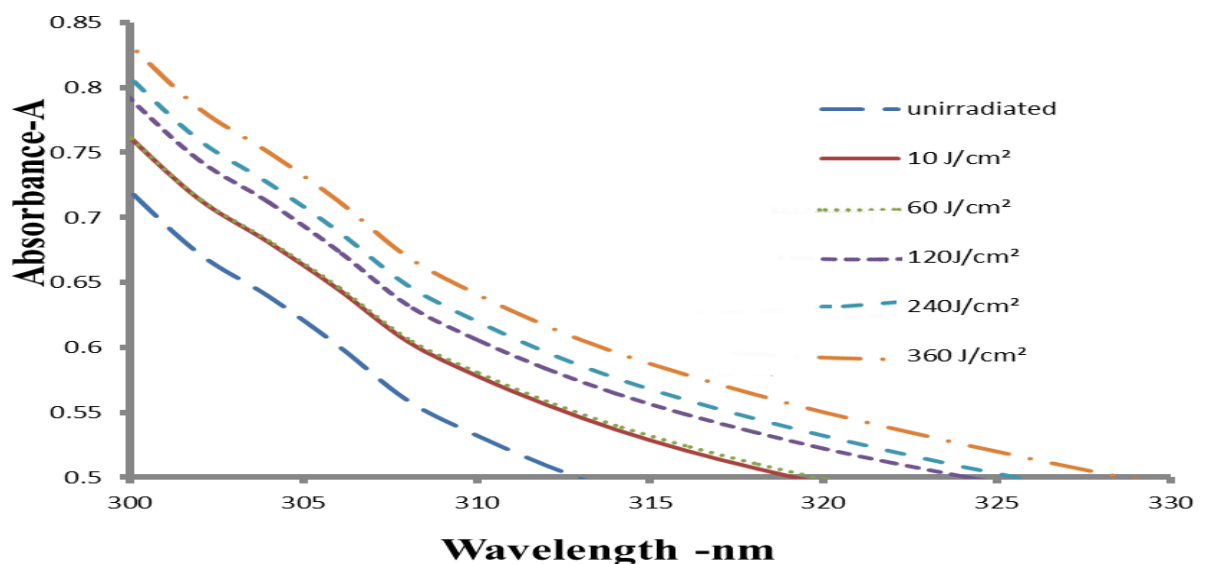
Figure 3.16 Absorbance-A measured by uv-Visible spectroscopy technique
with wavelength range (290 – 330 nm) for un-irradiated and
uv- irradiated   samples at dose range of
(10 ,60 ,120 ,240 ,360J/cm²) for Lexan detector

The maximum absorbance-A with irradiation dose was appear at the wavelengths 300 and   305 nm as shown in figure (3.17) and figure (3.18) respectively.

Figure (3.17) and figure (3.18) shows the polynomial relationship which determine the absorbance-A and uv-irradiation dose at 300 and   305 nm respectively. Equation (3.12) and equation   (3.13) are obtained   from polynomial relationship of figures 3.17 and 3.18 respectively . The radiation response of   uv- irradiation dose (J/cm²) with absorbance-A   by   uv-visible spectroscopy technique , appears as given by the following equations

$$D(J/cm^2) \ = \ 1 \times 10^4 A^2 \ - \ 1 \times 10^4 A \ + \ 5.7 \times 10^3 \qquad (3.12)$$

$$D \ (J/cm^2) \ = \ 9.2 \times 10^3 A^2 \ - \ 1 \times 10^4 A \ + \ 4.7 \times 1 \qquad (3.13)$$

Where D(J/cm²): uv- irradiation dose , A: absorbance

The maximum response of uv-radiation dose 360 J/cm² at wavelength 305 nm correspond at absorbance-A value 0.84 as shown in figure (3.18).
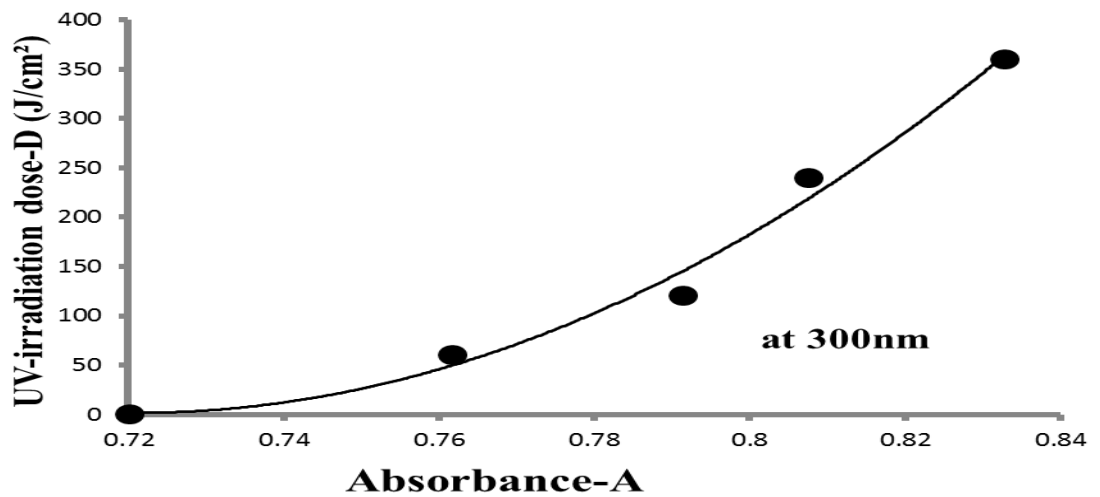

Figure 3.17 Absorbance-A vs. uv-irradiation dose-D (J/cm²) for Lexan detector at wavelength 300 nm
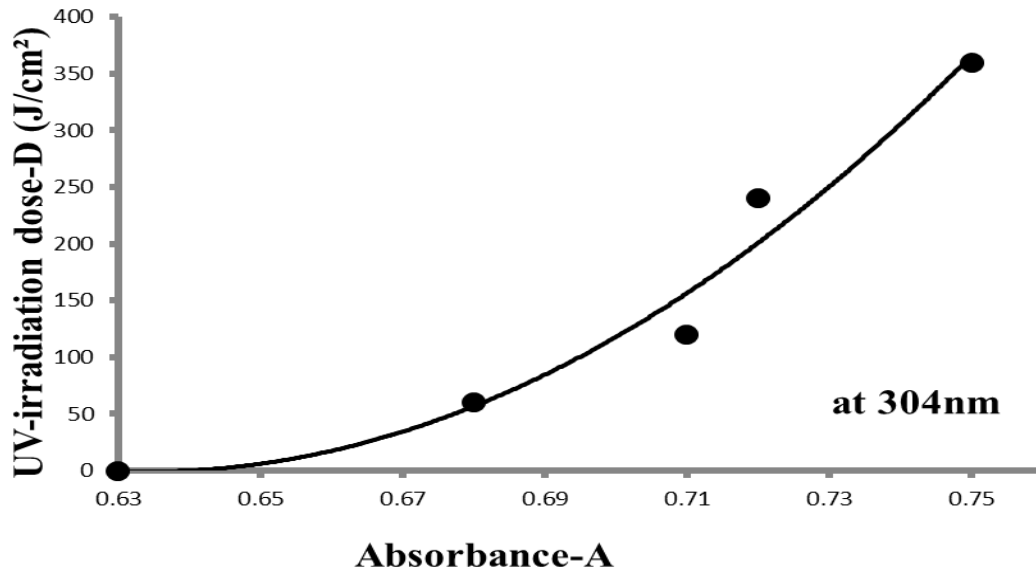

Figure 3.18 Absorbance-A vs. uv-irradiation dose-D (J/cm²) for Lexan detector at wavelength 305 nm

3.1.2.3. NTD type LR-115

Figure (3.19) shows the increase   in absorbance-A measured by uv-visible technique at range 600-700 nm to the samples of nuclear track detector type LR-115 with irradiation dose of uv-radiation at the range   (10 , 60 , 120 , 240 , 360 J/cm²) compared with un-irradiated sample. The increase in absorbance-A with irradiation dose appears at the wavelengths 600 and 650 nm as shown in figure (3.20) and figure (3.21) respectively.
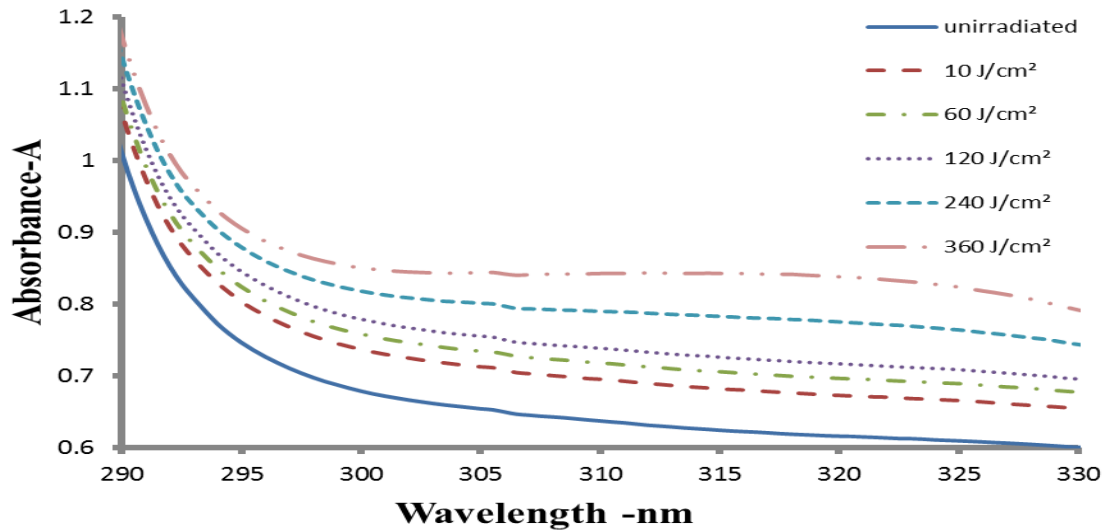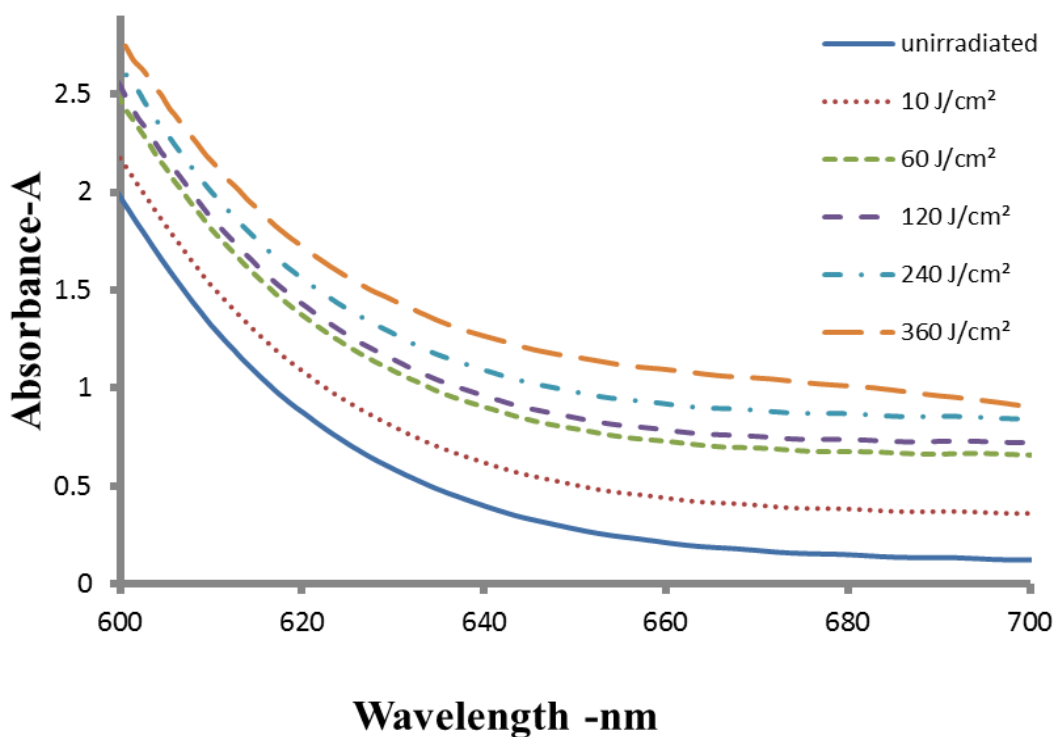

Figure 3.19 Absorbance-A measured by uv-visible spectroscopy technique
           with wavelength range (600 – 700 nm) for un-irradiated and uv-
            irradiated samples at dose range (10 , 60 , 120 , 240 , 360J/cm²)
           for LR-115 detector

Figure (3.20) and figure (3.21) shown the polynomial relationship between the absorbance-A and uv-irradiation dose at wavelengths 600 and 650 nm respectively. Equation (3.14) and equation (3.15) are obtained from the polynomial relationship of figures 3.20 and 3.21 respectively .The radiation response of uv-irradiation dose (J/cm²) with absorbance-A measured by uv-visible spectroscopy technique , appears to be given by the following equations

$$D \ (J/cm^2) \ = \ 8.5 \times 10^2 A^2 \ - \ 3.5 \times 10^3 A \ + \ 3.1 \times 10^3 \qquad (3.14)$$

$$D(J/cm^2) \ = \ 6.7 \times 10^2 A^2 \ - \ 5.2 \times 10^2 A \ + \ 1.8 \times 10^2 \qquad (3.15)$$

where D(J/cm²): uv- irradiation dose , A: absorbance

The maximum response of uv-radiation 360 J/cm² at wavelength 650 nm was correspond at absorbance-A value 2.7 as shown in figure (3.20).
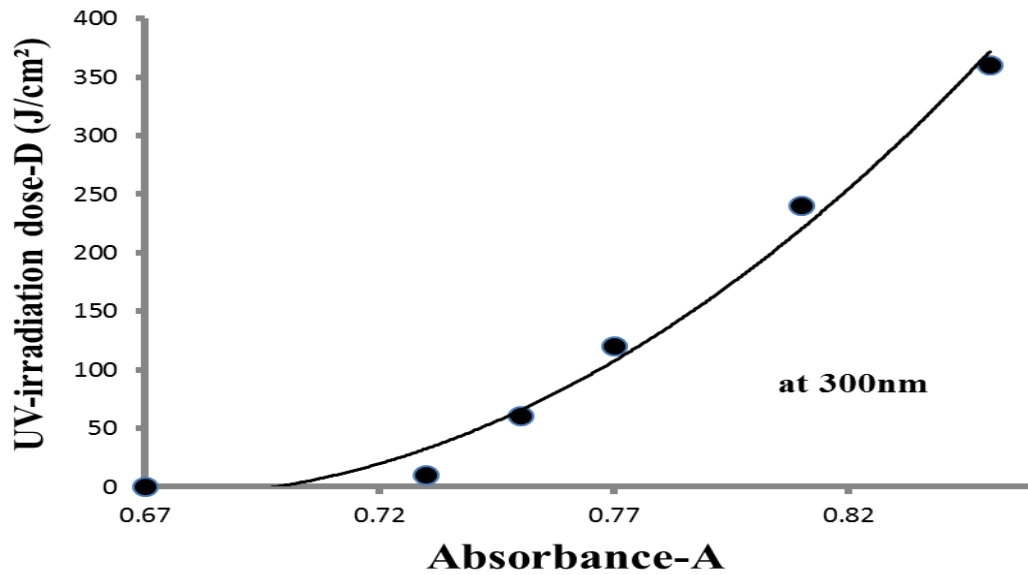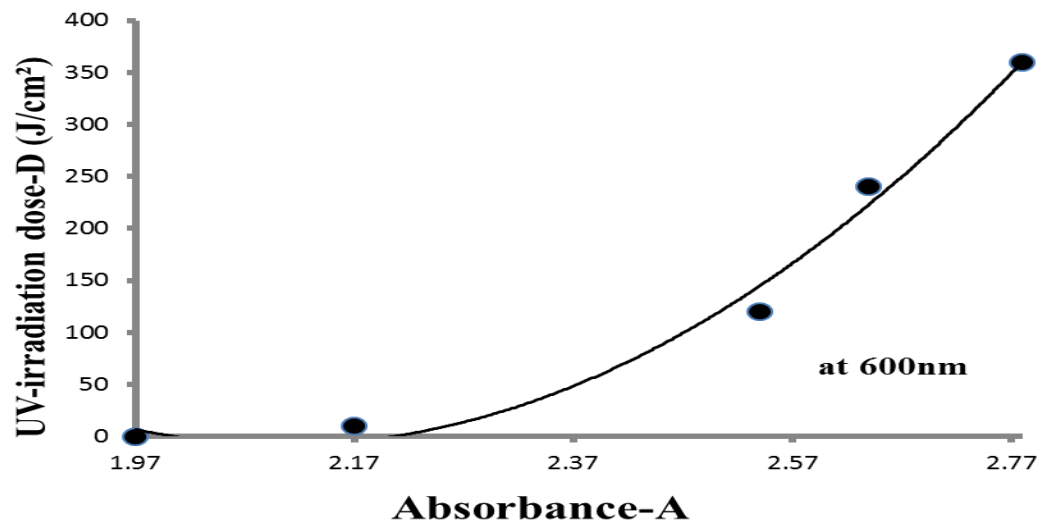

Figure 3.20 Absorbance-A vs. uv-irradiation dose-D (J/cm²) for LR-115 detector at wavelength 600 nm
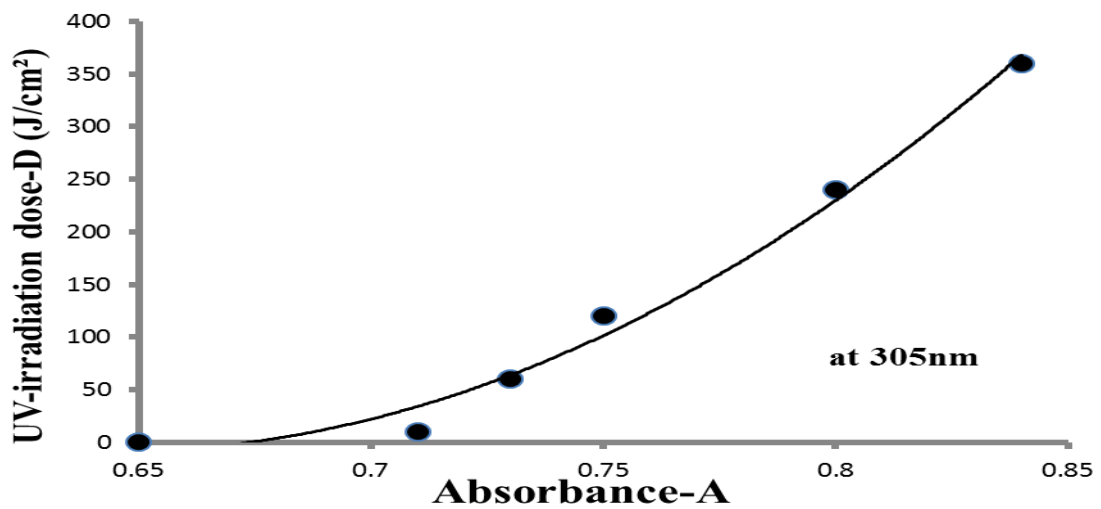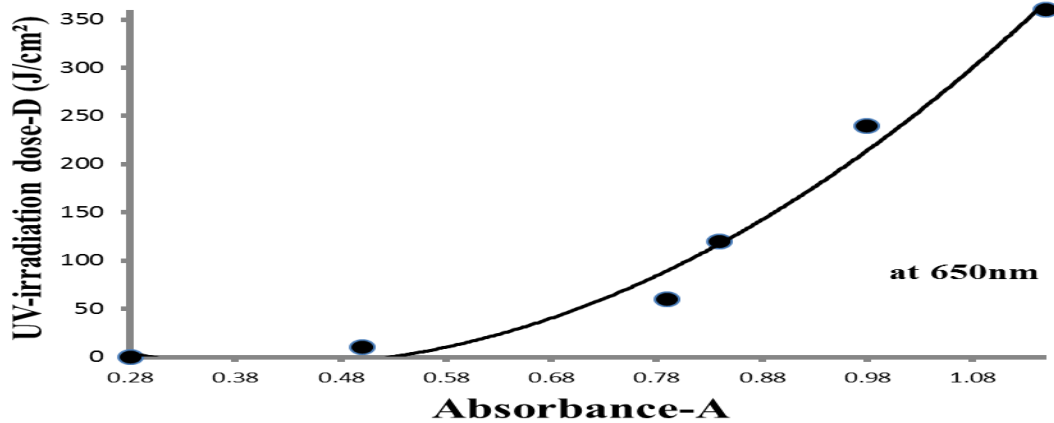
Figure 3.21 Absorbance-A vs. uv-irradiation dose -D (J/cm²) for LR-115 detector at wavelength 650 nm

Table (3.2) shows the equations obtained by the relationship between uv-irradiation dose with absorbance-A measured by uv-visible spectroscopy technique for the NTDs types CR-39 , Lexan and LR-115 .

Table 3.2 UV irradiation dose -J/cm² vs. absorbance-A obtained equations for NTDs types CR-39 , Lexan and LR-115 at different wavelengths using uv-visible spectroscopy technique .

Types of NTDs	Equations	equation no.	Wavelength (nm)
CR-39	$D\ (J/cm^2) = 2 \times 10^4 A^2 - 4 \times 10^4 A + 1 \times 10^4$	3.10	300
	$D(J/cm^2) = 2 \times 10^4 A^2 - 3 \times 10^4 A + 1 \times 10^4$	3.11	304
Lexan	$D(J/cm^2) = 1 \times 10^4 A^2 - 1 \times 10^4 A + 5.7 \times 10^3$	3.12	300
	$D\ (J/cm^2) = 9.2 \times 10^3 A^2 - 1 \times 10^4 A + 4.7 \times 10^3$	3.13	305
LR-115	$D\ (J/cm^2) = 8.5 \times 10^2 A^2 - 3.5 \times 10^3 A + 3.1 \times 10^3$	3.14	600
	$D(J/cm^2) = 6.7 \times 10^2 A^2 - 5.2 \times 10^2 A + 1.8 \times 10^2$	3.15	650

That means may use the change in absorbance-A value with uv-visible spectroscopy are technique to determine the uv- radiation dose (J/cm²) absorbed by NTDs CR-39 , Lexan and LR-115. The polynomial relationship between uv- radiation dose (J/cm²) and absorbance-A in table (3.2) for NTDs type LR-115 was better than the radiation response which appear in CR-39 and Lexan as shown in figure (3.20) . And these figure reflect this response for uv radiation at wave length 600 nm .

3.2. Effect of Gamma-ray and UV-irradiation on NTDs
Using FTIR-Spectroscopy Technique

In this study we used FTIR-spectroscopy technique to measure the effect of gamma-ray and UV radiation.

3.2.1. Effect of gamma irradiation on NTDs by using of FTIR-spectroscopy technique
3.2.1.1. NTD type CR-39

FTIR spectrum appears in figure (3.22) showing the change that appears in transmission percent–T% measured by FTIR-spectroscopy technique at range $500 - 4000$ cm^{-1} to the samples of nuclear track detector CR-39 irradiated by gamma-ray at range from 1 Gy to 10Gy compared with un-irradiated sample . The change in the shape of FTIR-spectrum with irradiation dose (Gy) appears at wavenumber 1405 and 1456 cm^{-1} as shown in figure (3.23) .
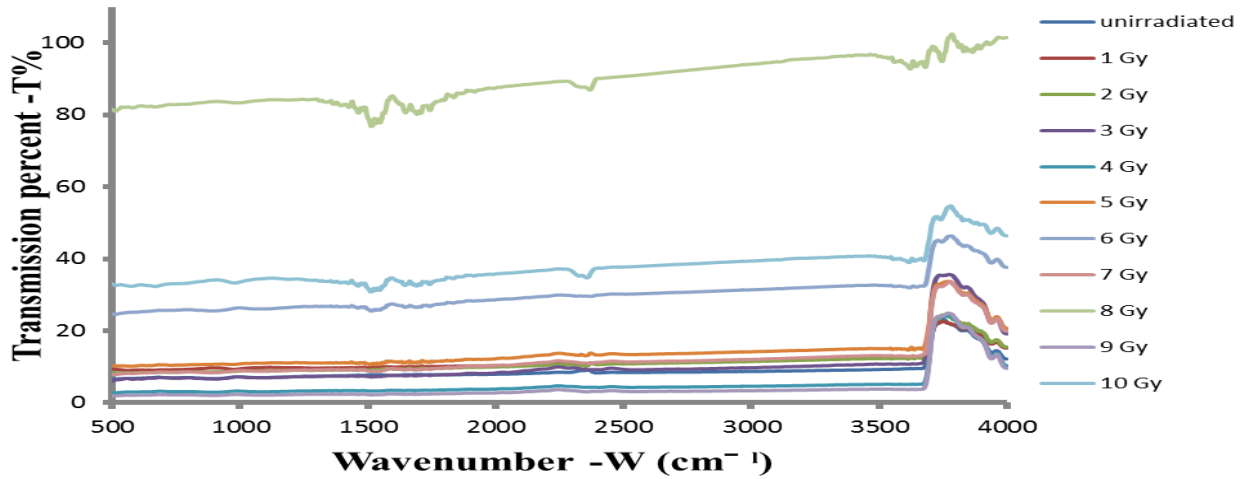
Figure 3.22 Transmission percent – T% measured by FTIR-spectroscopy technique at wavenumber-W range (500 – 4000 cm^{-1}) for un-irradiated and gamma irradiated samples at dose range from 1 to 10Gy for CR-39 detector
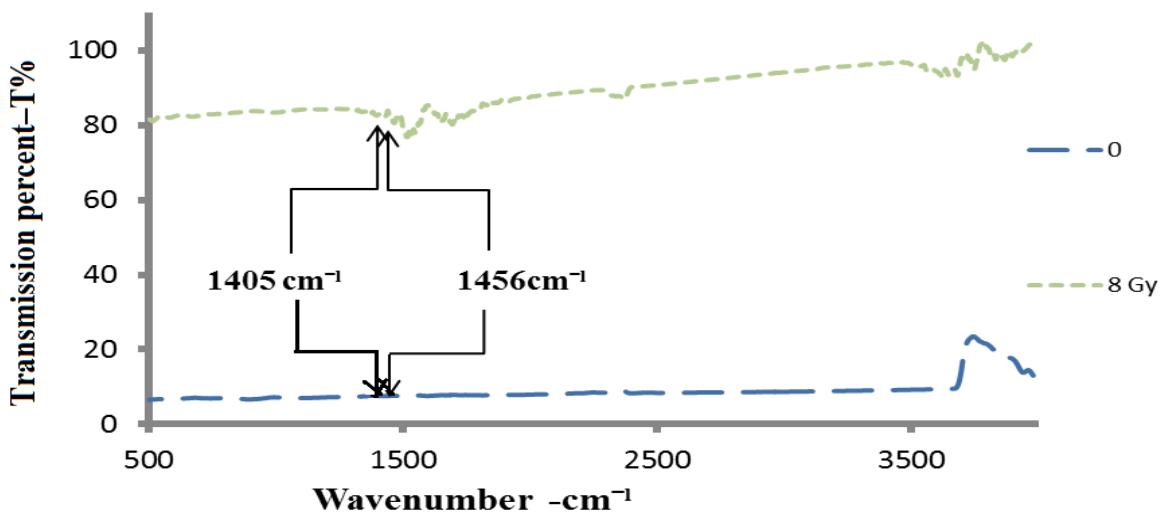
Figure 3. 23 Transmission percent–T% measured by FTIR-spectroscopy technique at wavenumber-W range (500 – 4000cm^{-1}) for un-irradiated and gamma irradiated at radiation dose 8 Gy for CR-39 detector
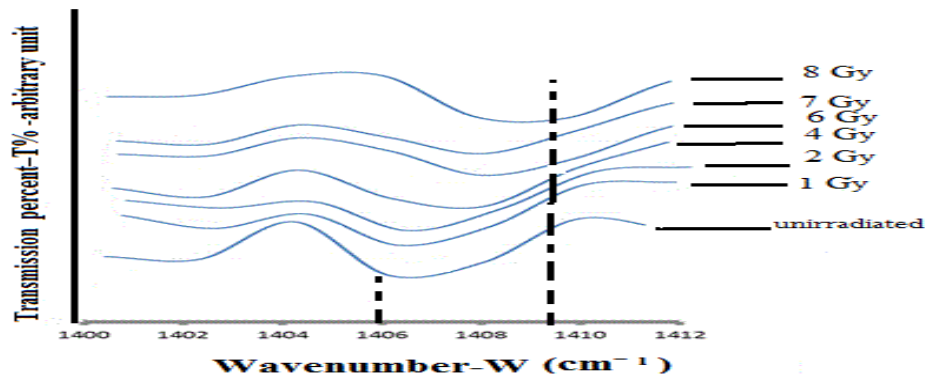
Figure 3.24 Deviation for FTIR-spectrum at the wavenumber -W value 1405cm⁻¹ for CR-39 detector with gamma irradiation dose range from 1 Gy to 8 Gy

Figure (3.24) shows the change in behavior as deviation at wavenumber value 1405 cm⁻¹ with irradiation dose -Gy for (1 , 2 , 4 , 6 , 7 , 8 Gy) . And figure (3.25) shows the polynomial relationship between the gamma irradiation dose and the deviation in wavenumber–W at 1405 cm⁻¹ . And the gamma radiation dose-Gy (1 , 2 , 4 , 6 , 7 to 8 Gy) measured by FTIR-spectroscopy technique . This behavior between irradiation dose (Gy) and wavenumber-W may be given by following equation

$$D \ (Gy) = \ -0.07 \ W^2 + \ 203.1 \ W \ - \ 1 \times 10^5 \qquad (3.16)$$

where D (Gy): gamma irradiation dose , W: wavenumber cm⁻¹
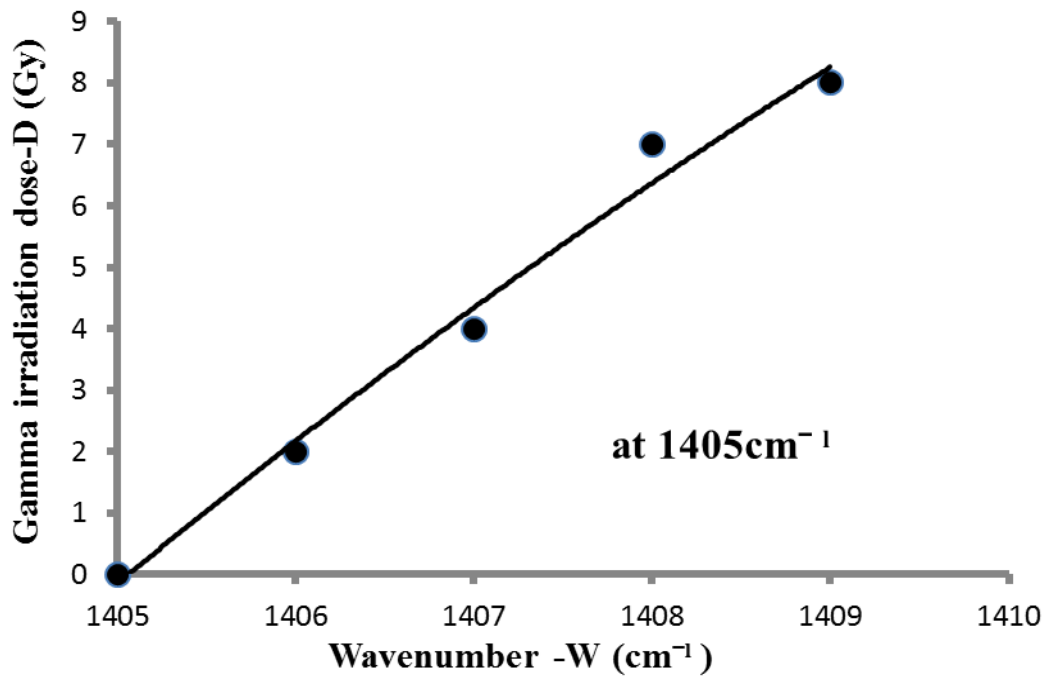
Figure 3.25 Behavior of deviation for FTIR-spectrum at wavenumber-W 1405cm^{-1} for CR-39 detector vs. gamma irradiation dose range from 1 to 8Gy

Figure (3.26) shows the change in deviation of wavenumber value1456 cm^{-1} with irradiation dose (Gy) for (1 , 2 , 3 , 4 , 6 , 7 , 8 Gy) .
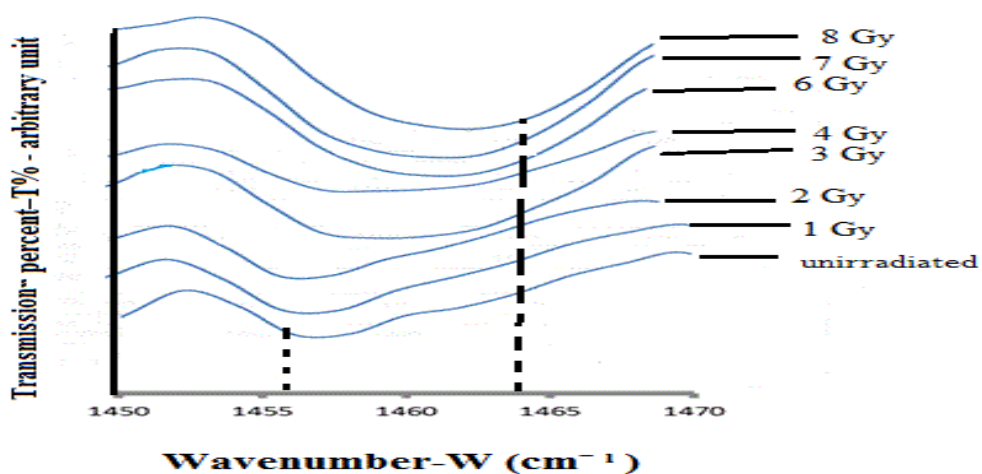
Figure 3.26 Deviation for FTIR-spectrum at wavenumber-W 1456cm^{-1} for CR-39 detector with gamma irradiation dose range from 1 Gy to 8 Gy

Figure (3.27) shows the polynomial relationship between the gamma irradiation dose(Gy) and the behavior of deviation in wavenumber –W at 1456 cm⁻¹ at the range (1 , 2 , 3 , 4 , 6 , 7 to 8Gy) measured by FTIR- spectroscopy technique .This behavior for irradiation dose D (Gy) and wavenumber-W may be written by the following equation

$$D(Gy) = 0.03\ W^2 - 88.5\ W + 6 \times 10^4 \qquad (3.17)$$

where D (Gy): gamma irradiation dose , W: wavenumber (cm⁻¹)
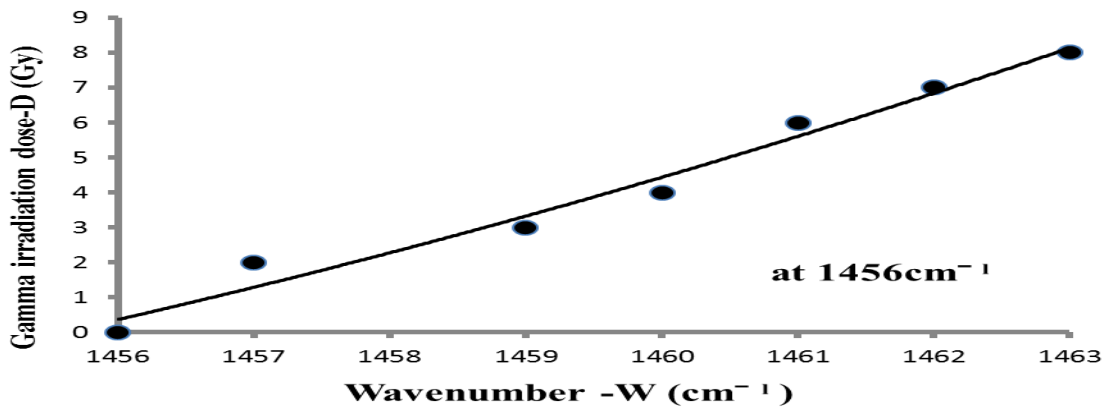
Figure 3.27 Behavior of deviation for FTIR-spectrum at wavenumber-W 1456cm⁻¹ for CR-39 detector vs. gamma irradiation dose range from 1Gy to 8Gy

Table (3.3) shows the relationships of gamma irradiation dose – (Gy) and wavenumber-W by FTIR –spectroscopy technique for CR-39 detector by equation (3.16) and equation (3.17) at wavenumber-W 1405 and 1456 cm⁻¹ . These equations reflect the gamma radiation dose with transitions percent–T% . No response for NTDs types (Lexan , LR-115) for gamma irradiation dose was

registered when measuring by FTIR –spectroscopy technique. The relation of wavenumbers –W 1405 cm⁻¹ and 1456 cm⁻¹ which appear in figure (3.25) and figure (3.27) respectively may be used to determine the change in bond CH_2 deformation vibrations as shown in table (1.2) as measuring by Tse Chun Chun [81].

Table 3.3 Gamma irradiation dose-Gy vs. wavenumber –cm⁻¹ - W equations for NTD type CR-39 at different doses using FTIR - spectroscopy technique

Type of NTD	Equation	Equation No.	Wavenumber –W (cm⁻¹)
CR-39	$D\,(Gy) = -0.07\,W^2 + 203.1\,W - 1 \times 10^5$	3.16	1405
	$D(Gy) = 0.03\,W^2 - 88.5\,W + 6 \times 10^4$	3.17	1456

3.2.2. Effect of uv-irradiation on NTDs by using of FTIR-spectroscopy technique

3.2.2.1. NTD type CR-39

A FTIR –spectrum appears in figure (3.28) showing the change that appears in transmission percent–T% measured by FTIR-spectroscopy technique at range 500 – 4000 cm⁻¹ to the samples of nuclear track detector CR-39 irradiated by uv radiation at the range (10 , 60 ,120 , 240 , 360 J/cm²) compared with un-irradiated sample . The change in the shape of FTIR-spectrum with irradiation dose (J/cm²) appear at wavenumber 1338 cm⁻¹ as shown in figure (3.29) .

Figure 3.28 Transmission percent–T% measured by FTIR-spectroscopy technique at wavenumber range $(500 - 4000 \text{ cm}^{-1})$ for un-irradiated and uv-irradiated samples at dose range (10 , 60 , 120 , 240 and 360J/cm²) for CR-39 detector
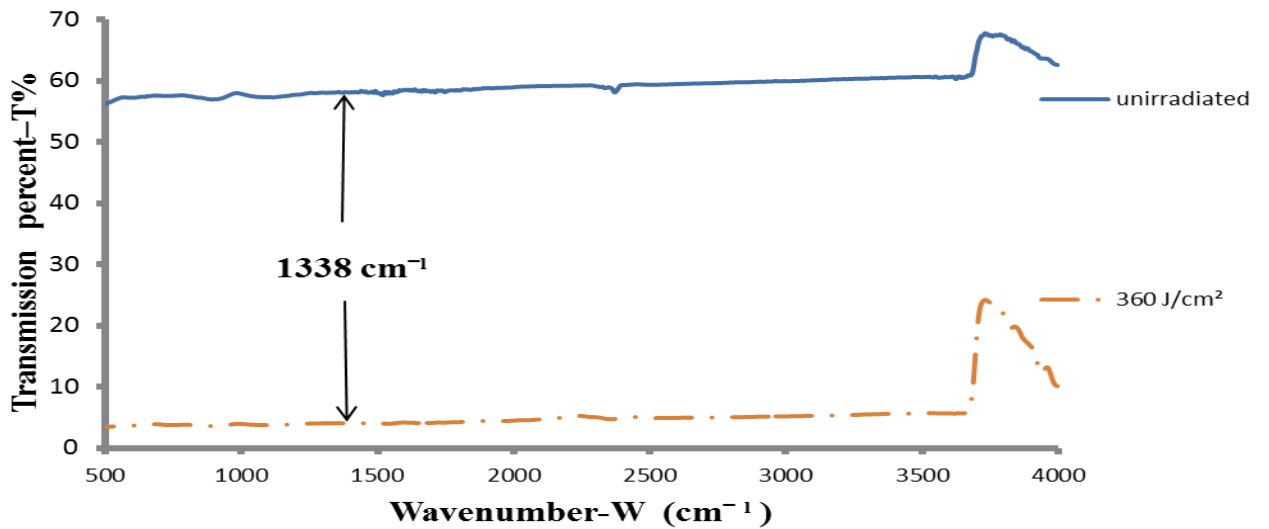
Figure 3. 29 Transmission percent–T% by FTIR-spectroscopy technique at wavenumber range $(500 - 4000 \text{cm}^{-1})$ for un-irradiated and uv-irradiated at radiation dose 360 J/cm² for CR-39 detector
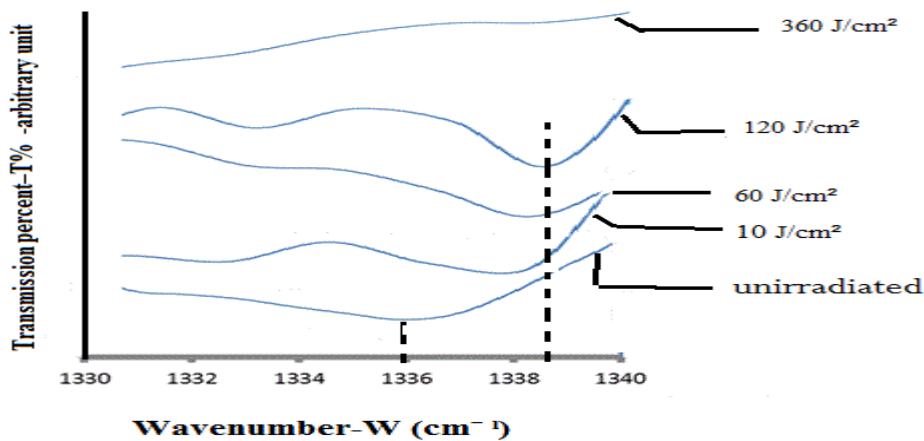
Figure 3.30 Deviation for FTIR-spectrum at wavenumber -W 1338cm^{-1} for CR-39 detector with uv-irradiation dose range (10 to 360 J/cm²)

Figure (3.30) shown the change in deviation of wavenumber value 1338 cm^{-1} with irradiation doses (J/cm²) from 10 J/cm² to 360J/cm² .

Figure (3.31) shows the polynomial relationship between the uv irradiation dose and the deviation in wavenumber–W at 1338 cm^{-1} and the uv- radiation dose from 10 J/cm² to 360J/cm² measured by FTIR- spectroscopy technique . The behavior of between radiation dose-D (J/cm²) and wavenumber-W may be writing in the following equation

$$D \ (J/cm^2) \ = \ 4.6 \ W^2 \ - \ 1 \times 10^4 \ W \ + \ 8 \times 10^6 \qquad (3.18)$$

where D (J/cm²): uv irradiation dose , W: wavenumber cm^{-1}
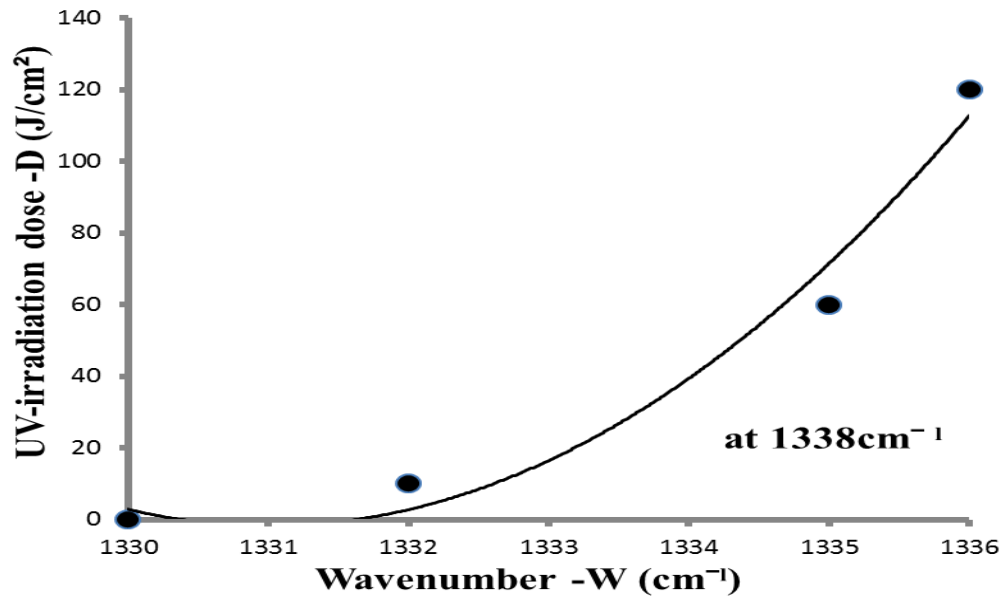
Figure 3.31 Behavior of deviation for FTIR-spectrum at wavenumber
1338cm⁻ᴵ for CR-39 vs. uv- irradiation dose range from 10 J/cm²
to 360J/cm²

3.2.2.2. NTD type Lexan

FTIR-spectrum appear in figure (3.32) showing the change that appears in transmission percent – T%   measured by FTIR-spectroscopy technique at range $300 – 3800$ cm⁻ᴵ to the samples of nuclear track detector Lexan irradiated by uv-radiation at range (1 , 5 , 10 , 60 , 120 , 240 J/cm²) compared with un-irradiated sample . The change in the shape of FTIR-spectrum with irradiation dose (J/cm²) appears   at wavenumber   940 cm⁻ ᴵ as shown in figure (3.33) .
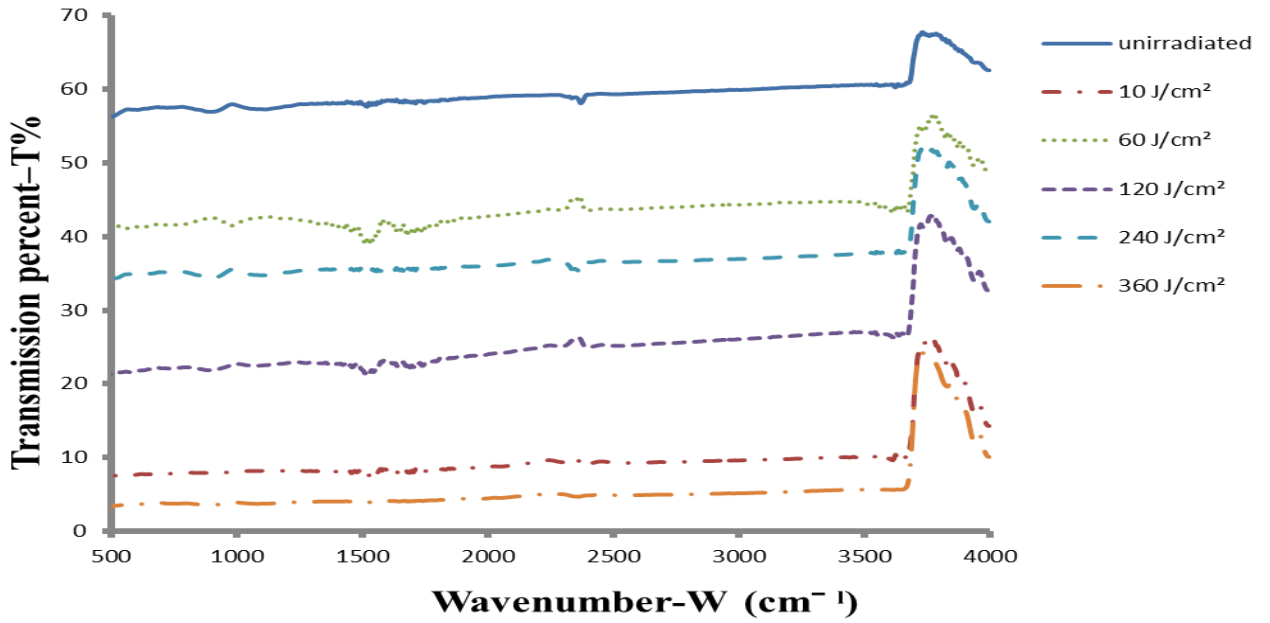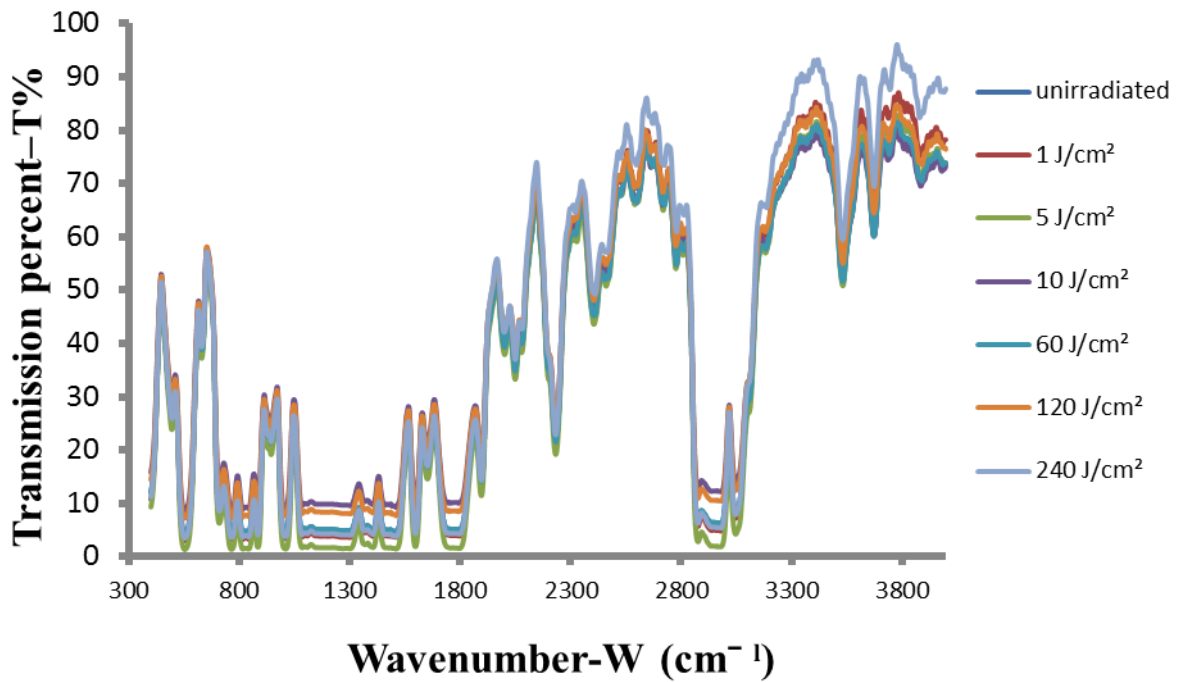
Figure 3.32 Transmission percent–T% measured by FTIR-spectroscopy technique at wavenumber-W range (300 – 3800 cm⁻ⁱ) for un-irradiated and uv-irradiated samples at dose range (1 ,5 ,10 ,60 ,120 ,240 J/cm²) for Lexan detector

Figure 3. 33 Transmissions percent–T% measured by FTIR-spectroscopy technique at wavenumber-W range (300 – 3800cm⁻ ¹) for un-irradiated and uv-irradiated at dose 240 J/cm² for Lexan detector
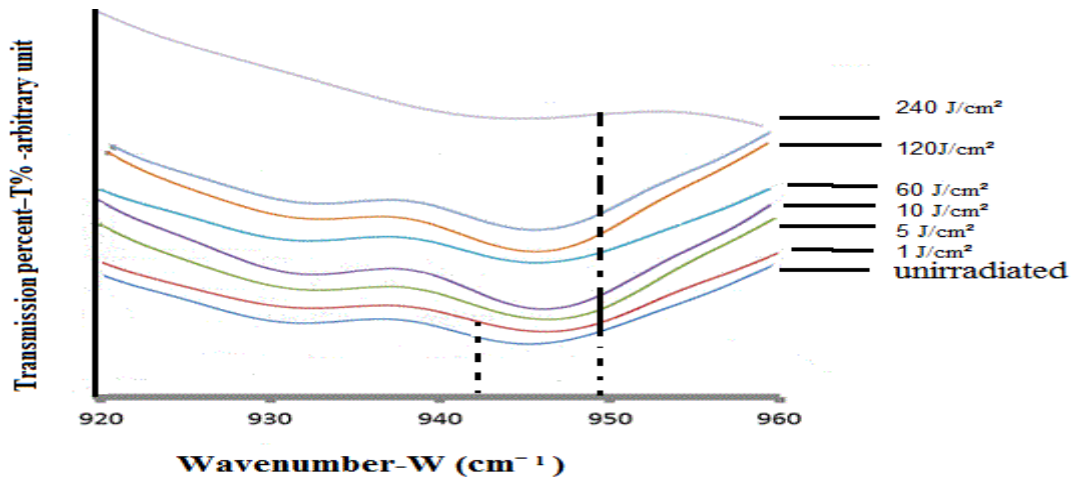
Figure 3.34 Deviation for FTIR-spectrum at wavenumber - W 940cm^{-1} for Lexan
detector with uv-irradiation dose range from1 J/cm² to 240 J/cm²

Figure (3.34) shows the change in deviation of wavenumber value 940 cm^{-1} with irradiation doses (J/cm²) from (1 to 240 J/cm²). Figure (3.35) shows the polynomial relationship between the uv-irradiation dose and the deviation in wavenumber–W at 940 cm^{-1} and the uv- radiation dose (J/cm²) from 1 J/cm² to 240 J/cm² measured by FTIR- spectroscopy technique .

The behavior between radiation dose (J/cm²) and wavenumber-W may be written in the following equation

$$D\ (J/cm^2) \ = \ 1.9W^4 \ - \ 7.8 \times 10^3W^3 \ + \ 1 \times 10^7W^2 \ - \ 7 \times 10^9W \ + \ 2 \times 10^{12} \qquad (3.19)$$

where D (J/cm²): uv- irradiation dose , W: wavenumber cm^{-1}
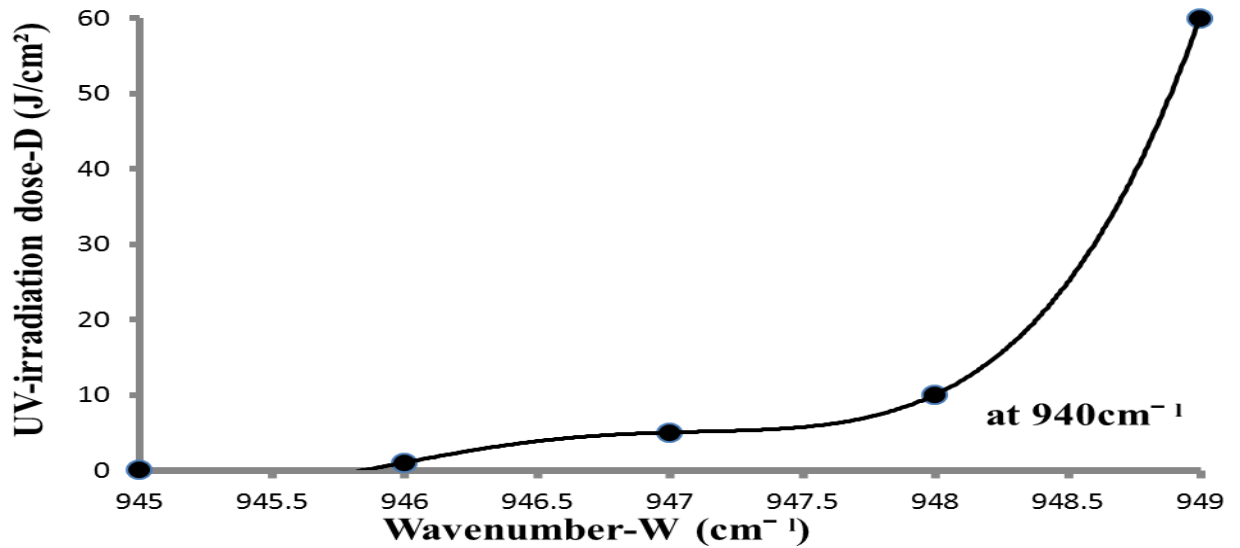
Figure 3.35 Behavior of deviation for FTIR-spectrum at wavenumber-W 940cm⁻¹ for Lexan vs. uv- irradiation dose range from 1 J/cm² to 240 J/cm²

3.2.2.3. NTD type LR-115

A FTIR -spectrum appear in figure (3.36) showing the change that appears in transmission percent–T%   measured by FTIR-spectroscopy technique at range 400 – 3800 cm⁻¹ to the samples of nuclear track detector LR-115 which irradiated by uv radiation at the range (5 , 10 , 60 , 120 , 240 , 360 J/cm²) compared with un-irradiated sample . The change in the shape of FTIR-spectrum with irradiation dose (J/cm²) appears at the wavenumber 2907 cm⁻ ¹ as shown in figure (3.37) .
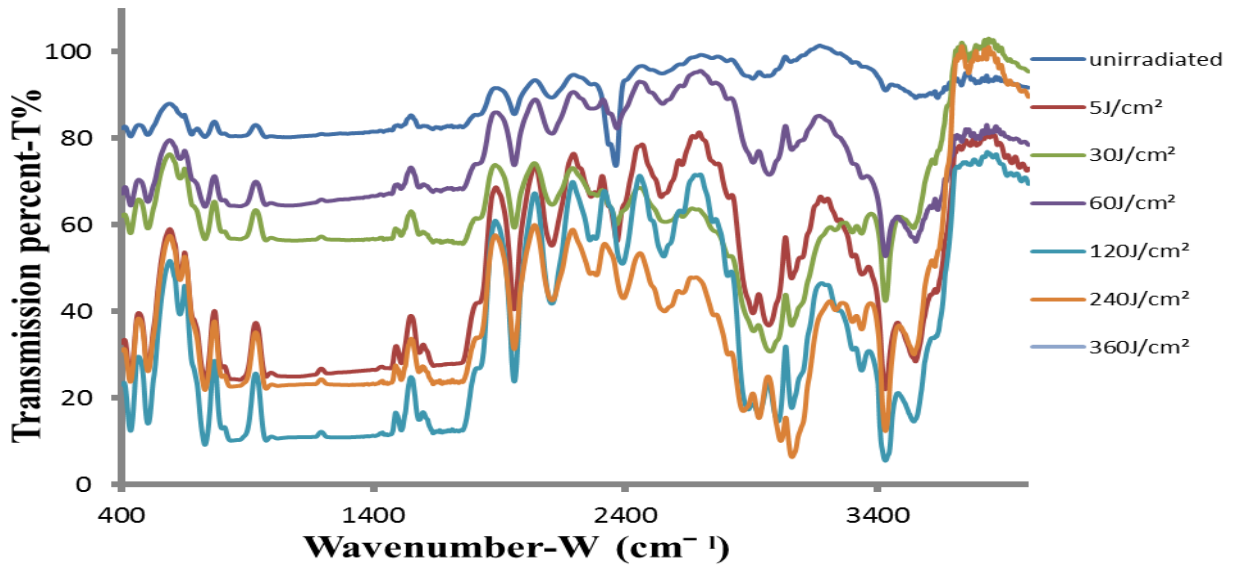
Figure 3.36 Transmission percent– T% measured by FTIR - spectroscopy technique at wavenumber-W range (400 – 3800 cm^{-1}) for un-irradiated and uv- irradiated samples at dose range (5 , 10 , 60 , 120 , 240 , 360 J/cm²) for LR-115 detector
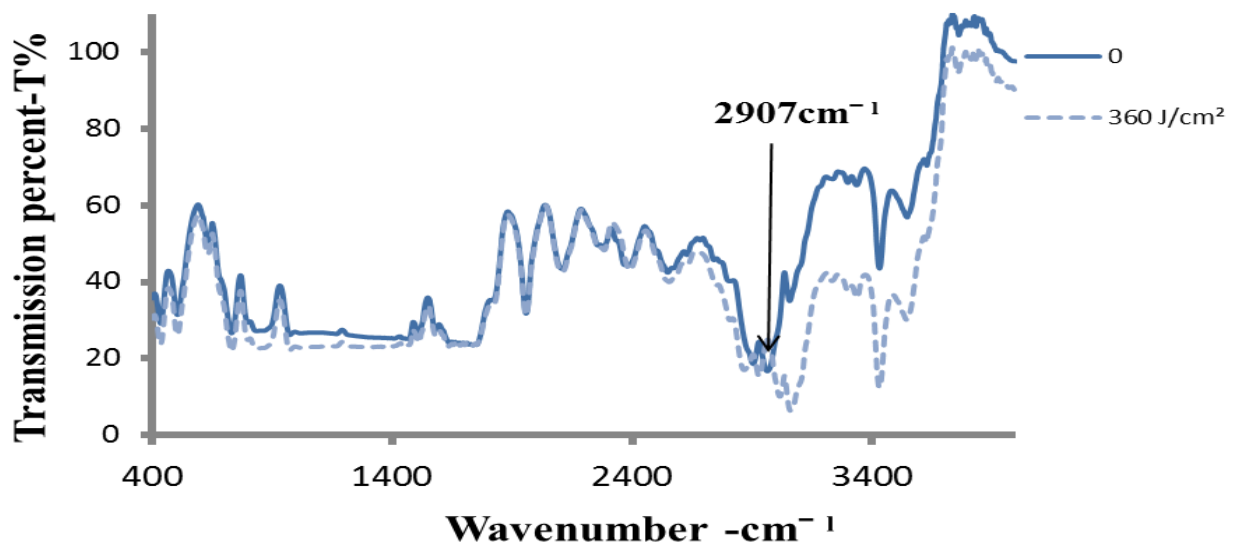
Figure 3. 37 Transmission percent–T% measured by FTIR-spectroscopy technique at wavenumber-W range (400 – 3800cm^{-1}) for unirradiated and uv- irradiated samples at dose 360 J/cm² for LR-115 detector
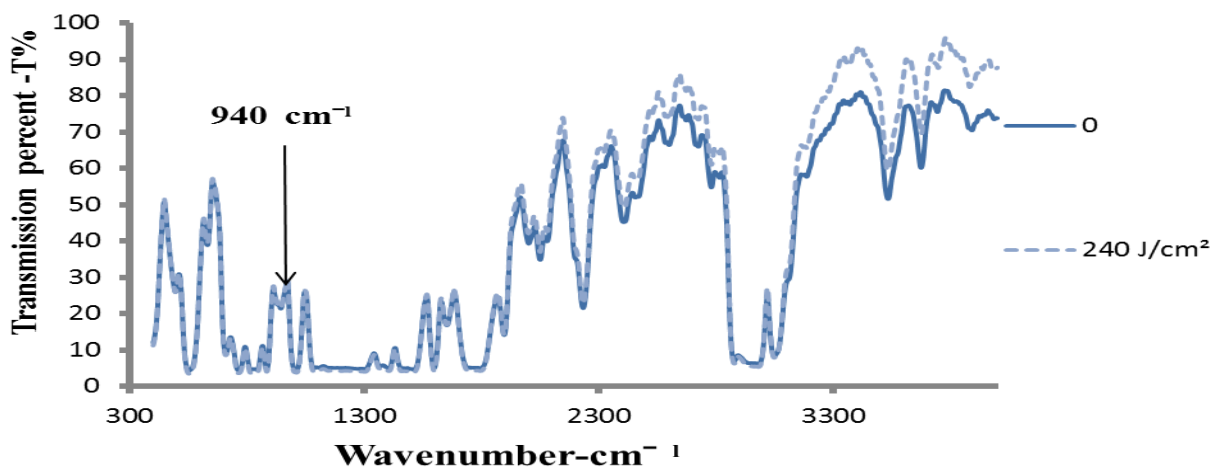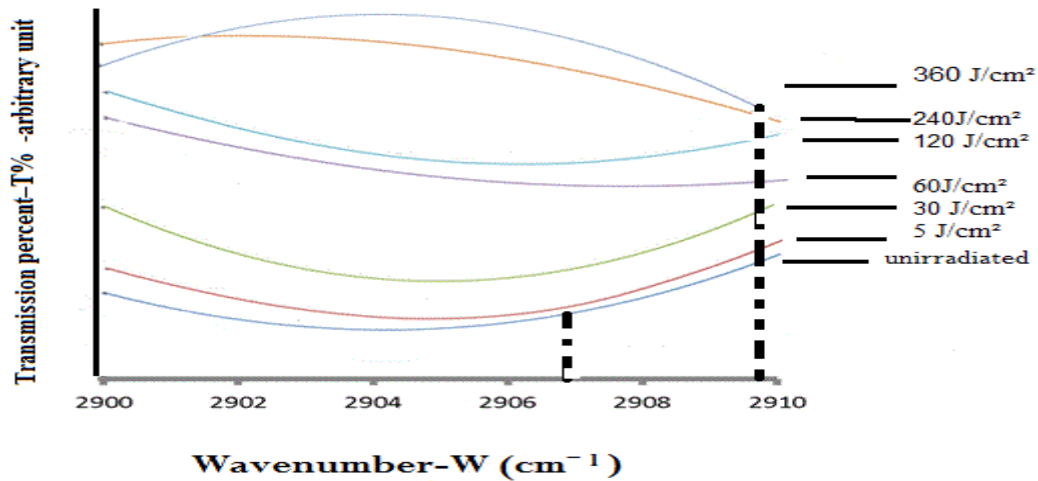
Figure 3.38 Deviation for FTIR-spectrum at wavenumber -W 2907cm^{-1} for LR-115 detector with uv-irradiation dose range (5 to 360 J/cm²)

Figure (3.38) shows the change in deviation of wavenumber value 2907 cm^{-1} with irradiation doses from 5 J/cm² to 360 J/cm² .

Figure 3.39 shown the polynomial relationship between the uv-irradiation dose and the deviation in wavenumber − W at 2907 cm^{-1} and the uv- radiation dose from 5 J/cm² to 360 J/cm² measured by FTIR- spectroscopy technique .

The behavior between radiation dose-(J/cm²) and wavenumber-W may be written in the following equation

$$D \ (J/cm^2) \ = \ 7.5W^3 \ - \ 5 \times 10^4 W^2 \ + \ 1 \times 10^8 W \ - \ 1 \times 10^{11} \quad (3.20)$$

where D (J/cm²): uv- irradiation dose , W: wavenumber cm^{-1}
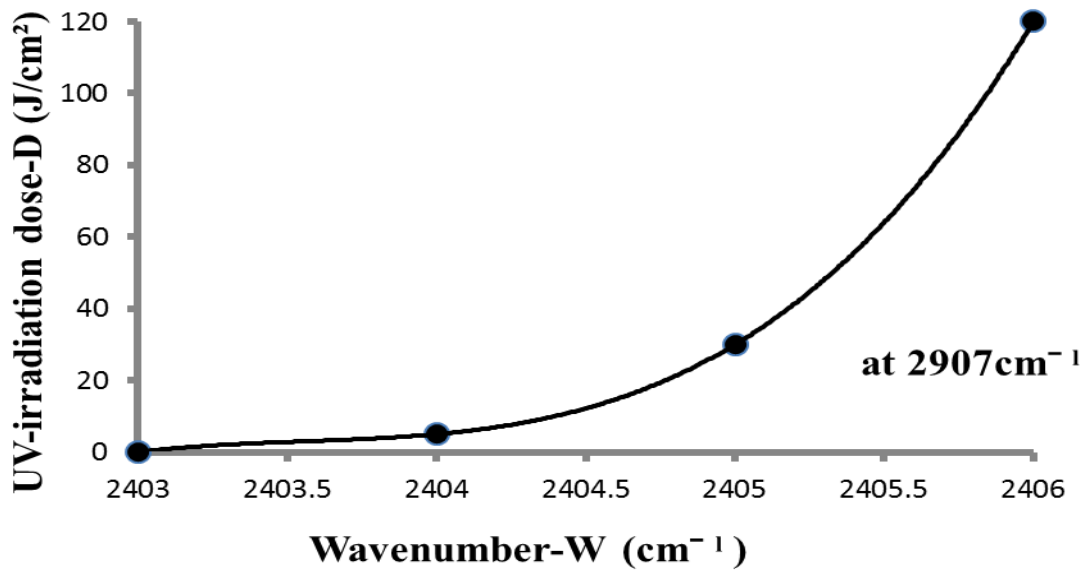
Figure 3.39 Behavior of deviation for FTIR-spectrum at wavenumber-W
2907cm⁻¹ for LR-115 vs. uv- irradiation dose range from 5 J/cm²
to 360 J/cm²

It can be shown that the deviation spectral of spectrum (FTIR) at wavenumbers-W (1338 , 940 , 2907 cm⁻¹) for the detectors (CR-39 , Lexan , LR-115) respectively , it was observed is better for the detectors CR-39 and Lexan than detector LR-115.

Table (3.4) shows the uv- irradiation dose – (J/cm²) and wavenumber-W measured by FTIR –spectroscopy technique for NTDs CR-39 , Lexan and LR-115 using equations (3.18) , (3.19) and (3.20) respectively . These equations reflect the uv-radiation dose relation with transmission percent–T%.

Table 3.4 UV- irradiation dose- J/cm² vs. wavenumber - W equations for NTDs types CR-39 , Lexan and LR-115 at different doses using FTIR - spectroscopy technique

Type of NTD	Equation	Equation No.	Wavenumber–W (cm⁻¹)
CR-39	$D\ (J/cm^2) = 4.6W^2 - 1 \times 10^4 W + 8 \times 10^6$	3.18	1338
Lexan	$D\ (J/cm^2) = 1.9W^4 - 7.8 \times 10^3 W^3 + 1 \times 10^7 W^2 - 7 \times 10^9 W + 2 \times 10^{12}$	3.19	940
LR-115	$D\ (J/cm^2) = 7.5W^3 - 5 \times 10^4 W^2 + 1 \times 10^8 W - 1 \times 10^{11}$	3.20	2907

The wavenumber –W 1338 cm⁻¹ for CR-39 detector which appear in figure (3.31) reflected the change in band CH_2 deformation vibrations [81] as shown in table (1.2), and the wavenumber –W 940 cm⁻¹ for Lexan detector appearing in figure (3.35) reflected the change in band CH wag (in –plane) deformation vibrations [82] as shown in table (1.3), and the wavenumber –W 2907cm⁻¹ for LR-115 detector that's appears in figure (3.35) reflects the change in band C-H stretch deformation vibrations [83] as shown in table (1.4) .

It can be shown that there is a possibility of using the NTDs to the assessment of doses of exposure to uv-radiation and gamma radiation in the medical and environmental fields .

3.3. Comparison of some results of the present work with previous studies

A comparison of some results of the present work with previous studies for range of wavelength results using uv-visible spectroscopy technique is shown in table (3.5) and for range of wavenumber results using FTIR- spectroscopy technique is shown in table (3.6).

Table 3.5 Comparison of some results of the present work with previous studies for range of wavelength results using uv-visible spectroscopy technique

Radiation	Types of NTDs	Thickness (µm)	The range of wavelength (nm)	Reference
Gamma-ray	CR-39	60	220-370	N. E. Ipe and P. L. Ziemer (1986)
	CR-39	500	300-350	M. F. Zaki (2008)
	CR-39	**1200**	**300-400**	**The present work**
UV-radiation	CR-39	250	315-350	Qusay Kh. O. AlDulamy (2010)
	CR-39	**1200**	**300-330**	**The present work**
	Lexan	200	330-385	K. Hareesh . Ganesh et al. (2013)
	Lexan	**175**	**290-330**	**The present work**

Table 3.6   Comparison of some results of the present work with previous studies for range of wavenumber results using FTIR- spectroscopy technique

Radiation	Types of NTDs	Thickness (μm)	wavenumber (cm⁻¹) and type band	Reference
Gamma-ray	CR-39	100	1745 (C=O) , and 1140 , 1100 (C-O-C) Stretch	T. Yamauchi et al.(2013)
	CR-39	**1200**	**1405,1456 (in bound CH$_2$ deformation vibrations)**	**The present work**
UV-radiation	Lexan	200	1690 (C=O) Stretch	K. Hareesh . Ganesh et al. (2013)
	Lexan	**175**	**940 (in band CH wag (in–plane) deformation vibrations**	**The present work**

Chapter Four

Conclusions and Recommendations for Future Works

Chapter Four

Conclusions and Recommendations for Future Works

4.1. Conclusions

1. No gamma ray response appears at the range from 1Gy to 10 Gy for CR-39 detector by measuring absorbance-A at uv-visible   spectroscopy , while the radiation response appears at the wavelengths   300 and 304 nm for 195 kGy.

2. The gamma ray   response appears at the range from 1Gy to 10 Gy for Lexan detector by measuring absorbance-A at uv-visible spectroscopy at the wavelengths   400 , 500 , 600 , 700 and 800 nm for 10 Gy , While for LR-115 detector it appears at the wavelengths 700 and 710 nm for 10 Gy.

3. The polynomial relationship between gamma radiation dose (Gy) and absorbance-A for Lexan type was better than the radiation response which appears in CR-39 and LR-115 at wavelengths 700 and 800 nm.

4. The uv radiation response appears at the range 10 - 360 J/cm² for CR-39 detector by measuring absorbance-A at uv-visible spectroscopy at the wavelengths 300 and 304 nm for   360 J/cm². While, for the Lexan detector it appears at the wavelengths 300 and 305 nm for   360 J/cm². And for the LR-115 detector appears at 600 and 650 nm for 360 J/cm².

5. The polynomial relationship between uv- radiation dose (J/cm²) and absorbance-A for NTDs   types LR-115 was

better than the radiation response which appears in CR-39 and Lexan at wavelength 650 nm.

6. The change in the shape of FTIR-spectrum with gamma irradiation dose (Gy) appears at wavenumbers 1405 and 1456 cm^{-1} for CR-39 but did not show any change in the measurement of Lexan and LR-115 detectors .

7. The deviation in spectrum (FTIR) is observed at wavenumbers-W 1338 , 940 and 2907 cm^{-1} for CR-39 , Lexan and LR-115 detectors respectively , it was observed better in the detectors CR-39 and Lexan than detector LR-115. While, the deviation at CR-39 and Lexan detectors was better than LR-115 detector.

4.2. Recommendations for Future Works

1. The NTDs may be used as a measuring tools radiation dosimeter for other studies , at the medical and environment fields .

2. Use of UV-VIS and FTIR spectroscopy techniques in the field of exposure radiation dose to gamma ray and uv-radiation for other polymer materials .

3. The NTDs may be used for another radiation like micro-wave radiation which from mobile phone .

4. Use of AFM , TEM technique to measure the effect of gamma ray and uv radiation on NTDs and comparing with this study .

5. Another study may use some of nanomaterial's coated with NTDs to increase the uv radiation response .

6. Use of digital image detector for the analyses of NTDs image irradiation by gamma ray and uv radiation .

References

Reference

[1]   Frederick William Herschel ., "Herschel Discovers Infrared Light" , activities. Retrieved 4 March (2013).

[2]   Davidson., W. Michael, "Johann Wilhelm Ritter" , (1776 -1810) .

[3]   Mehta, Akul. "Introduction to the Electromagnetic Spectrum and Spectroscopy". Pharmaxchange.info. Retrieved (2011).

[4]   Mohr, J. Peter; Taylor, N. Barry; Newell, B. David, "CODATA Recommended Values of the Fundamental Physical Constants", (2008).

[5]   Kwan-Hoong Ng., "Non-Ionizing Radiations–Sources, Biological Effects , Emissions and Exposures ", Proceedings of the International Conference on Non-Ionizing Radiation at UNITEN ICNIR2003 Electromagnetic Fields and Our Health ., (2003).

[6]   " ICRP Publication 103, the 2007 Recommendations of the International Commission on Protection". ICRP. Retrieved 12 December (2013).

[7]   Jim Clark Ionization energy . chemguide. c o. uk. The ionization energies of hydrogen and oxygen (first ionization) are both about 14 eV. last modified August (2012) .

[8]   Questions and Answers about Biological Effects and Potential Hazards of Radiofrequency Electromagnetic Fields. Office of Engineering and Technology. Bulletin 56, Fourth Edition, August (1999).

[9]   John Moulder, Professor of Radiation Oncology, Medical College of Wisconsin , Milwaukee , Wisc, U.S.A, 13-Aug . (2006).

[10]   A. A. Morsy , Eygp. J. Biophys., 3 , 29 (1997) .

[11] S. A. Durrani , Proceedings of the 20th Inter.Conf. on SSNTDs, Sloenia, (2000) ,p.1.

[12] D. A.Young , " Etching of Radiation Damage in Lithium Fluoride" Nature , 182 (1958) 375.

[13] E. C. Silk and R. S. Barnes , Phil.Mag., "Examination of fission fragment tracks with an electron microscope", 4 ,970 (1959) .

[14] Price and Walker ," Electron Microscope Observation of Etched Tracks from Spallation Recoils in Mica ", Phys. Rev. Lett. , 8 ,217(1962) .

[15] P. B. Price and R. M. Walker ," Observation of Charged Particle Tracks in Solids ", J. Appl. Phys. 33, 2625 , 3400. 3407 (1962) .

[16] R. L. Fleischer and P. B. Price, " Tracks of Charged Particales in High Polymers" , Science, 140 (1963) 1221.

[17] R. L. Fleischer, P. B. Price , R.M. Walker and R. L. Hubbard. " Effects of temperature, pressure, and ionization of the formation and stability of fission tracks in minerals and glasses Phys .Rev., A133 (1964) 1443.

[18] S. A. Durrani , Proceedings of the 20th Inter.Conf. on SSNTDs , Sloenia, (2000),p.1.

[19] S. A. Durrani. "Nuclear track detection",pergammon press, London,(1976).

[20] F. Granzer , H.G. Paretze and E. Schopper., Nuclear Inst.and Meth,147(1977)1.

[21] D. Velickovic , I. Miric & P. Bonjoric , " Proceeding of the 11th Inter. Conf. on Solid State Nuclear Track Detectors", Lyon,(1981) 583.

[22] C.E. Gohn & R. Golden," Rev. Sci. Inst. ", 43, (1972) 13.

[23] M. M. Monnin, Nuclear Inst.and Meth. Vol.173:ppl:(1980).

[24] c. Hepburn & A. H. Windle ," Solid state nuclear track detectors" , J. Material Science, 15, (1980) 279.

[25] R. L. Fleischer, P. B. Price, R. M. Walker: Nuclear Tracks in Solids: Principles and Applications. University of California Press, Berkeley,(1975).

[26] H. A. Khan, S. A. Durrani " Measurement of Spontaneous-Fission Decay Constant of U^{238} with a Mica Solid State Track Detector. Rad Effects" , 17:133-135, (1973).

[27] S. C. L. Charama and G. K. Mehta, Nucl. Instr. Meth., 178(1980)217.

[28] E. Cieslak, J. Piekarz and J. Z. akrzewski , Nucl. Instr. Meth., 39(1966)244.

[29] P. Vater, H. Freiesleben , H. J. Becker and R. Brandt," The Study of Nuclear Fission Induced by High-Energy Protons", Nucl. Instr.Meth., 147(1977)271.

[30] P. Vater , H. J. Becker, R. Brandt and H. Freiesleben ," Ion Tracks and Microtechnology " , Phys. Rev. Lett., 39 (1977) 594.

[31] S. A. Durrani and R. K. Bull '' Solid State Nuclear Track Detection: Principles, Methods and Applications '' , Pergammon press, U.K., (1987).

[32] D. J. Gore, M. C. Thorne and R. H. Watts, " The visualisation of fissionable radionuclides in rat lung using neutron induced autoradiography ", Phys. Med. Bio., 23(1978)149.

[33] A. P. Fews and D. L. Henshaw, Proc. of the 10th Inte. Confer. On SSNTDs, Bristol,(1979), p.705.

[34] D. L. Henshaw, A. P. Fews and D. J.Webster, Proc. of the 11th Inter.Confer. on SSNTDs, Lyon, (1981), p.649-654.

[35] D. L. Henshaw, K. J. Heyward, J. P. Thomas, A. P. Fews, P. Gallerano and G. Sanzone ," Environmental radiochemistry and radioactivity A current bibliography Nucl. Tracks, 8(1984) 453.

[36] R. L. Fleischer , P. B. Price and R. M.Walker, " On the Simultaneous Origin of Tektites and Other Natural Glasses", Geochim. Cosmochim. Acta., 29(1965) 161.

[37] P. Vater , Nucl. Tracks and Radia. Measure., 15(1988) 473.

[38] S. L. Guo , H. Hao , R. Brandt and P. Vater , Nucl. Tracks and Radia. Measure., 15(1988)159.

[39] G. Trees , M. Ellinger , E. U. Khan, P. Vater, P. Brandt and M. Kadner , Nucl. Tracks, 6(1988)159.

[40] C. Hepburn and A. H. Windle, Solid State Nuclear Track Detectors,J.Mater.Sci.15,279-301,(1980).

[41] T. Heins, and W. Enge, "Oxygen effect on the etch rate in CR-39 polymer" , Nucl. Tracks Radiat. Meas, 12: 87-92 (1996).

[42] Kumar, S. Chander, S., Yadov, J.S, and Sharma, A.P., Some environmental effect studies on CR-39 polymer , Nucl. Tracks Radiat.Meas.,12:129-135(1996).

[43] R. Isabey, E. Duverger, J. L. Decossas, and J. C. Varielle, " Theoretical and experimental study of the CR-39 behavior under electron beam" , Nucl. Tracks Radiat. Measur., 31: 85-90 (1999).

[44] D. Nikezic , Yu KN . Materials Science and Engineering , Reports ;46:51(2004) .

[45] A. Tidjani " Nuclear Istruments and Methods in Physics Research Section B: Beam Interactions with Materials and Atoms" ;58:43(1991) .

[46] F. Abu-Jarad, M. A. Islam, I. Abu-Abdoun, M. A. Khan " Nuclear Tracks and Radiation Measurements" ; 20:531(1992) .

[47] T. Sharma, S. Aggarwal, A. Sharma, S. Kumar, V. K. Mittal, P. C. Kalsi, V. K. Manchanda," Modification of optical properties of polycarbonate by gamma irradiation". Radiat Eff Defects Solids 163: 161–167(2008).

[48] M. F. Zaki, and Y. H. El-Shaer, " Particularization of alpha contamination using CR- 39 track detectors " , Paramana , 69 (4): 567 – 574 (2007).

[49] S. M. Farid, " A study on the radon concentrations in drinking water in Saudi Arabia and the associated health effects", J.Environ.Radioactivity,38:97-101(1998).

[50] M. I. Al-Jarallah, F. Rehman, A. Musazay and A. Aksoy, " Correlation between radon exhalation and radium content in granite samples used as construction material in Saudi Arabia" , Nucl.TracksRadiat.Meas.,40:625_629(2005).

[51] F. S. Erees , G. Yener, M. Salk, and O. Ozbal, " Measurement of radon content in soil gas and in thermal wayers in Western Turkey, " Nucl. Tracks Radiat. Measur., 41: 354 – 361 (2006).

[52] D. Al- Azmi , A. I. Abu-Shady, A. M. Sayed, and A. Al-Zayed, " Indoor radon in Kuwait Health Phys." , 94 (1): 49 – 56 (2008).

[53] T. Heins and W. Enge, " Oxygen effect on the etch rate in CR-39 polymer" , Nucl. Tracks Radiat. Meas, 12: 87-92 (1996).

[54] R. Isabey , E. Duverger , J. L. Decossas and J.C. Varielle, " Theoretical and experimental study of the CR-39 behavior under electron beam" , Nucl. Tracks Radiat. Measur., 31: 85-90 (1999).

[55] S. Kumar , S. Chander , J. S. Yadov , and A. P. Sharma ," Some environmental effect studies on CR-39 polymer " , Nucl. Tracks Radiat. Meas., 12:129-135 (1996).

[56] B. T. Anthony " Lexan polycarbonate for automotive forward lighting ".Mater Des6 :293-302 (1985).

[57] H. G. Raj Prakash, G. Sanjeev, K. B. Vijay Kumar, K. Siddappa, B. K. Nayak, A. Saxena, "Experimental determination of

photofission   cross-section of ^{232}Th using electron accelerator". Ann Nucl Energy 38: 757–766 (2011).

[58] S. Banisadr , H. Asempour ,"Effect of ferric salt of orange peel solid fraction on photo-oxidation and biodegradability of LDPE films. Iran Polym J 21:463–471(2012).

[59] Tse K. C. C., Ng F. M. F., Yu K. N Photo-degradation of PADC by UVradiation at various wavelengths. Polym Degrad Stab2388_91:2380(2006).

[60] A. Chapiro ,General consideration of the radiation chemistry of polymers. Nucl Instr Methods Phys Res B 105:5–7(1995).

[61] T. Sangappa Demappa, S. Mahadevaiah Ganesha, S. Divakara, M. Pattabi, R. Somashekar, Physical and thermal properties of 8 MeV electron beam irradiated HPMC polymer films. Nucl Instrum Methods Phys Res B 266:3975–3980(2008).

[62] R. C. Ramola, S. Chandra, A. Negi, J. M. S. Rana, S. Annapoorni, R. G. Sonkawade , P. K. Kulriya ,Srivastava, A Study of optical bandgap, carbonaceous clusters and structuring in CR-39 and PETpolymers irradiated by 100 MeV O^{+7} ions. Phys B 404:26–30(2009).

[63] R. C. Ramola, S. Chandra , J. M. S. Rana, R. G. Sonkawade, P. K. Kulriya, S. Fouran, D. K. Avasthi, S. Annapoorni ,A comparative study of the effect of O^{+7} ion beam on polypyrrole and CR-39 (DOP) polymers. J Phys D Appl Phys 41:115411 (1–6)(2008).

[64] J. Jagielski, A. Turos, D. Bielinski, A. M. Abdul-Kader, Piatkowska A " Ion-beam modified polymers for biomedical applications". Nucl Instrum Methods Phys Res B 261:690–693(2007).

[65] A. Srivastava, T. V. Singh, S. Mule, C. R. Rajan, S. Ponrathnam, "Study of chemical, optical and thermal modifications induced

by100 MeV silicon ions in a polycarbonate film". Nucl Instrum Methods Phys Res B 192:402–406(2002) .

[66] K. Hareesh , A. K. Pandey , Y. Sangappa , Ravishankar Bhat , A. Venkataraman , Ganesh Sanjeev" Changes in the properties of Lexan polycarbonate by UV irradiation", Nuclear Instruments and Methods in Physics Research B 295 (2013) 61–68.

[67] D. Nikezic and K.N. Yu, Mater, " Formation and growth of tracks in nuclear track materials ", Sci. Eng. R 46 51(2004).

[68] R. L. Fleisher, Ion tracks, in: J.H. Westbrook, R.L. Fleischer (Eds.) (Intermetallic Compounds Principles and Practice) , John Wiley, (2002)).

[69] C.W.Y. Yip, J.P.Y. Ho, V.S.Y. Koo, Nikezic D., K.N. Yu, " Effects of stirring on the bulk etch rate of LR-115 detector", Radiat. Meas. 37 (2003) 197-200.

[70] C.W.Y. Yip, Nikezic D., J.P.Y. Ho, K.N. Yu, "Chemical etching characteristics for cellulose nitrate", Mater. Chem. Phys. 95 (2006) 307–312.

[71] C.W.Y. Yip, J.P.Y. Ho, D. Nikezic, K.N. Yu, "A fast method to measure the thickness of removed layer from etching of LR-115 detector based on EDXRF", Radiat. Meas. 36 (2003) 161–164.

[72] Z. S. Kocsis, K. K. Dwivedi, and R. Brandt, Radiat . " Studies on The Track Formation Mechanism of The Heavy Ions in CR-39 " Meas.28 Radiation Measurements, Vol. 28, Nos I-6, pp. 177-180, (1997) .

[73] C.W.Y. Yip, J.P.Y. Ho, D. Nikezic, K.N. Yu, "A fast method to measure the thickness of removed layer from etching of LR-115 detector based on EDXRF", Radiat. Meas. 36 (2003) 161–164.

[74]　D. T. Clark , P. J. Stephenson," Electron-spectroscopy for chemical applications (ESCA) applied to polymers—an ESCA study of the surface chemistry of cellulose nitrates and double based propellants", with particular reference to their degradation in UV-light, Polym. Degrad. Stab. 4 (1982) 185–193.

[75]　A. H. K. Fowler, H. S. Munro, D. T. Clark, E. S. C. , "A studies of the thermal and X-ray induced degradation of cellulose nitrates", Polym. Degrad. Stab. 11(1985) 287–296.

[76]　F. M. F. Ng, K. N. Yu, " X-ray irradiation induced degradation of cellulose nitrate", Materials Chemistry and Physics 100 (2006) 38–40.

[77]　K. N. Yu and F. M. F. Ng, " Alternative Method to Determine the Bulk Etch Rate of LR-115 Detectors" , Nucl. Instrum. Methods Phys. Res. J.B 226 (2004) 365.

[78]　 C. Darrand, B. Bennamane, C. Gagnadr, J. L. Decossas, J .C. Vareille,"Optical modification of polymers by ion beam irradiation ".Polymer, 35,2447-2451(1994).

[79] C. Gagndre, J. L. Decossas, J. C. Varcille," IR Spectroscopy Studies of Polycarbonate irradiated by H^+ and Li^+ ions .Nucl. Inst. Meth. B73, 48-52 (1993).

[80] M. A. Malek, C. S. Chong ," FTIR study of H_2O in polyallyldiglycol carbonate". Vibration Spectroscopy, 24,181-184 (2000).

[81]　Tse Chun Chun ," Investigations of The Effects of UV Irradiation on The Etching Behavior of CR-39 Solid State Nuclear Track" , Master of Phiolosophy City University of Hong Kong march (2007).

[82]　Koichi Nishikida and John Coates ," HANDBOOK OF PLASTICS ANALYSIS", chapter 7 (Infrared and Raman Analysis of Polymers) , (2003).

[83] K. C. C. Tse , F. M. F. Ng , D. Nikezic , K. N. Yu ," Bulk etch characteristics of colorless LR-115 SSNTD", Nuclear Instruments and Methods in Physics Research B 263 - 294–299(2007).

[84] N. E. IPE , P. L. Ziemer, .," Effect of Pre-Gamma Irradiation on CR-39", SLAC - PUB - 3800 October (1985) (M).

[85] D. Sinha , S. Ghosh, A. Srivastava , V. G. Dedgaonkar , and K. K. Dwivedi," Effect of Gamma Rays on PADC Detectors", Radiation Measurements. Vol. 28, Nos 1-6, pp. 145-148, (1997).

[86] Sinha D. G. K. Sarker, Ghosh S. Ghosh , A. Kulshreshtha , K. K. Dwivedl and D. Fink ," Gamma Ray Photon-Induced Modifications in Triafol -TN and Triafol-BN Polymeric Track Detectors ", Radiation Measurements Vol. 29, No. 6, pp. 599-604, (1998).

[87] D. Sinha, R. Mishra, S. P. Tripathy, K. K. Dwivedi, " Effect of high gamma doses on the etching behavior of different types of PADC detectors", Radiation Measurements 33 (2001) 139-143.

[88] T. Yamauchi, H. Ichijo, K. Oda ," Depth-dependence of the bulk etch rate of gamma-ray irradiated CR-39 track detector ", Radiation Measurements 34 (2001) 85–89.

[89] M. A. Maleka , C. S. Chongb," CO_2 diffusion from X-ray and γ -ray irradiated CR-39 plastic", Radiation Measurements 35 (2002) 203 – 206.

[90] Ahmed K. Abdullah," The Effect of High Irradiation Energy (Gamma, UV- light) Radiation on the Energy Gap of Polymers Doped with Anthrancene", Iraqi Journal of Science, Vol.47, No.1, (2006), PP. 99-103.

[91] P. C. Kalsi, V. S. Nadkarni, V. K. Manchanda," Effect of gamma irradiation on the etching and optical properties of a newly developed nuclear track detector called (PNADAC) homopolymer", Radiation Physics and Chemistry 77 (2008) 1002– 1004.

[92] Jyotsna A. Sapkal , P. C. Kalsi, Chhavi Agarwal , Thanamani M. , Murali S. ," The etching and optical response of Tuffak polycarbonate nuclear track detector to gamma irradiation", Radiation PhysicsandChemistry78(2009)81–84.

[93] Abdel Raouf Kh. M.," Study of CR-39 SSNDs irradiated with different types of radiation by FTIR spectroscopy and α-range determination", American Journal of Environmental Protection (2013) ; 2(2): 53-57.

[94] R. Shweikani , G. Raja, A. A. Sawaf," The possibility of using plastic detectors CR-39 as UV dosimeters", Radiation Measurements 35 (2002) 281 – 285.

[95] K. C. C. Tse, F. M. F. Ng, K.N. Yu " Photo-degradation of PADC by UV radiation at various wavelengths", Polymer   Degradation and Stability 91 (2006) 2380_2388.

[96] Chhavi A garwal, P. C. Kalsi ," UV-irradiation effects on polyester nuclear track detector", Radiation Physicsand Chemistry 79 (2010) 844–847.

[97] Rana H. Mahmmod " Study the Effect of UV Radiation Dose on the Optical Properties of SSNTD – CN-85", Mosul University , Rafidain journal of scienc , Volume: 23 Issue: 1A Pages: 130-140 (2011).

[98] Firas M. Al-Jomaily , Hussain A. Al-jobouri, Ahmed K. Mheemeed ," Ultraviolet Radiation Dosimetry by Using of

CN-85 , CR- 39, LR-115 Nuclear Track Detectors", Iraqi Journal of Science, 355 - 3, 35 (2012).

[99] K. Hareesh , Ganesh Sanjeev , A. K. Pandey, Vijayalakshmi Rao." Characterization of UV-irradiated Lexan polycarbonate films", (Iran Polym J (2013) 22:341–349 DOI 10.1007/s13726-013- 0133-7) (2013).

[100] Chong C.S. C.S. Chong, I. Ishak , R. H. Mahat and Y. M. Amin, " UV-VIS and FTIR Spectral Studies of CR-39 Plastics Irradiated with X-ray", Radiation Measurements. Vol. 28. Nos 1-6. pp. 119-122, (1997).

[101] D. D. Nikezic, K.N. Yu," Profiles and parameters of tracks in the LR115 detector irradiated with alpha particles", Nuclear Instruments and Methods in Physics Research B 196 (2002) 105–112.

[102] Amer H. Ali," Effect of Laser Radiation on the Nuclear Track Detector LR-115", Tikrit University , Tikrit Journal of Pure Science , Volume: 15, Issue: 2 Pages: 302-305 (2009).

[103] Sallama . S. Hummadi ," Determination of Uranium Concentration In Female And Male Children's Teeth Samples Using Fission Tracks In CR-39 From Different Countries." , Journal of college of education , No.1.(2010).

[104] Hussain Ali Al-Jobouri, Jameel M. A. Sulaiman and Ahamed S. Jarallah," Effect of X-Ray Radiation on Electro-Optical Characteristics of CR-39 Sheets", Journal of Al-Nahrain University,Vol.15 (4), December, (2012), pp.318-343.

[105] G. H. Dieke, A. B. F. Dunce, '' Spectroscopic Properties of Uranium Compounds; National Nuclear Energy Series'', Div. III, Vol.2, McGraw-Hill, New York, (1949).

[106] P. Griffiths, J. A. de Hasseth, Fourier Transform Infrared Spectrometry (2nd ed.). Wiley-Blackwell. ISBN 0-471-19404 - 2(18 May 2007).

الخلاصة

الغرض من هذه الدراسة هو تخمين الجرعة الإشعاعية لأشعة كاما-γ والاشعة الفوق البنفسجية-UV على كواشف الأثر النووي LR-115 , Lexan , CR-39 من خلال قياس الامتصاصية الضوئية-A باستخدام تقنية مطيافية الضوء المرئي وفوق البنفسجي (UV-visible) , و قياس الانحراف الطيفي باستخدام تقنية تحول فورير للأشعة تحت الحمراء-FTIR . وتم قياس الاستجابة الإشعاعية لأشعة كاما-γ بمدى الجرع الواطئة من 1 Gy الى 10 Gy ومدى الجرع العالية من 10 Gy الى 195 kGy . تبين ان هناك استجابة إشعاعية لأشعة كاما-γ لكافة كواشف الأثر النووي المستخدمة في هذه الدراسة . حيث لوحظ ان هناك استجابة اشعاعية لأشعة كاما-γ للكاشفين Lexan و LR-115 من خلال قياس الامتصاصية الضوئية-A بينما الاستجابة الاشعاعية للكاشف CR-39 تظهر في مدى الجرع العالية فقط.

وقد اوضحت النتائج ان الامتصاصية الضوئية-A تزداد بزيادة الجرعة الإشعاعية لأشعة كاما-γ, حيث لوحظ ان الكاشف Lexan يمتلك استجابة اشعاعية افضل بكثير من الكاشفين CR-39 و LR-115 من خلال قياس ارتفاع قيمة الامتصاصية الضوئية-A عند الطول الموجي   800 nm .

وظهر ان هناك انحراف في بعض الاعداد الموجية-W في طيف-FTIR للكاشف CR-39 عند مدى الجرع الواطئة من 1 Gy الى 10 Gy مع زيادة الجرعة الإشعاعية لأشعة كاما-γ. وظهر الانحراف في الاعداد الموجية- W 1405 cm^{-1} و 1456 cm^{-1} لطيف –FTIR , بينما لم يظهر ذلك الانحراف باستخدام الكاشفين Lexan و LR-115 .

وعند التشعيع بالأشعة الفوق البنفسجية UV للكواشف وجد ان الامتصاصية الضوئية-A تزداد مع زيادة الجرعة الإشعاعية لأشعة UV ايضا" عند مدى الجرع من 1 J/cm² الى   360 J/cm² . حيث يمتلك الكاشف LR-115 استجابة اشعاعية افضل بكثير من الكاشفين Lexan , CR-39 من خلال قياس ارتفاع قيمة الامتصاصية الضوئية-A عند الطول الموجي 650 nm.

وظهر الانحراف في طيف –FTIR الناجم عن الأشعة الفوق البنفسجية UV عند الاعداد الموجية W-1338, 2907 cm^{-1} , 940 للكواشف LR-115 , Lexan , CR-39 على التوالي , وكان الانحراف في CR-39 و Lexan اكثر وضوحا" من الكاشف LR-115 .

من هذه الدراسة لوحظ امكانية استخدام كواشف الأثر النووي LR-115 , Lexan , CR-39 كمقاييس للجرع الاشعاعية لأشعة كاما-γ والاشعة الفوق البنفسجية-UV في المجال الطبي والبيئي.

تخمين الجرعة الإشعاعية للأشعة المؤينة وفوق البنفسجية باستخدام كواشف الاثر النووي LR-115، Lexan، CR-39

رساله

مقدمه الى كلية العلوم/ جامعة النهرين
وهي جزء من متطلبات نيل درجة الماجستير في علوم الفيزياء

من قبل

فلا حاتم طه

بكلوريوس علوم فيزياء (٢٠١١)

إشراف

أ.م.د.حسين علي الجبوري